Towards geriatric use of exoskeletons: Improving human-device interaction with a tutorial and optimal control

by

Jan C. L. Lau

A thesis
presented to the University of Waterloo
in fulfillment of the
thesis requirement for the degree of
Master of Applied Science
in
Systems Design Engineering

Waterloo, Ontario, Canada, 2023

Author's Declaration

This thesis consists of material all of which I authored or co-authored: see Statement of Contributions included in the thesis. This is a true copy of the thesis, including any required final revisions, as accepted by my examiners.

I understand that my thesis may be made electronically available to the public.

Statement of Contributions

The results of this thesis have led to one published manuscript, two poster presentations, and two accepted conference abstracts, listed in reverse chronological order:

1. Jan C. L. Lau and Katja Mombaur. **Motion analysis and motion synthesis on crutch-less sit-to-stand for geriatric users with an exoskeleton using optimal control**. *Accepted to TGCS 2023 Symposium on Computer Simulation in Biomechanics (ISB TGCS 2023).*

2. Jan C. L. Lau and Katja Mombaur. **Towards crutch-less exoskeleton-assisted geriatric sit-to-stand motions – an experimental and optimization-based study**. *Accepted to 2023 International Society of Biomechanics-Japanese Society of Biomechanics Conference.*

3. Jan C. L. Lau and Katja Mombaur. **How can we make exoskeletons less intimidating for geriatric users?**. *Poster presented at the Internationales Wissenschaftsforum Heidelberg Hengstberger Symposium on Aging and Technology*, Heidelberg, Germany. May 2022.

4. Jan C. L. Lau and Katja Mombaur. **Preliminary Study on a Novel Protocol for Improving Familiarity with a Lower-Limb Robotic Exoskeleton in Able-Bodied, First-Time Users**. *Front Robot AI*, 8:785251, January 2022.

5. Jan C. L. Lau and Katja Mombaur. **Protocol for improving familiarity with a lower-limb robotic exoskeleton in able-bodied, first-time users**. *Poster presented at the International Society of Biomechanics Conference*, virtual. July 2021.

For the paper, presentations, and abstracts, I was responsible for designing the experiment, carrying out the experiments, developing code, analyzing the data, and drafting and submitting the documents. Prof. Dr. Katja Mombaur provided guidance throughout the research performed and feedback on the published, presented, and submitted documents.

Abstract

With the global geriatric population expected to reach 1.5 billion by 2050, there has been growing interest to tackle age-associated movement impairments by developing assistive technologies. Rehabilitative lower-limb exoskeletons have been primarily developed for people with spinal cord injuries. Since the needs of older adults are different than those of individuals with spinal cord injuries, the existing exoskeletons must undergo further modifications to be appropriate for the elderly. This thesis covers two preliminary approaches taken to improve human-exoskeleton interaction.

The first approach is to develop a novel protocol to teach first-time exoskeleton users how to move with the device. A pre-test involving two graduate students (healthy young adults) who had no prior exoskeleton experience suggests that moving with the device for the first time may be intimidating. It is assumed that this initial experience would be even worse for older adults. Moreover, there are little-to-no instructions provided on how to move with it, nor is there research done in this direction so far. To test the effectiveness of the developed protocol, a preliminary study was conducted with IIT's TWIN exoskeleton. Due to COVID-19 restrictions, only healthy, able-bodied lab members could be invited. One group received the tutorial and the other group did not receive any training. The preliminary results suggest that the novel protocol is beneficial for first-time exoskeleton users and has a positive influence on the usability of the device, though this came at a cost of higher mental and physical demands and poorer perceived performance. Details on expanding the study to a larger population and making the tutorial suitable for older adults are discussed.

The second approach is an attempt to modify an existing lower-limb exoskeleton, which is originally made for a different target population, so that it would be suitable for older adults. Using optimal control and a simulation model of an elderly woman wearing TWIN, the crutch-less sit-to-stand trajectories are analyzed and generated. To first better understand the kinematics and forces of the movement involving a human-exoskeleton system, motion capture and force plate data on various "crutched" and crutch-less sit-to-stand conditions are collected. Note that the crutch-less sit-to-stand scenarios do not reflect the intended use of the exoskeleton, but are collected to show the possibility of doing so with TWIN and analyze the underlying biomechanics. Motion analysis is performed on one of the crutch-less cases, allowing us to determine the torques needed to perform the motion successfully. The feasible solution is compared against an optimal solution obtained via motion synthesis. Similarities and differences between the feasible and optimal solutions are discussed. The limitations are identified and suggestions on formulating the optimal control problem to be suitable for the geriatric population are also discussed.

Acknowledgements

I would like to thank my supervisor, Dr. Katja Mombaur, for her guidance, encouragement, support, patience, and the learning opportunities provided throughout my master's degree. Her passion in human-centred robotics and optimal control has inspired research topics that I did not know is possible. I would like to thank Dr. Arash Arami and Dr. Yue Hu for their comments and insights on improving this thesis. I learned a lot.

I would like to thank all my lab colleagues from the Human-Centred Robotics and Machine Intelligence Lab, for their continuous encouragement and support in getting through the MASc degree during the COVID-19 global pandemic. Jonas, thank you for your talks and insights on numerics and optimization, and also allowing me to practice speaking German with you. Jonathan, thank you for the help in many aspects, including and not limited to using motion capture equipment and handling ethics. I also want to thank you for being a great listener and offering great advice for overcoming different challenges. Francisco, thank you for your continuous support, including coming up with ideas for debugging code and understanding the exoskeleton. Robert, thank you for helping me out with running the experiments and also teaching some machining knowledge here and there. Branca, thank you for the homemade baked goods. I really love your cookies. To the lab members who participated in my preliminary protocol study because COVID-19 restrictions would not let me recruit external participants, but must remain anonymous due to confidentiality issues, thank you for your help. To Menna, Kareem, Pranav, Anas, Will, Jiwon, Christian, and Mahsa, thank you for the help and encouragement throughout the courses and lab experiments. Whether it is grabbing 6 cups of coffee per day or not being able to walk the next day from "squatting till we drop" just for a course project, I will miss those times of us surviving and stu*dying* together.

I would like to thank the UWaterloo Karate & Jujitsu and UWaterloo Muay Thai clubs for the friendships made, fun memories, and of course, the countless opportunities to release stress and tension.

Including and not limited to a partially-torn thumb, various foot injuries, and a concussion, I would like to thank the Ontario healthcare professionals for, quite literally, keeping me alive. It is fascinating to learn more about human biomechanics when receiving physiotherapy, though I admit that it is not the healthiest way to learn about this subject matter.

Last but not least, to Mom and Dad: engineering and science may not be the field you had hoped I would pursue back in high school, but thank you for your love, understanding, continuous support, and now being two of my biggest cheerleaders as I continue on this journey.

Dedication

I would like to dedicate this thesis to my grandmother living in Hong Kong. Before having a stroke at the age of 90, she also had knee pain that affected her walking capabilities. Being fully recovered from stroke and knee pain, she turns 98 this year. Her story has inspired me to do something for the geriatric population.

Table of Contents

List of Figures

xiii

List of Tables

Chapter 1

Introduction

An active lower-limb exoskeleton is a wearable robotic system made to augment and/or assist human motion in the legs. The onboard motors can help a person walk, sit, and stand. Benefits of exoskeletons over wheelchairs include reducing chances for injured individuals to live a sedentary lifestyle, improving cardiopulmonary function, metabolic function, and promoting quality of life [90]. Compared to walkers and rollators, exoskeletons occupy less space in the environment and can directly administer movement aid in the lower limbs via motors, so it has the potential to provide mobility assistance to the geriatric population.

Osteoporosis and sarcopenia are two examples of gait impairments associated with ageing that can reduce the quality of life in older adults [88, 46]. The global population of people aged 65 years or above in 2019 was 703 million, and it is projected to reach 1.5 billion by 2050 [23]. According to a one-year study conducted with nursing home residents in Bavaria (Germany), walking and improper sit-to-stand (STS) transfers are responsible for 36% and 41% of the falls in older adults respectively [71]. Walking canes, walkers, and wheelchairs are passive devices currently used by older adults that require gait and/or STS assistance. In this context, passive means that the movement is human-driven and the device does not have components that actively move the person. Although robotic interventions have the potential to improve the quality of life in older adults, these solutions come with various challenges related to the interaction between a human and exoskeleton.

Learning how to move with an exoskeleton can be a strenuous process with a steep learning curve because it usually requires multiple training sessions. From a user acceptance perspective, unless really needed, older adults are reluctant to wear an assistive device because of lack of familiarity, its bulkiness, and the fact that it looks rather intimidating. Control design is also challenging because not only should the motions acting on the human

be smooth, comfortable, and safe, the movement trajectories should also resemble as closely as the movements of an able-bodied healthy person. Various trajectory generation methods have been developed, yet there is no research done so far on improving user familiarity with an exoskeleton.

The contributions of this thesis involve two approaches that are considered preliminary works towards improving human-exoskeleton interaction in the geriatric population. The first approach is to develop a novel familiarity protocol to teach first-time exoskeleton users how to move with the device. Due to COVID-19 restrictions, the protocol could only be tested on a small group of lab members as a preliminary study. Utilizing a simulation model of an elderly woman wearing the TWIN exoskeleton, the second approach is to generate a crutch-less full-body sit-to-stand trajectory with optimal control, which is considered as an attempt to modify an existing exoskeleton for it to be suitable for the elderly. A novelty of this approach is the consideration of arm movements when performing crutch-less sit-to-stand, since this is something that has not been done so far. Other contributions of this thesis are the kinematics and forces involved in performing sit-to-stand with the 25-kg TWIN with and without crutches at two different seat heights. They include force trajectories and peak values exerted in the crutches in "crutched" cases, force trajectories and peak values exerted in the feet in crutch-less cases, and the kinematics (particularly the arm and hip joint movements) prior to lifting from being seated. The trajectories and maximum magnitude of lower-limb joint torques obtained with optimal control are also contributions of this thesis. It is once again emphasized that these contributions are from preliminary works, so more effort and formulation are required before being fully suitable for the geriatric users. Note that healthy geriatric users would not require exoskeleton support, so the target elderly population would be older adults living with either very mild or mild frailty. Suggestions on how the findings/results can be expanded to this target population are another set of contributions of this thesis.

Chapter 2 covers lower-limb exoskeleton state of the art and control methods. It begins with describing existing hardware developed in a lab and on the market, then proceeds into the underlying controls and trajectory generation methods.

Chapter 3 is about the novel familiarity protocol developed. It begins with a pre-test conducted with two graduate students, then expands into a preliminary study where the protocol was deployed to train a small group of able-bodied, first-time users. Preliminary results, future recommendations, and interdisciplinary exchanges on how the protocol can be tailored to older adults are discussed in this chapter.

Chapter 4 starts with a literature review on sit-to-stand trajectory generation, then describes a motion capture experiment conducted on performing six scenarios of sit-to-stand

with the TWIN exoskeleton.

Chapter 5 is dedicated to modeling human movement and describing the lumped model created for the optimal control simulations.

Chapter 6 is the optimal control chapter. It first covers optimal control concepts then describes the formulation of optimal control problems. Results, limitations, and future improvements on the simulations performed are also discussed.

Chapter 7 explains how the novel protocol and optimal control approaches complement each other, and concludes with future prospects on this type of research.

Appendix A contains the survey questions used for the novel protocol, and Appendix B illustrates the marker layout used in this thesis.

Chapter 2

State of the Art in Lower Limb Exoskeletons

Lower-limb exoskeletons are devices designed to be worn by an individual. Active exoskeletons are equipped with motors meant to move the human limbs, whereas passive exoskeletons primarily use beams and/or springs for passive actuation. The former is more commonly found in healthcare, particularly helping people with spinal cord injuries (SCI) to regain locomotion. The latter is more for industrial and military applications that require ergonomic support to carry heavy loads. There are also devices called exosuits (soft exoskeletons), which are often driven by cables to assist walking and aid rehabilitation. They are not equipped with heavy motors, nor do they have an external rigid frame, so these devices weigh less and do not restrict the user's movements. None of the active exoskeletons developed so far are targeted for the geriatric population, whereas some exosuits are marketed to be suitable for the elderly among other target populations. However, exosuits deliver less power than exoskeletons due to their design, so exosuits may not be able to support individuals such as frailer older adults. In this thesis, the standalone "exoskeleton" keyword stands for lower-limb rehabilitative exoskeletons given the focus of this research. Depending on the design, some exoskeletons may or may not be used with crutches, though majority of the designs require external support because they are not actuated along the frontal plane for stability. This chapter first covers the active lower-limb exoskeletons and a few exosuits that are either developed or being sold in the market, then describes the controls adapted in these devices.

2.1 Existing Hardware and Target Application

2.1.1 Exoskeletons

TWIN is a 25-kg lower-limb exoskeleton developed by Istituto Italiano di Tecnologia (IIT) made for persons with spinal cord injury (SCI). It has four active degrees of freedom (DOF) at the hips and knees with passive ankle joints, and the device must be used with a set of crutches [84]. The exoskeleton has a modular design with each component coming in various sizes to enable a more customized fit to the user. TWIN can sit, stand, and walk, and its functionalities are controlled by a tablet via Bluetooth connection.

Developed by Ecole Polytechnique Fédérale de Lausanne, the AUTONOMYO is targeted for users with moderate neurological disorders such as Parkinson's disease, multiple sclerosis, and stroke [67]. Weighing at 22.5 kg, the exoskeleton has three passive degrees of freedom (DOFs) at the ankle and six active DOFs to enable hip flexion/extension, hip abduction/adduction, and knee flexion/extension. The possibility of frontal-plane actuation eliminates the need for crutches. Controlled via a smartphone application, the device provides partial or full assistance at the hips and knees for sit-to-stand, walking, and stair climbing.

The 13-kg Indego exoskeleton from Parker Hannifin is made for persons with SCI and has a modular design composed of a pelvis, two upper legs, and two lower legs [81]. Used with crutches or other stability aids, it has four active DOFs for hip and knee flexion/extension, and has two adjustable ankle-foot orthoses. The embedded sensors track the user's posture and tilt, and the device is used with an external tablet connected via Bluetooth. Although it is not intended for sports or stair climbing, it can sit, stand, and walk.

Cyberdyne's HAL lower-limb exoskeleton weighs around 14 kg and has six active DOFs for flexion/extension at the hips, knees, and ankles [82]. Designed for persons with SCI, users can choose to move from two types of control while using stability aids. The voluntary control augments the wearer's joint torque based on the muscle activity estimated with electromyographic (EMG) sensors [36], whereas autonomous control considers the wearer's preliminary motion as part of the intention to provide support for a functional motion [79]. HAL's sitting, standing, and walking functions can be controlled by an external device.

The FDA-approved EksoNR exoskeleton weighs 27 kg and is made for persons with SCI, stroke, multiple sclerosis, and acquired brain injury [20]. With four active DOFs for hip and knee flexion/extension, it provides partial or full assistance for walking and monitors leg movement for adaptive gait training [21]. The device is controlled by an external touch-screen tablet and must be used with a set of crutches.

ReWalk by ReWalk Robotics (formerly Argo Medical Technologies) is another exoskeleton for users with SCI that received an FDA approval [21]. Weighing 23.3 kg, it has passive spring-loaded ankles and four active DOFs at the hips and knees for flexion/extension. The device can sit, stand, walk, and turn. To take a step when walking, users would shift their body weight forward to trigger the tilt sensor located in the chest strap. Instead of using a tablet, the exoskeleton can be controlled with a wireless remote control worn on the wrist. Walking aids must be used with the exoskeleton.

Weighing at 12.3 kg, the Vanderbilt Powered Orthosis from Vanderbilt University is designed for persons with paraplegia and has four active DOFs at the hips and knees for movement on the sagittal plane [69]. Instead of having built-in ankle or foot components, the design is to be utilized with a set of ankle foot orthosis (AFO) for stabilizing ankles and preventing foot-drops. Using voice control to switch among states, the device can perform sit-to-stand, stand-to-sit, walking, stair ascent, and stair descent [26]. For safety and stability reasons, the device is to be used with a walker or a set of crutches.

WPAL stands for Wearable Power-Assist Locomotor. It is a lower-limb exoskeleton with a walker made by ASKA Corporation targeted for persons with paraplegia [45]. With six active sagittal DOFs at the hips, knees, and ankles, the device can perform sit-to-stand, stand-to-sit, and walking. Similar to other exoskeletons that can only perform motions on the sagittal plane, WPAL must be used together with its walker for stability reasons. To control the exoskeleton's functions, the user can interact with a tablet attached on the walker. The exoskeleton portion of WPAL weighs approximately 13 kg.

ATALANTE is a 12-DOF lower-limb exoskeleton developed by Wandercraft, a French start-up company. With four 3-axis force sensors in each foot, it weighs 75 kg and is made for people with paraplegia [31]. Aside from performing sit-to-stand, stand-to-sit, and walking, the exoskeleton is self-balanced, therefore eliminating the need for crutches or walkers. A smartphone is used for controlling the exoskeleton, and it can be strapped to a user's wrist for convenience as exhibited in Cybathlon 2020.

The Asian Institute of Technology developed a 12-DOF lower-limb exoskeleton called ALEX-I to assist mobility in users that suffer from paraplegia or weaker lower limbs. Each foot contains four load cells for sensing ground contact forces. Weighing at 117.5kg excluding the battery backpack, it is intended to support the user's weight and external loads [12]. Aside from walking, the developers of this exoskeleton did not comment whether it can also perform sit-to-stand, stand-to-sit, stair-ascend or stair-descend. They also did not mention if the device is controlled via a tablet or with other means. Although the device has the same DOF as a person's lower limbs, it is meant to be utilized with a set of crutches since the trajectories generated assumed the wearer is using crutches for balancing [11].

The Angeleg Exoskeleton is developed by SG Mechatronics from Korea and made for people with partial lower limb mobility. It uses series elastic actuators to actuate 3 DOFs at the hip and 1 DOF at the knee. It also has 3 passive DOFs at the ankle and weighs 13 kg in total. The device follows the movements of the wearer and can provide partial assistance in sitting, standing, and walking. According to SG Mechatronics' website, there are a few exoskeleton products that require crutches, but none of them resemble the one used in [40]. Therefore, it is unknown how this version of Angeleg is controlled and whether it must be used with crutches.

Figure 2.1 is a collage of the devices covered. The images are either obtained from the company websites or papers cited above.
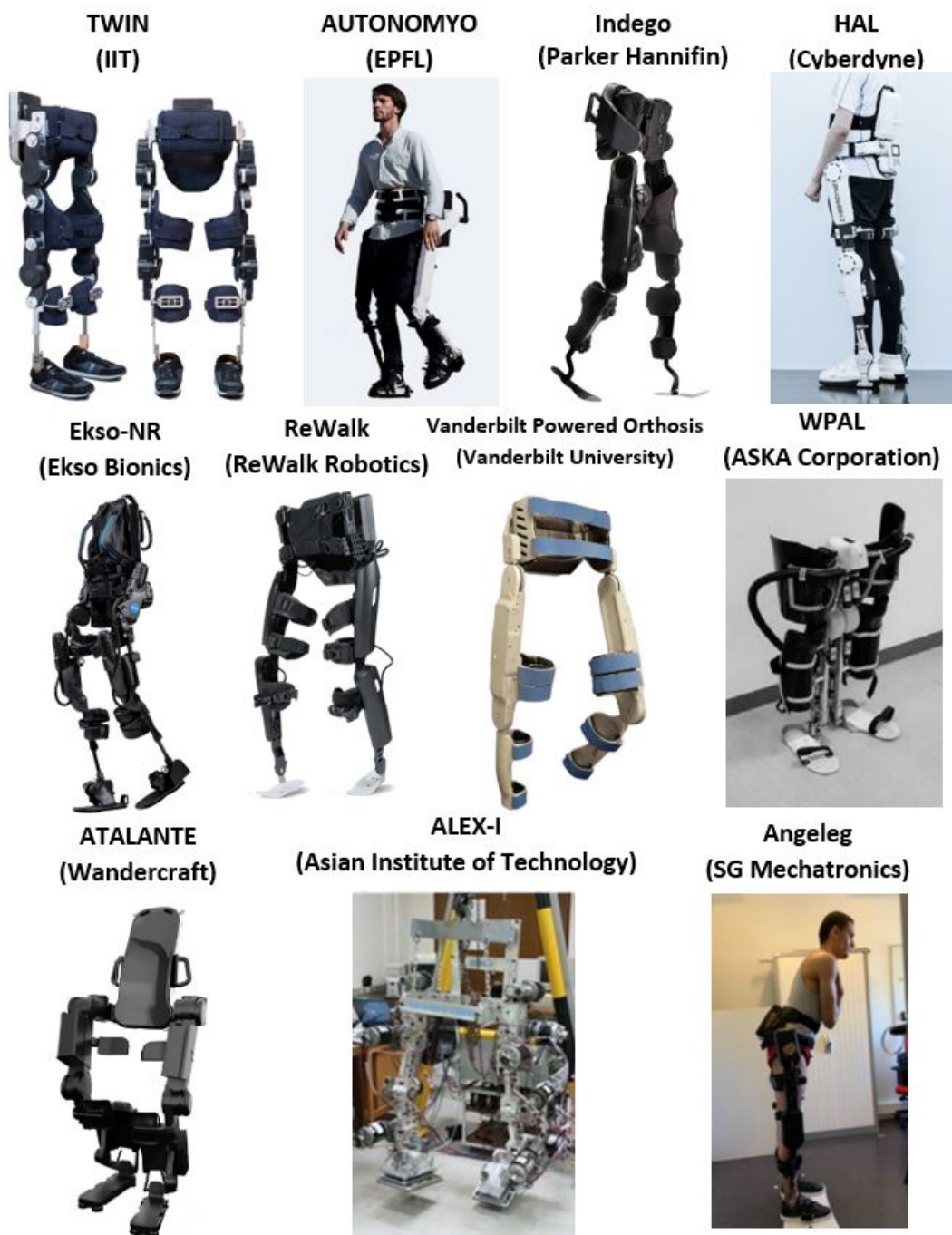
Figure 2.1: Lower-limb exoskeletons covered in the state of the art of this thesis.

2.1.2 Exosuits (Soft Exoskeletons)

ReStore is another lower-limb assistive device developed by ReWalk Robotics. Also cleared by the FDA, it is made for stroke rehabilitation and post-stroke individuals with lower limb disabilities. Driven by cables, the exosuit provides unilateral assistance to the ankle for plantarflexion and dorsiflexion during gait training [3]. It analyzes the user's movements and controls the support timing with the help of the sensors on the user's shoes [4]. ReStore is controlled via a hand controller and weighs 5 kg [5].

EasyWalk is a soft exoskeleton developed by Siyi Intelligent Technology. Driven by Bowden cables with the motor situated behind the waist, the device actuates one of wearer's ankles for walking assistance and physical rehabilitation [1]. Made for individuals including older adults and people with motor dysfunction, EasyWalk weighs 3 kg and can assist and adapt to walking modes such as flat-ground, downhill, and stair ascent [6]. In case of emergency, the device can be stopped via voice control.

Developed by MyoSwiss, Myosuit is a soft exoskeleton made for supporting individuals during rehabilitation and physiotherapy training. It can support older adults, people with incomplete spinal cord injury, and individuals with neurological conditions like stroke or multiple sclerosis [2]. Myosuit is a cable-driven exosuit with two electric motors located in the device's backpack, and it can generate 12 to 22 Nm of torque in the hip and 8 to 15 Nm of torque in the knee [35]. The device can assist walking, standing, sitting transfers, and stair walking. The sources did not comment on how the user can choose the exosuit's functions, but according to Figure 2.2, it is suspected that one can do so by interacting with a device located on the backpack strap. This device requires the wearer to have residual muscle function.

The images for the exosuits described above are either obtained from the company website or the Exoskeleton Report website.

**ReStore
(ReWalk Robotics)**   **EasyWalk
(Siyi Intelligent Technology)**   **Myosuit
(MyoSwiss)**

Figure 2.2: Exosuits covered in the state of the art of this thesis.

2.2 Exoskeleton Control

This section covers the methods of high-level control from the user, trajectory generation, and control approaches. Exoskeletons can provide full or partial assistance to the user, and the trajectories can be predefined or adjusted to environmental changes in real-time.

2.2.1 High-level Control

One approach for a user to control an exoskeleton is via manual user input, which involves the device wearer or an external person to give commands via voice control or pressing buttons on a tablet or smartphone. Lower risk of errors, high predictability, and ease of implementation are the benefits of this type of control, but these advantages can come at a cost of less natural user experience, long user interface learning time, and manipulation errors. Tablet-controlled exoskeletons highly reduce user autonomy because an external person is in control of their movements. For exoskeleton models that must be used with

crutches, it is almost impossible for the user to use the device on their own because they are unable to operate the tablet at the same time. Voice-control may relief the user's hands from a tablet or smartphone, but there are also disadvantages with this approach. The user may find it awkward to give spoken commands in public and noisy environments can create higher errors of registering the commands [15].

Some researchers have explored the possibility of integrating brain-computer interface (BCI) to control exoskeletons. The most predominant BCI method is electroencephalography (EEG), which picks up brain electrical signals from the head's superficial layer. The idea is that the brain's electrical signal patterns can be utilized as a method of sending specific commands to the exoskeleton. Although BCI enables user autonomy and is safe to use, it has several disadvantages. EEG signals are around 100 μV, which are around ten times less than muscle signals (electromyography, "EMG"). This means any minor muscle twitches near the scalp would be detected instead, thereby making EEG signals noisy. Users must limit any muscle movement when sending commands to the exoskeleton via BCI, so the tremendous amount of concentration required from the user can easily cause fatigue. From a researcher's point of view, BCI is time-consuming because electrode placement is a lengthy process, they need to train both the users and algorithms, and only a few event classifications can be created [15]. That said, BCI-controlled exoskeletons may offer user autonomy to individuals with complete spinal cord injury, since it allows them to control their movements with their mind.

Movement recognition utilizes the wearer's movements or intention to move to trigger exoskeleton events. IMU data and joint sensors coupled with machine learning algorithms are one of the most common approaches of this method of device control. Other exoskeletons also utilize EMG signals in the lower limbs and ground reaction forces (GRF) to detect user movement intention. For instance, Cyberdyne's HAL exoskeleton incorporates EMG for movement detection [82, 36, 79]. Compared to manual user input and BCI, movement recognition is more advantageous because it does not draw much nor strain the user's cognitive load while preserving user autonomy. However, movement recognition is only suitable for individuals that have residual function in their lower limbs. Such users include people with incomplete spinal cord injury, mobility impairments associated with old age, or mobility impairments associated with neurological disorders (e.g. stroke or multiple sclerosis).

Gait phases can be estimated based on user's joint angles using machine learning. Implemented on the Indego exoskeleton, Shushtari et al. developed a real-time gait phase estimator involving a time-delay neural network that takes hip and knee joint angles as input, which has demonstrated robustness against sudden changes in stride length, gait speed, stops or starts of walking [75]. Real-time gait phase estimation is only applicable for

11

exoskeleton users with residual lower limb function, including and not limited to the types of users mentioned above.

2.2.2 Trajectory Generation

Predefined trajectories mean that the joint angles are set and cannot be varied in stride length, gait speed, or gait pattern in real-time. Common methods for this type of trajectory generation in exoskeletons include and are not limited to polynomial minimum jerk trajectory, fuzzy logic control (FLC), and optimal control. To obtain appropriate joint angles throughout a gait cycle, these trajectory generation methods may be combined with motion capture analysis on recordings of healthy human walking data as done in WPAL [45], TWIN [84], Vanderbilt Powered Orthosis [26], and ALEX-I [12].

Polynomial minimum jerk trajectory is the process of determining a polynomial function that minimizes acceleration changes to yield a smooth motion trajectory. WPAL uses a fifth-order polynomial and constraints to determine the exoskeleton's movements [45]. TWIN uses a sixth-order polynomial as a basis function to normalize the initial and final state positions in amplitude and over time [84].

FLC is a nonlinear controller that yields a crisp output value while recognizing that there is a smooth transition between classification groups (also known as "membership" and "non-membership") [78]. It is described to resemble human thinking since it incorporates linguistic or qualitative information in its algorithm [54]. To yield a crisp output value from a crisp input value, the input is fed into a multi-staged process with decision-based rules to characterize its value (fuzzification, inference, and defuzzification) and ultimately yield a crisp output. In 2009, ALEX-I used FLC to determine the appropriate roll and pitch ankle angles to bring the zero-moment point (ZMP) within the convex hull of the supporting area for stability when walking [12]. In 2010, Aphiratsakun, Chairungsarpsook, and Parnichkun generated walking trajectories for ALEX-I by tracking the its center of gravity (CoG) position on MATLAB Simulinks/SimMechanics, and only retained gait trajectories where the ZMP falls within the convex hull.

Optimal control is a technique that determines the control and state trajectories over a period of time, such that the objective functions involving such controls and/or states are minimized. The concepts of optimal control are further described in Chapter 6. For example, Hu and Mombaur generated the motion needed for the HeiCub humanoid robot to recover from perturbation [38]. Optimal control can also be used in the context of state tracking, which requires reference data that is often motion capture recordings from human

data. An example of state tracking optimal control is Koch and Mombaur determining the required exoskeleton kinematics and torques for ground-level and sloped walking [48].

One major drawback of implementing predefined gait trajectory is the lack of adjustment to the desired pace and patterns when walking. Some of the aforementioned trajectory generation methods can be combined with other techniques, such that trajectories can be made online to accommodate for sudden changes in the environment or exoskeleton behaviour. For example, the ATALANTE uses the Guided Trajectory Learning for gait generation. This novel algorithm first generates walking trajectories using optimization based on the direct collocation framework, then uses these solutions to train a function approximation to output a trajectory that achieves a specified task [24]. There also exists a novel method developed by Shushtari et al. that is able to adapt a walking reference trajectory in real-time [76]. Their formulation has an adaptation term that relates the initial and subsequent reference trajectories, which contains a vector of coefficients generated such that a cost function is minimized. The role of their cost function is to 1) minimize the interaction force between human and exoskeleton, and 2) minimize deviation from the initial trajectory. After testing their proposed adaptation method via simulation and against experimental data, the results on gait stability and spatiotemporal parameters show potential to be implemented in lower-limb exoskeletons. Details can be found in [76].

2.2.3 Control Approaches

Position control is a method that attempts to track a predefined reference trajectory as closely as possible. Note that the term "reference trajectory" mentioned in this subsection refers to trajectory that can be prerecorded healthy human motion capture data or generated via methods mentioned previously in the Trajectory Generation subsection. IIT implemented this controller in the TWIN exoskeleton to perform active sit-to-stand and walking motions (Manual and Automatic walk modes) [84].

Impedance control, also known as "assist-as-needed" (AAN), is a method where the exoskeleton's motors are engaged to guide the user's limbs to a reference trajectory [15]. With the user initiating the movements, it is believed that this type of controller can encourage mobility learning and recovery. Another advantage of impedance controllers is preserving human autonomy, since the motors are engaged only when the actual behaviour deviates too much from a reference. These trajectories can be time-dependent, meaning the user's timing is also governed. For example, Sylos-Labini et al. analyzed the EMG patterns during exoskeleton-assisted walking, in which the device's guidance is based on a time-dependent impedance controller [80]. Unluhisarcikli et al. implemented an algorithm

on top of their exoskeleton's impedance controller to prevent the human from walking out of phase from the exoskeleton [83].

There are also impedance controllers that do not impose the fixed timing of the reference trajectory. Duschau-Wicke et al. developed the path control algorithm to allow users to freely influence the timing of their movement while being guided around the desired spatial path [25]. Martinez et al. developed a time-invariant torque-field controller that guides leg swing movement during walking [59]. Forming a path that relates the hip and knee joint angles throughout a gait cycle, they calculated the smallest Euclidean distance and normal unit vector between each point outside the path and the corresponding points on the path, and used these values to formulate the torque vector responsible for guiding the action [59]. After discovering balance disturbance issues caused by the corrective torque's homogeneous behaviour, they proposed a flow controller that only provides path guidance based on velocity error and details can be found in [58].

The Virtual Energy Regulator (VER) is another type of AAN controller developed by Nasiri et al. [65]. It is time-independent and does not impose a reference trajectory either. Instead, it controls the system's mechanical energy. The idea is to regulate the system's virtual energy within a constrained unit-circle that describes the state-space of each joint, so VER allows the exoskeleton user to start the motion at any time point throughout the gait cycle. Details can be found in [65].

The exoskeletons on the market offer different features and functionalities to address specific populations, though so far none has been made specifically for the geriatric population. A paper evaluated which exoskeletons might be suitable for elderly walking assistance, and concluded that a lot of work still has to be done for these exoskeletons to be appropriate for the elderly [47]. Although user manuals are provided with the devices, neither of them have a solid protocol in place to help familiarize users how to move with one.

Chapter 3

Protocol for Improving Exoskeleton Familiarity

In 2020, the TWIN exoskeleton (made by IIT) was purchased. Along with the device, instructions on device operation and software installation were provided, but there was no documentation on how one would move with the exoskeleton. We requested for instructions on moving with it, and only three techniques were provided. This chapter first begins with describing studies done on exoskeleton usage, acceptance, and diversity. It then documents a pre-test conducted with two graduate students on their first time moving with the exoskeleton, and proceeds into a novel tutorial developed and a preliminary study conducted. Results, discussion, and future works are covered in this chapter.

3.1 Studies on Exoskeleton Usage, Acceptance, and Diversity

A study was conducted to investigate the diversity in exoskeleton design [19]. Involving three subjects, the results showed that the adjustable exoskeleton was not designed to fit a woman's body and the woman subject (aged 18-35) experienced higher energy expenditure throughout the experiment than a 71-year-old man subject. In addition to gender differences, another subject who was a wheelchair user stated his lack of confidence in performing daily-life activities while wearing the device, since the exoskeleton did not feel comfortable nor safe. The authors concluded that making exoskeletons adjustable to physically fit users alone is insufficient in improving the safety of these devices.

Research has also been done on exoskeleton usage and acceptance in older adults. In one study, participants with SCI were trained to use an exoskeleton for 12 weeks [56]. Each person shared their experiences and expectations in the form of an interview, and one participant stated that adjusting to the exoskeleton's movements required physical and mental effort.

In another study, a group of older adults with reduced motion were interviewed to acquire their acceptance on lower-limb exoskeletons [22]. While some thought the device would enhance user autonomy, some were afraid it would remove it instead. Meanwhile, the participants believed that it requires an ample learning process to use an exoskeleton.

An interview on exoskeleton technology perception was conducted with seven older adults and six clinicians [44]. Five older adults utilize a cane, rollator, mobility scooter, or even wheelchair for mobility. Although the older adults did not express an immediate usage for an exoskeleton, they stated that if the need arises, older adults would be willing to use it for daily living activities such as walking, prolonged standing, stair climbing, and lifting.

Another study also explored elderly acceptance and perception in robotic assistive devices and concluded that the technologies for geriatric users must be easy and comfortable to use [74]. Older adults are conscious about their competencies and they maintain it to avoid being alienated from society. Not meeting their needs may cause them to be frustrated embarrassed, and even abandon the device [74].

To summarize, older adults would be willing to use lower-limb exoskeletons if they really need to. They think that the learning process should be encouraging and easy to follow, and the device should be easy and comfortable to use.

3.2   Pre-Test with Two Graduate Students

The TWIN exoskeleton is used for this pre-test. IIT provided three techniques on how one can move with the device:

1. Draw a circle on the ground with the bottom end of the crutches to bring them back as far as possible to push up for sit-to-stand (see Figure 3.1)

2. Bring weight of upper torso forward so that the center of mass (CoM) lands between the feet (or close to that).

3. Shift weight to the stationary leg when taking each walking step.

Figure 3.1: Crutch positioning per IIT's instructions.

The author of this thesis is the first graduate student to wear TWIN and they had no prior experience in moving with one. They reviewed all the user manuals, documentations provided, and even the three techniques described above. Meanwhile, the user manuals and documentations did not include any instructions on how to move with the exoskeleton. When performing the sit-to-stand motion, they could not stand up at all because the 3-kg battery pack on the back of the trunk made it difficult to bring the weight of the upper torso forward. When walking, they were startled because they had no idea how the exoskeleton would move their legs and the motion was jerkier than they had expected.

A second graduate student with no exoskeleton usage experience prior to this session was invited. He struggled to perform sit-to-stand and required external help to stand up. Although he was not as startled by the motor's predefined movements, he stated that the motions were sudden, it was challenging to move with the exoskeleton while maintaining balance, and the overall experience was uncomfortable. He even experienced lower back pain the day after wearing the device.

Based on these observations and qualitative feedback, it is assumed that the initial exoskeleton usage session with older adults and patients would be even worse. This calls for a need to better prepare users for their first time moving with an exoskeleton. The proposed protocol outlined in the following section is tested with young-to-middle-aged healthy adults that do not require walking assistance. This is because COVID-19 restrictions did not allow study participants external to the lab.

3.3 Methods

3.3.1 Proposed Protocol

COVID-19 restrictions limited the population size to be small and only allowed lab members to participate. Ten volunteers who had never worn an exoskeleton prior to the preliminary study were originally invited, but the exoskeleton experienced hardware malfunction at the start of the tenth experiment, so this session was excluded and the device had to be sent back to the manufacturer for repairs. Therefore, nine healthy, able-bodied adult lab members took part in this preliminary study and were randomly divided to receive the tutorial (T) or no tutorial (NT). The average age, height, and mass were 28 ± 11 years old (note: age range is 18 to 55), 1.70 ± 0.08 m, and 66.3 ± 9.1 kg respectively. Four men and one woman did not receive the tutorial, and this group of volunteers would be referred to as NT throughout this thesis for simplicity. Two men and two women received the tutorial, and this group of volunteers would be referred to as T. They received instructions in the form of video clips and live demos, and had the opportunity to practice each exercise during the tutorial at their own pace. The crutches exercises do not involve the exoskeleton, but the device demonstration and "air walking" experience (explained later) involve the exoskeleton. This preliminary study received ethics clearance (REB43135).

The exoskeleton used is TWIN, and the specifications can be found in the "Existing Hardware and Target Application" section in Chapter 2. The device has two modes for partial assistance (human leads the motion) and two modes for imposing a predefined gait trajectory (exoskeleton leads the motion). In this preliminary study, only the latter two modes – Manual Walk Mode (MWM) and Automatic Walk Mode (AWM) – are considered since the purpose is to improve the wearer's familiarity with the exoskeleton's predefined gait patterns. MWM consists of manually triggering each walking step via the TWIN tablet, meaning the exoskeleton wearer would have to indicate their walking intent to the person controlling the tablet. In AWM, the exoskeleton wearer can trigger each walking step with their forward incline without the need to externally express their walking intent, and the forward incline is calculated with an inertial measurement unit (IMU) located on the back of the trunk. The times for walking, stand-up, and sit-down are 2 s, 4 s, and 4 respectively, and they are the default settings from IIT. The ceiling lift used is the Guldmann GH3 Ceiling Hoist and it can support a total of 400 lbs.

The proposed protocol shown below contains four parts: Preparation, Tutorial, Exo Session, and Ending. NT and T underwent Preparation, Exo Session, and Ending, but only T experienced the Tutorial.

1. Preparation

   (a) Invite member to complete a pre-study survey.

   (b) Adjust the forearm crutches appropriate to the member.

   (c) Obtain member's stature, mass, lower limb segment lengths, and lower limb segment masses.

   (d) Create a new profile of the member on the TWIN tablet with anonymous naming.

2. Tutorial

   (a) Perform crutches exercises without exoskeleton.

      i. Bring crutches backwards while sitting.
      ii. Perform sit-to-stand and stand-to-sit with crutches.
      iii. Walk around with crutches.
      iv. Repeat iii but shift weight to stationary leg for each step.
      v. Practice turning by pivoting.

   (b) Demonstrate TWIN's sit-to-stand, stand-to-sit, and walking motions with member wearing it.

   (c) Don TWIN on member and attach TWIN to ceiling lift via straps.

   (d) Lift member slightly off the ground with the ceiling lift.

   (e) Activate walking motion to familiarize member with TWIN's gait pattern without the risk of falling.

3. Exo Session

   (a) Perform sit-to-stand and stand-to-sit wearing TWIN.

   (b) Walk in TWIN while being supported by a lift (Guldmann GH3 Ceiling Hoist).

      i. Manual walk mode for 7 m.
      ii. Automatic walk mode for 7 m.

   (c) Walk in TWIN while being supported by a person.

      i. Manual walk mode for 7 m.
      ii. Automatic walk mode for 7 m.

4. Ending

(a) Doff TWIN from member.

(b) Member completes post-study survey, SUS, and RTLX.

The overall approach of this tutorial is to start off with something simple and gradually increase the content's complexity. Each crutches exercise is designed to build nicely into the next one, and each step of the Tutorial session acts as a foundation for the subsequent steps. The volunteers are encouraged to practice until they are comfortable to move on to the next step of the tutorial. Note that the tutorial described above is not designed specifically for older adults. The idea is to implement the suggestions received at an interdisciplinary exchange in the next stage, recruit older adults, and modify the tutorial based on their feedback. Details will be covered in the Future Improvements and Conclusions sections.

In the series of crutches exercises, the first part is to only bring the crutches backwards while sitting. T is taught to perform this by pretending to draw a circle on the ground with the bottom end of the crutches. This is one of the three techniques provided by IIT in terms of how to move with the exoskeleton.

The second technique provided is how to perform sit-to-stand. IIT said to shift weight of upper torso forward so that the center of mass (CoM) lands between the feet (or close to that), and the crutches must be set behind at an angle. Performing stand-to-sit would simply be a reverse of the sit-to-stand process, where the user would set the crutches at an angle first, then sit down. T is taught to perform sit-to-stand and stand-to-sit with these techniques, shown in Figure 3.2.

Figure 3.2: Crutches sequence for sit-to-stand.

The sequence for walking with crutches is inspired by a YouTube video showcasing the TWIN at an event [8]. Before taking the first step, both crutches are placed at one step

length away. After taking the first step, the crutch on the opposite side of the upcoming swinging leg is placed at one step length away. Figure 3.3 visualizes the crutch-walking sequence.
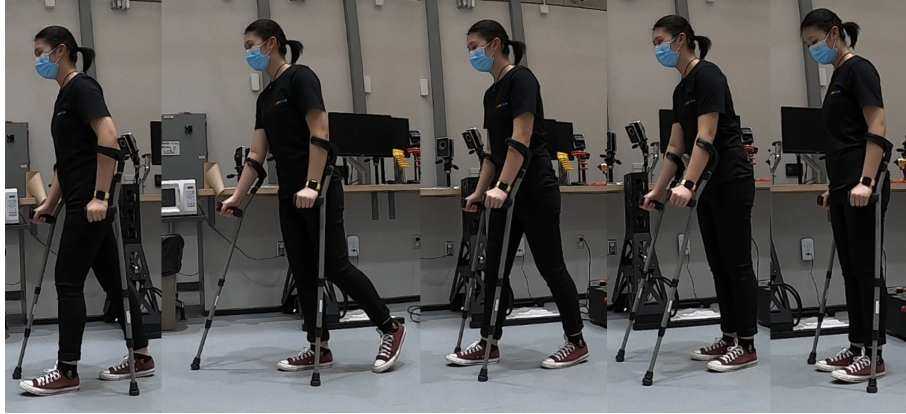
Figure 3.3: Crutches sequence for walking.

The fourth crutches exercise, which is to walk around with crutches but shift weight to stationary leg for each step, is the third and last technique provided by IIT. In this exercise, the volunteers are asked to repeat walking with the crutches sequence from the previous exercise, but this time, shift weight to the stationary leg when taking a step. TWIN does not have motors that can support any turning motion, but IIT said it is possible for the user to turn by pivoting, yet they did not provide exact techniques to perform this movement. Therefore, the following sequence is developed for the turning method, which is also visualized in Figure 3.4:

- To turn left, first place the left crutch to the left of the left foot and the right crutch in front of the right foot.

- Shift the weight to the left heel, so that the heel becomes the pivot point for the turning motion.

- Twist the body to the left with the aid of pushing both crutches to the right without causing injuries.
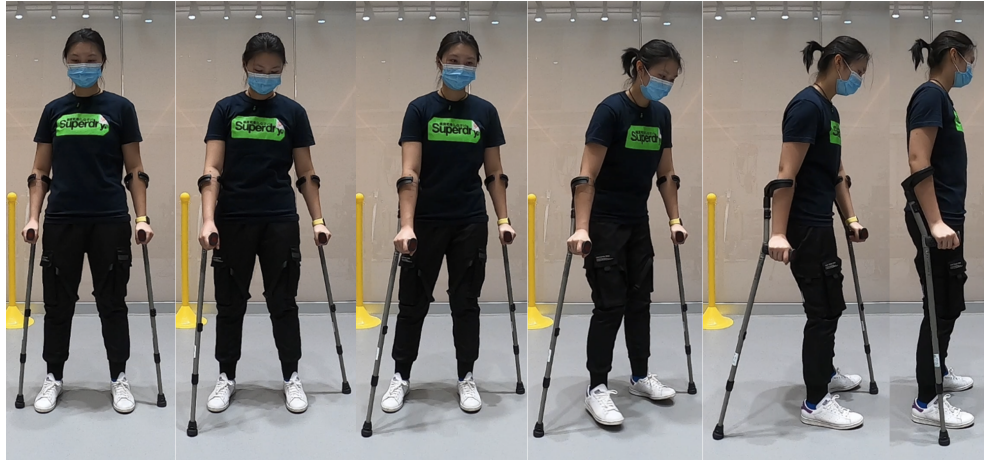
Figure 3.4: Crutches sequence for turning.

The purpose of demonstrating the TWIN's motions with no one wearing it is to give the users an idea on how the movements look like, and the purpose of the air-walking sequence is to let the users feel how the motors move their legs. By having the person-less demonstration first, it is believed that the users can have a sense of how the movement looks like, and particularly the range of motion in the joints. Since the two graduate students from the pre-test had no clue how the motors would interact with their legs, it is thought that the air-walking experience could minimize the "fear of the unknown" while not having to worry about falling over when the motors are in action. Similar to the crutches exercises, the volunteers are allowed to go through these steps at their own pace.

The volunteers are asked to perform four walking trials – twice supported by a ceiling lift and twice supported by a person. The purpose of running trials with ceiling and human support is to see if users have a preference on one safety support type over the other. The walking distance for each trial is set to 7 m because that is the space available in the lab. To avoid fatigue, all nine users only experience one walk mode per safety support type. The order of the walking sequence is not randomized because doing so on a small sample size would make the data harder to interpret. Meanwhile, the purpose of asking each person to fill out a pre-study and post-study survey is to note any changes in subjective opinions after the exoskeleton experience.

3.3.2 Qualitative Analysis

Qualitative data are collected with the System Usability Scale (SUS), NASA Raw Task Load Index (RTLX), and a set of two custom surveys. They are used for measuring device usability, user's perceived cognitive workload, and user's comfort level respectively. Collecting data on these aspects can provide more information on each person's experience, and the decision to use SUS and RTLX is inspired by a study on evaluating the wearability of a wrist exoskeleton [49]. SUS is a survey containing ten questions with Likert scales as response options and it is an established tool for evaluating device usability [14]. The survey results yield a score from 0 to 100 that should not be interpreted as percentages [18]. The purpose of utilizing SUS in this preliminary study is not to evaluate TWIN's usability. It is instead used for measuring whether the protocol has any influence on the usability of the device. The procedure for calculating the SUS score is outlined below [52].

1. Convert Likert scale options to values from 0 to 4.

   (a) "Strong Agree" = 4

   (b) "Agree" = 3

   (c) "Neutral" = 2

   (d) "Disagree" = 1

   (e) "Strongly Disagree" = 0

2. Add scores from all odd-numbered questions and subtract 5 from the sum.

3. Add scores from all even-numbered questions and subtract sum from 25.

4. Add adjusted scores from steps 2 and 3, then multiply by 2.5 to obtain the SUS score for one participant.

5. Repeat steps 1 to 4 for the remaining participants.

6. Calculate the mean SUS score per group by taking the average of the values in the corresponding group.

RTLX is utilized for evaluating each person's perceived cognitive workload when performing five tasks: sit-to-stand, stand-to-sit, turning, MWM, and AWM. The six aspects of perceived cognitive workload gathered per task are mental demand, physical demand,

23

temporal demand, performance, effort, and frustration [34]. Users would rank their perceived cognitive workload for each aspect on a scale containing 20 equal intervals and each task would result in a score ranging from 0 to 100. A higher score stands for poorer perceived cognitive workload, meaning the person finds the task to be more demanding, they found themselves less successful in accomplishing what they were asked to do, they had to exert higher levels of effort to accomplish their level of performance, and/or they experienced higher levels of frustration. RTLX applies equal weights for all aspects, though there exists a full version incorporating different weights for each aspect [34]. For simplicity, this preliminary study uses equal weights. Below is the procedure for calculating the RTLX score [33].

1. Count the number of lines from left to right (1 to 21) marked by the participant.

2. Subtract 1 from the marked line and multiply by 5.

3. Repeat steps 1 and 2 for the other five aspects.

4. Repeat step 3 for all tasks evaluated and the remaining participants.

5. Calculate the mean score for each aspect per group by taking the average of all the scores in the corresponding aspect per group.

6. Calculate the average workload score by averaging the mean scores from the six aspects per group.

The two custom surveys are completed before and after the exoskeleton usage to capture the user's comfort level. The statements in the two surveys are phrased as similarly as possible to avoid triggering a change in emotion that would otherwise influence the user's response. The survey statements between NT and T are slightly different, since T's included statements about the tutorial received (see Appendix A for details). Users would respond to each statement using a Likert scale, and the results are treated as subjective opinions since Likert scales can be problematic when applying statistical analyses [68].

The SUS and RTLX scores between the groups NT and T are compared. The custom survey results are compared between the two groups and also within each person. Outliers in small datasets can skew the overall representation. Given the small sample size due to COVID-19 restrictions, statistical analysis is not performed in this preliminary study, thus statements on significance in the scores are not made.

3.4 Results

3.4.1 General Observations

Majority of the NT and T users were unsuccessful in performing sit-to-stand with the crutches especially in their first try. Meanwhile, NT and T users' stand-to-sit performance seemed relatively smoother than their sit-to-stand. In general, T managed to turn easier with the TWIN than NT. It seems that most users initially had difficulty walking, but they eventually were able to adapt to TWIN's movements throughout the session at their own pace. Most, if not all users, found it challenging to trigger the AWM steps. The IMU is located on the back of the trunk and the trunk tilt angle must reach 9.7 degrees forward to trigger a step in this walk mode. These users naturally tilted their torso forward to trigger the steps. Despite having a proper fit between the person's trunk and the exoskeleton's trunk brace, tilting the torso alone does not tilt the trunk module, therefore the AWM steps could not be initiated. The volunteers must tilt forward by the ankles to activate the steps, but the movement is described as unnatural because the natural instinct to initiate a step is to tilt the torso forward.

Some user-specific observations are also made. One NT members' performance illustrated a few safety concerns related to walking posture and crutch hold. While walking, his back was severely hunched forward (see Figure 3.5) and he had unstable gait caused by large lateral deviations, though he did not fall because he was strongly supported by either the ceiling lift or a person (see Figure 3.6). When holding the crutches during walking, his arms were rotated internally, and this configuration caused the exoskeleton frame and crutch handle to nearly pinch his index finger twice.

Figure 3.5: A NT member walking with large lateral deviations.

Figure 3.6: A NT member walking with a severely hunched back.

On the contrary, one NT member naturally outperformed all NT and T users. He only had a minor struggle with balancing after standing up from sitting, and he was the sole volunteer who performed sit-to-stand without losing balance on the first try.

By the end of the exoskeleton session, one T member's palm was sweating and left sweat stains on the crutch handles (see Figure 3.7).

Figure 3.7: Sweat marks from a T member after the end of the exoskeleton session.

Another T member's hands turned red and even had darkened marks on the superficial layer of the thenar eminence (see Figure 3.8). No pain was reported from both volunteers.

Figure 3.8: Red hands and darkened thenar eminence from another T member after the end of the exoskeleton session.

3.4.2 SUS Score

As mentioned earlier, it is not possible to perform statistical analysis on a small sample size. Therefore, SUS score comparisons are only done in a form of percentage difference.

Tutorial vs No Tutorial

NT has mean and median usability scores of 34.5 and 35 respectively, with a standard deviation (SD) and interquartile range (IQR) of 13.3 and 18.1 respectively. T has a mean usability score of 45, median usability score of 47.5, SD of 10.8, and IQR of 15. Figure 3.9 shows the spread of the scores in both groups and Table 3.1 summarizes the values. The bottom and top lines of each box represent the first and third quartiles, and the red line represents the median. The top and bottom error bars in each boxplot extend to maximum and minimum values that are within one standard error.
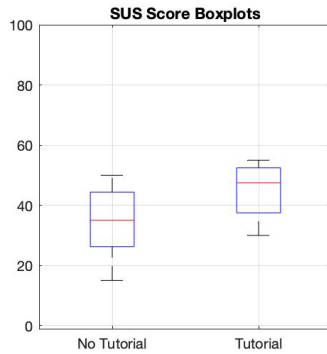
Figure 3.9: SUS scores of users receiving tutorial and those who did not.

Table 3.1: Mean, median, standard deviation, and interquartile range of SUS scores in NT and T.

	NT	T
Mean SUS score	34.5	45
Median SUS score	35	47.5
Standard deviation	13.3	10.8
Interquartile range	18.1	15

Female vs Male

According to a EUROBENCH report on identifying areas of improvement on regulating lower-limb exoskeletons, the authors identified that ISO 13482:2014 lacks specific requirements for different categories of people, including individuals of different sexes [29]. With the field of mechanical and robotics being historically male-dominated, they stated that the development of new technology may reflect these biases. In this thesis, we recognize that the small sample size of this preliminary study cannot yield any conclusion on sex differences. With the tutorial acting as a tool designed for using lower limb exoskeleton, it has some relation to these devices, so we believe it would be thorough to compare results between male and female participants. It is hypothesized that there would be no difference in usability scores between male and female participants. Note that the hypothesis does not contain any wordings related to significance because no statistical analysis can be drawn from a sample size of nine individuals. Mean SUS scores between male and female are compared and the values grouped by sex can be viewed in Table 3.8.

With a higher mean SUS score by 63.3%, it seems that the female volunteer in the NT group find TWIN to be more usable than the male volunteers in the same group (50 vs 30.6). Meanwhile, with a lower mean SUS score by 28.6%, the female volunteers in the T group appear to find TWIN to be less usable than the male T volunteers (37.5 vs 52.5). Comparing the scores within the same sex, the female T users seem to have a 25% lower score than the female NT user, whereas the male T users appear to have a 71.4% higher score than male NT users.

Table 3.2: Average SUS scores in female and male volunteers in T and NT groups.

Group	Female	Male
No Tutorial	50	30.6
Tutorial	37.5	52.5

3.4.3 RTLX Score

Similar to what is done for SUS scores, percentage difference in RTLX scores are calculated and compared since statistical analysis cannot be applied on a small sample size.

Tutorial vs No Tutorial

All volunteers filled out five RTLX questionnaires, one for each task. Unlike SUS, the RTLX does not have a threshold to categorize a demand as "too high", so only a relative comparison between conditions and/or within subjects can be made [34].

In the sit-to-stand task, T's average workload score is 22.7% less than NT's. Breaking down the average score, T found sit-to-stand to be less demanding in the mental, physical, and temporal aspects. They also experienced less frustration and did not have to work as hard to perform the motion. Table 3.3 summarizes the average score for NT and T across the six aspects.

Table 3.3: Mean RTLX scores for sit-to-stand task of users receiving tutorial and those who did not.

Sit-to-stand	NT	T
Mental Demand	36	31.25
Physical Demand	66	45
Temporal Demand	35	27.5
Performance	35.5	41.25
Effort	58.5	33.75
Frustration	32.5	25
Average Workload Score	43.92	33.96

In the stand-to-sit task, T's average workload score is 54.3% higher than NT's. Although T found the task to be less demanding in a temporal sense, they found it to be mentally and physically more demanding, exerted more effort, and were more frustrated with stand-to-sit. A summary of the scores is shown in Table 3.4.

Table 3.4: Mean RTLX scores for stand-to-sit task of users receiving tutorial and those who did not.

Stand-to-sit	NT	T
Mental Demand	20	52.5
Physical Demand	25	50
Temporal Demand	40	32.5
Performance	24.5	35
Effort	22.5	40
Frustration	26	33.75
Average Workload Score	26.33	40.63

In the turning task, T's average workload score is 18.6% higher than NT's. T found the task to be physically less demanding and required less effort, but this came at a cost of higher mental demand, temporal demand, and frustration. The breakdown of the score for turning is summarized in Table 3.5.

Table 3.5: Mean RTLX scores for turning task of users receiving tutorial and those who did not.

Turning	NT	T
Mental Demand	28.5	51.25
Physical Demand	66	52.5
Temporal Demand	29.5	35
Performance	27	36.25
Effort	67	55
Frustration	17	48.75
Average Workload Score	39.17	46.46

In MWM and AWM tasks, T consistently scored higher than NT across all aspects, with the average workload score for MWM and AWM being 54.8% and 36.5% higher than NT's respectively. T considered both walking tasks to be more rushed, mentally demanding, and physically demanding. They also were more frustrated, had to exert more effort, and found themselves less successful in performing the walking tasks. Details on the scores for MWM and AWM are listed in Tables 3.6 and 3.7.

Table 3.6: Mean RTLX scores for MWM task of users receiving tutorial and those who did not.

MWM	NT	T
Mental Demand	35	71.25
Physical Demand	56.5	77.5
Temporal Demand	25.5	51.25
Performance	38.5	58.75
Effort	69	77.5
Frustration	35.5	66.25
Average Workload Score	43.33	67.08

Table 3.7: Mean RTLX scores for the five tasks of users receiving tutorial and those who did not.

AWM	NT	T
Mental Demand	46.5	67.5
Physical Demand	58.5	65
Temporal Demand	33	47.5
Performance	34.5	50
Effort	59	76.25
Frustration	34	56.25
Average Workload Score	44.25	60.42

Another clear trend is found related to performance. T had a higher score than NT across all tasks, indicating that they perceived themselves as less successful in performing the tasks well.

Female vs Male

The EUROBENCH report on lower-limb exoskeletons states that ISO 13482:2014 lacks specific requirements for different categories of people, including individuals of different sexes [29], so the RTLX scores between male and female participants are also made to enable a more thorough analysis. It is hypothesized that there would be no difference in perceived cognitive workloads between male and female participants. The hypothesis does not contain any wordings related to significance because no statistical analysis can be drawn from a sample size of nine individuals. The RTLX scores separated by sex can be viewed in Table 3.8.

In the NT group, the female volunteer's RTLX score is lower than the male volunteers' scores across all five tasks. The percentage difference for sit-to-stand is 52.4% lower, stand-to-sit is 70.1% lower, turning is 43.7% lower, MWM is 57.4% lower, and AWM is 74.3% lower. This may mean the female member perceived these tasks to be less difficult.

As for the T group, the female volunteers' RTLX scores in sit-to-stand and stand-to-sit tasks are lower than the male volunteers' (20.9% and 52.3% respectively). This may indicate that the female members found the sit-to-stand and stand-to-sit tasks less difficult than the male members. On the other hand, the female members' scores for turning, MWM, and AWM tasks are higher by 0.901%, 28.4%, and 39.7% respectively, meaning they may have more difficulty in performing these tasks compared to the male members.

Comparing the female members' scores, the T group may perceive all five tasks to be more challenging than the NT group. The former group's scores in sit-to-stand, stand-to-sit, turning, MWM, and AWM are 28.6%, 186%, 93.1%, 262%, and 428% higher respectively.

The RTLX scores for the male volunteers in T are 22.7% and 3.01% lower than those in NT for sit-to-stand and AWM tasks respectively, though the T group scored higher in stand-to-sit, turning, and MWM by 79.6%, 7.77%, and 20% respectively. This may indicate that the male T members perceived sit-to-stand and AWM to be less difficult, but not for stand-to-sit, turning, and MWM.

It is once again emphasized that any score comparisons made between the sexes cannot yield any sound conclusion given the small sample size.

Table 3.8: Average RTLX scores in female and male volunteers in T and NT groups.

	No Tutorial		Tutorial	
Task	Female	Male	Female	Male
Sit-to-stand	23.33	49.06	30	37.92
Stand-to-sit	9.167	30.63	26.25	55.00
Turning	24.17	42.92	46.67	46.25
MWM	20.83	48.96	75.42	58.75
AWM	13.33	51.98	70.42	50.42

3.4.4 Custom Surveys

As mentioned in the Methods section, the phrasing of some statements on the "before" and "after" surveys are kept the same to track the change in user's comfort level with minimal

additional influence. Since a person's decision to choose between "strongly disagree" and "disagree" or "strongly agree" and "agree" are subjective, it is challenging to determine the true change in comfort level when the responses remain on the same side of the spectrum. Therefore, it is decided that "strongly disagree" and "disagree" would be considered as one collective spectrum (referred to as "disagree spectrum"), whereas "strongly agree" and "agree" are considered as another collective spectrum (referred to as "agree spectrum"). This means a change in response is only registered when the responses go from one collective spectrum to neutral or to the other collective spectrum.

Statements 1 to 4 appear on the "before" and "after" surveys for both the NT and T versions, therefore the results from both groups of volunteers are shown together. The remaining statements only appear on the "after" survey, and since they are different between the NT and T versions, the results are shared in two separate sub-subsections for clarity.

Comfort Level Before VS. After Exoskeleton Session

- *Statement 1: "I am excited to wear the Twin Exoskeleton."*

In the group that did not receive the tutorial, two people's response to Statement 1 worsened. Before the exoskeleton session, all five members responded with "strongly agree" or "agree." After the exoskeleton session, three of them remained in the "agree spectrum", whereas the remaining two responded with "neutral." Meanwhile, no response change was observed in the group that received the tutorial; all four T members' responses are in the "agree spectrum."

- *Statement 2: [Before Exo Session] I think I am comfortable with wearing the Twin Exoskeleton.*

- *Statement 2: [After Exo Session] I felt comfortable wearing the Twin Exoskeleton.*

Two NT members' comfort level worsened in Statement 2 – one went from "neutral" to "disagree," and the other went from "agree" to "neutral." One person stayed in the "agree spectrum," and the remaining two remained neutral. Among the T members, only one person had a negative change (from "agree" to "neutral"), whereas the remaining three people still agreed that they were comfortable wearing TWIN after the session.

- *Statement 3: I am nervous to wear the Twin Exoskeleton.*

34

Before the exoskeleton session, one NT member was neutral on their nervousness, but afterwards they were very nervous to wear TWIN. Meanwhile, another NT member started being nervous to wear the device, but was less nervous after the exoskeleton session. One NT user remained neutral and two NT users remained not nervous before and after the session. As for the volunteers who received the tutorial, two T members' level of nervousness increased throughout the session, since their response to this statement went from "disagree" to "agree." One person's response stayed at "neutral," though one person was less nervous after wearing the exoskeleton (from "neutral" to "disagree").

- *Statement 4: I am scared to wear the Twin Exoskeleton.*

Two NT volunteers originally were not scared to wear TWIN, but they were scared after the exoskeleton session. Three NT volunteers, on the other hand, remained not scared throughout the session. As for the T members, there are also two people whose comfort level worsened after the exoskeleton session. One person's response to Statement 4 remained neutral, and one person was less scared after wearing the device.

Table 3.9 shows a brief summary of NT and T's responses that contains the number of improvements, worsening, and unchanged comfort levels for statements 1 to 4.

Table 3.9: Change in comfort level before and after exoskeleton session in all volunteers.

Statement	Improvement	Worsening	No Change
I am excited to wear TWIN.	NT: 0 T: 0	NT: 2 T: 0	NT: 3 (agree) T: 4 (agree)
I felt comfortable wearing TWIN.	NT: 0 T: 0	NT: 2 T: 1	NT: 3 (1 agree, 2 neutral) T: 3 (agree)
I am nervous to wear TWIN.	NT: 1 T: 1	NT: 1 T: 2	NT: 2 (1 neutral, 2 disagree) T: 1 (neutral)
I am scared to wear TWIN.	NT: 0 T: 1	NT: 2 T: 2	NT: 3 (1 strongly disagree, 2 disagree) T: 1 (neutral)

35

Group-specific Responses After Exoskeleton Session

In the NT group, four members believe that receiving a tutorial would better prepare their first time wearing an exoskeleton, and one member disagreed. Three volunteers preferred to be supported by the ceiling lift than a person when wearing the device, though two volunteers were indifferent. One person who agreed to this statement explained that he felt safer with the ceiling lift because he was afraid to injure the person supporting him if he (the user) were to fall, and he assumed that in the event of a fall, he would only be suspended by the lift. While two people think they are comfortable with wearing the TWIN in the future, two people are neutral and one person disagreed. The "after" survey results for NT are summarized in Table 3.10

Table 3.10: Likert scale responses collected after the exoskeleton session from individuals who did not receive the tutorial.

Statements for NT Group	Strongly Agree	Agree	Neutral	Disagree	Strongly Disagree
I think having a tutorial on getting acquainted with the Twin Exoskeleton would better prepare my first time wearing the device.	1	3	0	1	0
I prefer to be supported by the lift than a person when wearing the Twin Exoskeleton. (If you are indifferent, select Neutral.)	2	1	2	0	0
I am comfortable with wearing the Twin Exoskeleton in the future.	1	1	2	1	0

In the T group, all members agreed that the tutorial was easy to follow and it helped prepare them for moving with TWIN. Three volunteers did not think that the tutorial should be improved in the future, whereas one was neutral about this statement. Two users prefer to be supported by the ceiling lift when walking with the device and the other two

users are indifferent. Three people agreed that they are comfortable with wearing TWIN in the future, though one person disagreed. Table 3.11 summarizes these Likert scale findings.

Table 3.11: Likert scale responses collected after the exoskeleton session from individuals who received the tutorial.

Statements for T Group	Strongly Agree	Agree	Neutral	Disagree	Strongly Disagree
The tutorial helped preparing me for the Twin Exoskeleton.	2	2	0	0	0
The tutorial is easy to follow.	2	2	0	0	0
The tutorial should be improved before I wear the Twin Exoskeleton in the future.	0	0	1	3	0
I prefer to be supported by the lift than a person when wearing the Twin Exoskeleton. (If you are indifferent, select Neutral.)	0	2	2	0	0
I am comfortable with wearing the Twin Exoskeleton in the future.	1	2	0	1	0

Ranking Task Difficulty

The volunteers were also asked to rank the five tasks from the easiest to the most difficult to perform. In the NT group, one person said MWM is the easiest, one said sit-to-stand is the easiest, one said stand-to-sit is the easiest, and two said AWM is the easiest. One of the two volunteers who put AWM as the easiest task said that it took him some time to realize that one's center of mass had a lot of impact on each of the walking motions, and that "in this walk mode, [he] was automatically braced for the movement." As for the most difficult task to perform, two members put turning, one put sit-to-stand, one put AWM, and another put MWM.

The results for ranking tasks based on level of difficulty are different in T compared to NT. Three users stated that stand-to-sit is the easiest and one user stated sit-to-stand is the easiest. As for the most difficult task, two put sit-to-stand and two put MWM. One of the users made the following additional comments:

- I could benefit from additional try-on / practice sessions. I will be more comfortable wearing the Twin exoskeleton if I were able to practice with the harness and the researcher/technician in the room.

- I preferred AWM since I felt more in control (rather than the manual where the person with the control has the power to choose my motions).

- Additional tutorial showing what not to do (wrong motion vs the proper motion) when wearing the exoskeleton and also showing the moves that it can trigger when used wrongly (twisting, slipping foot backward) can help set the first time wearer's expectations.

3.5 Discussion

The preliminary study involving the novel protocol has yielded interesting findings. As mentioned earlier, one must carefully handle results from small sample sizes, since the influence of outliers can skew the overall behaviour.

3.5.1 General Observations

It seems that T managed to turn easier with the TWIN than NT because the tutorial taught them how to turn with crutches via pivoting. The T member who left sweat marks on the crutch handles indicated that despite receiving the tutorial, she was nervous and had to exert a lot of effort when moving in the exoskeleton. This observation is supported by the fact that her effort scores for MWM and AWM tasks are 100 and 90 respectively, which are the highest effort scores in these two tasks among all nine users. As for the T member whose hands turned red, he reported that the darkened marks on the thenar eminence was a result from holding onto the crutches tightly. Meanwhile, his SUS score, RTLX scores per task, and responses on the two custom surveys did not provide hints on what could possibly be causing him to hold the crutches tightly.

3.5.2 SUS Score

Recall that the purpose of analyzing SUS scores is not to evaluate TWIN's usability, but rather to note how receiving the tutorial would influence its usability. With T having a higher average score by 30.4%, the tutorial seems to have some improvement towards the exoskeleton's usability after one session. The average scores fall within the "poor usability" spectrum [14], but this should not be taken as a surprise. The volunteers recruited for this preliminary study are healthy, able-bodied adults that do not need external support for walking, sitting, and standing. Moreover, it usually takes multiple training sessions before an individual can properly walk with an exoskeleton. Since this is the first time the lab members have ever worn such a device and they only had one session, the lower scores are expected.

It is hypothesized that there is no difference in usability scores between male and female participants. The novel protocol may seem to have a positive influence on the usability of the exoskeleton in the male population (note the 71.4% increase in the score), and it may also appear to have caused the female population to find the exoskeleton less usable (note the 25% decrease in the score). However, one must take these findings with a grain of salt because of the small sample size and gender imbalance between conditions (1 female participant in NT vs 3 female participants in T). Coupled with the possibility of having outliers in the data set, no conclusions can be made based on the comparison of mean SUS scores. It is recommended to increase the sample size and have similar population of male and female participants in NT and T groups for a fairer analysis.

3.5.3 RTLX Score

The first clear trend is T scoring higher in all RTLX aspects of the two walking tasks (MWM and AWM). The higher temporal demand can stem from the different walking pace in the tutorial and during the experiment. For instance, T walked at their own pace without TWIN in the tutorial, but the device's predefined gait trajectory moved their legs at a faster pace, therefore making them feel more rushed. The constant need to recall the techniques learned from the tutorial is responsible for the higher mental demand score. With the T members receiving the tutorial immediately before performing the walking trials in TWIN in one session, the longer testing duration explains the higher physical demand score. It is possible that with the higher mental, physical, and temporal demands, T ought to work harder to accomplish their level of performance while being more frustrated. The higher average workload score in MWM (compared to AWM) across all volunteers could be influenced by the task sequence. With MWM happening before AWM, the members

already had a better idea of what to do and how to walk with TWIN. With too few people to modulate conditions, randomizing task orders with a small population can make the data harder to interpret.

Another clear trend is T perceiving themselves as less successful in accomplishing what they were asked to do in all five tasks. This could be an unintentional effect of the tutorial, because T may think that they are expected to perform as well as the demonstrations and should be struggling less when moving. Although it is difficult to move perfectly with an exoskeleton in the first session, they may not realize that and therefore think they did not perform as well.

Comparing the scores between the sexes, the female volunteer in the NT group may seem to have outperformed both the average male volunteers in the NT group and the average female volunteers in the T group. This was based on her lower scores across all tasks. The female members in the T group may find sit-to-stand and stand-to-sit tasks to be easier than the male members in both NT and T groups, but may also find the turning and walking (MWM and AWM) tasks to be more challenging than the NT and T male members. Due to the small sample size, gender imbalance between conditions, and the possibility of having outliers in the data set, no conclusions can be made when comparing the perceived cognitive workloads between male and female participants. It is therefore recommended to increase the sample size and have similar number of male and female participants in each condition for a fairer analysis.

The sit-to-stand results may deem the tutorial as helpful for this task, but the stand-to-sit temporal scores suggest that tutorial is only helpful with the pacing. The true reasons are unknown because the volunteers did not comment anything on this regard, and no conclusions could be drawn from in-person observations. The turning technique can be considered helpful based on the scores, though the phenomena observed cannot be fully explained.

3.5.4 Custom Surveys

Only one person who did not receive the tutorial disagreed that having a tutorial would better prepare his first time wearing the exoskeleton, though he also naturally performed well when completing various tasks with TWIN. People have different levels of adaptation when interacting with an exoskeleton for the first time, suggesting that some may reach proficiency sooner than others. Meanwhile, the subjective opinions from T members strongly indicated that the proposed tutorial was useful.

The two NT members whose response for Statement 1 ("I am excited to wear TWIN") from the "agree spectrum" to "neutral" are the same two members who felt less comfortable wearing the device after the exoskeleton (Statement 2). With one of them being the NT user who almost had his finger pinched twice between the exoskeleton and crutch handle, although his response remained not nervous wearing TWIN, he is one of the two people who went from not scared to being scared after wearing it. One T member thought she would be comfortable wearing the exoskeleton (Statement 2), yet ended up being neutral about the statement. She is also the same person who made the additional comments listed in the "Ranking Task Difficulty" subsection of the Results section. Based on her comments, it is possible that the safety aspect of using the device, additional practice of moving with the exoskeleton, and having control over walking steps have an influence on her comfort level with TWIN.

In terms of ranking the five tasks based on performance difficulty, the protocol was relatively effective in teaching users stand-to-sit and how to turn with the exoskeleton. This is because three T volunteers and one NT volunteer said it was the easiest task. As for turning, two NT members said it was the most difficult task and no T members said it was difficult. Although one NT user put MWM as the easiest task, this is the same person who walked with an unstable gait (large lateral deviations) and a severely hunched back. This indicates that a person's perception of an easy task may not truly reflect their capability of executing the same task. It is interesting to note that two NT volunteers and no T volunteers found AWM to be the easiest task to perform. A possible reason for this phenomenon is that the users have more control on deciding when to take the next step. One of the two NT volunteers stated that he was "automatically braced for the movement," therefore he found it to be easier than MWM. Both groups agreed that sit-to-stand and MWM are the most difficult tasks to perform. Although the tutorial covers the skills required to perform these tasks and T volunteers were progressing through the tutorial at their own pace, these tasks can take time for users to become proficient. It is important to note that it takes a person multiple exoskeleton sessions to become proficient at walking with the device, therefore this does not necessarily mean the protocol is not sufficient in teaching sit-to-stand and MWM movements.

3.5.5 Overall Comments

According the preliminary results presented, the novel protocol has some improvement towards the usability of the exoskeleton for first-time users, and it is also considered beneficial by the volunteers who received it. That said, the workload scores for the MWM

and AWM walking tasks contradict these findings, so there is insufficient evidence to prove the true effectiveness of the protocol.

The performance safety concerns exhibited by one NT member could be mitigated if the proposed protocol were introduced, since it includes a tutorial on proper crutch usage and body weight shifting when walking.

One limitation of this preliminary is that NT did not go through anything to equalize with the experience T is getting with the exoskeleton. The arrangement for NT is to replicate the experiences of the two grad students from the pre-test, and also reflect the current experience of how exoskeletons are provided. Therefore, the original intent of doing so is to obtain a behavioural comparison between a scenario with no instruction at all and another scenario with a tutorial. However, with the design of this preliminary study, T was able to spend more time interacting with the device than NT, so the improved usability and positive comments about the tutorial could possibly be confounded by longer interaction time.

Another limitation is that regardless of whether the participant received the tutorial or not, there was not time allocated for them to freely interact with the device. Since different people take different approaches on learning new things, it is worthwhile to explore the difference in performance between receiving the tutorial and interacting with the device freely.

The small sample size and lack of quantitative data are the limitations of this preliminary study, since the survey results analyzed could not fully explain certain observed phenomena. The tutorial described in this thesis not designed specifically for older adults either. The next steps on expanding and improving this study are covered in the next section.

3.6 Future Improvements

It is recommended to increase the sample size in future related studies. Not only could the effects of outlier data be reduced, statistical analysis could also be performed and therefore provide a more in-depth analysis. As mentioned in the Results section, RTLX scores can only be compared relatively between conditions and/or within subjects since the scores do not have a threshold for a demand considered "too high." Aside from comparing RTLX scores between NT and T as it was performed in the preliminary study, the tool can be better utilized by also evaluating the users performing the same tasks but without an exoskeleton, since this could portray the change in perceived workload within an individual. Another recommendation is to incorporate electromyography (EMG), motion capture,

instrumented crutches, and pressure sensors / force plates for future related studies. This is because combining survey results and biomechanical analysis could provide a more complete perspective on the effectiveness of the protocol and explain the perceived cognitive workload phenomena that could not be explained purely based on qualitative data.

Another recommendation is to introduce a third group of participants who are allocated time to freely interact with the TWIN exoskeleton. To keep the exposure time consistent with the group receiving the tutorial, the interaction duration would be the same as the tutorial's duration. This approach grants a fairer evaluation on the effectiveness of the tutorial by equalizing exposure time, allows analysis on performance differences between self exploration and the tutorial, and enables comparisons against how exoskeletons are currently provided.

In May 2022, these preliminary results were presented at the Hengstberger Symposium on Aging and Technology at the Internationales Wissenschaftsforum Heidelberg in Heidelberg, Germany. Interdisciplinary exchanges were made on how the protocol could be further tailored to the geriatric population. In particular, some comments and recommendations were provided by Dr Anna Schlomann, a postdoctoral researcher from the Network of Aging Research at Heidelberg University. She commented that the results on perceived cognitive workload (RTLX) from young-to-middle-aged adults would be even more exaggerated in older adults. Her recommendations on tailoring the protocol to older adults include separating the tutorial into at least two sessions, adding a concise information sheet for the older adults to read, and asking the geriatric participants to "Think-Aloud" during the sessions. "Think-Aloud" is the process of verbalizing one's thoughts as they perform a task [30]. Although this technique requires practice and training, it is possible to obtain more information on the participants' perspectives on the exoskeleton and tutorial. Dr Schlomann stated that the first session could involve showing the older adults TWIN, its movements, and perhaps going through a little bit of the tutorial. The second and/or future sessions could include a quick review of the previous session, complete the rest of the tutorial, and perform the tasks with the exoskeleton. She added that the material covered in the sessions are dependent on the older adult, since some may want to cover more material in one session than others. Therefore, it is important to ask if they would like to continue with the tutorial or leave it to the next session. Dr Schlomann said that older adults prefer reading an information sheet than watching videos, and some even would treat it as a keep sake, which allows them to show their friends and families the things they learn.

With these recommendations on making the tutorial appropriate for the geriatric population, improvements include spreading out the tutorial over multiple sessions to reduce cognitive overload, providing handouts to help introduce the exoskeleton and its

functionalities, and adding an "acquaintance mode" to the exoskeleton. The "air walking" experience may be uncomfortable and unsafe for the geriatric users, an "acquaintance mode" can be created to move only one leg at a time to let the older adults feel how the motors move their legs. This "acquaintance mode" should be able to be activated whether the person is sitting or standing, and allow the operator to manually choose between the left or right leg. If the older adult wants to experience the "acquaintance mode" standing, it must be designed such that the stance leg remains stationary at all times, and the geriatric user should hold onto a stable object while being supported by a patient lift via harness, with at least one researcher next to them in case of an emergency. For future related studies involving only older adults, there would be two groups of participants instead of three: one group going through self-exploration by asking questions and requesting for demonstrations, and another group going through the tutorial. Due to safety reasons, the "no exposure" condition would be removed.

3.7 Conclusion

This preliminary study indicated that the novel protocol was potentially helpful to improve familiarity with wearing an exoskeleton for the first time, and the results suggested the importance of having a tutorial to teach people how to move with this type of device. Various ways of improving and expanding this study to a larger population and to older adults are identified and discussed. With more participants finding sit-to-stand and MWM to be the most difficult tasks to perform with the TWIN exoskeleton, a need exists to explore a different avenue to improve human-exoskeleton interaction via trajectory generation. Due to time constraints, only the sit-to-stand motion is considered so far, though the methods taken in this thesis can also be expanded to walking. The second approach to improve human-exoskeleton interaction involves optimal control, but before describing the problem formulation, we begin with understanding the biomechanics of sit-to-stand.

Chapter 4

Sit-to-Stand Biomechanics

Sit-to-Stand (STS) refers to the motion of standing up from a sitting position. Recall that STS was the leading cause of falls in nursing homes in Bavaria in 2012 [71] and is one of the most difficult predefined TWIN exoskeleton motions to move with. Moreover, the push-off with the crutches to stand up can be uncomfortable, so we are interested in generating a new STS trajectory that does not require crutches. The motion itself can be divided into four phases [53]:

1. Trunk forward rotation until hip leaves the seat.

2. Forward rotation of full body as hip leaves the seat until lower legs no longer flex forward.

3. Synchronized rising movement of trunk and hips until lower legs stop flexing backward.

4. Forward flexion of lower leg and thigh.

STS can also be simplified into two phases: sitting and lifting, as done in [64] and [9]. The main difference between the phases is that the seat contact is present in the first and absent in the second. In healthy younger adults, the average STS duration is 1.6 seconds, and it is suggested that the full STS duration in assistive devices be between 1.6 s and 5 s [53].

This task requires lower limb strength, but it becomes challenging as one ages because of sarcopenia (loss of muscle strength), osteoporosis (loss of bone mass and density), and other age-associated movement impairments. STS-related injuries are unfortunately a reality

the society must face, accounting for 41% of the falls in older adults in Bavaria, Germany. For decades, geriatric users can purchase passive walkers and/or canes to aid walking and sit-to-stand transfers. In recent years, researchers have been developing robotic assistive devices, such as a robotic STS device for wheelchair users [93] and a robotic walker that can also perform active STS assistance [55].
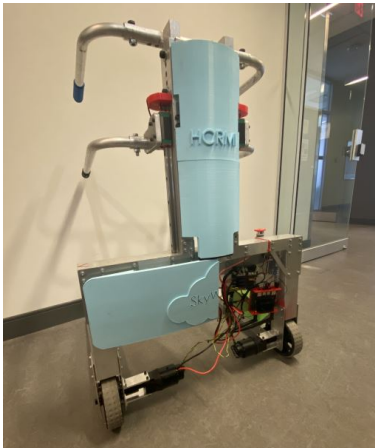
Figure 4.1: SkyWalker, a novel lightweight robotic rollator for walking and active STS assistance.

4.1 Trajectory Generation

Yamada and Demura compared STS movements in younger and older populations using ground reaction forces, and found that the stomping force and movement speed in the elderly are weaker and slower. They suggested that a stable STS movement does not solely require leg muscle strength, but also the ability to maintain the stability of the center of gravity [91].

The STS motion can be generated by performing inverse kinematics at the hip, knee, and ankle joints as done by Jatsun, Savin, Yatsun, and Malchikov [72]. This approach can be applied to an adaptive control system for a lower-limb exoskeleton to perform STS, with ZMP principles taken into account for maintaining balance in the system [42].

Yamasaki, Kamabara, and Koike predicted center-of-mass trajectories during STS movement with optimization. Comparing results from the minimum jerk and minimum torque-change models, the latter model is able to generate a trajectory that resembles

the center-of-mass trajectories. They concluded that STS can be described with dynamic optimization [92].

Mombaur and Ho Hoang applied optimal control into determining the best way for an assistive device to exert external forces on geriatric users for sit-to-stand transfer support [64]. Under three different support settings, they utilized a whole-body model and separated the entire STS motion into two phases – sitting phase (Lagrangian multipliers as contact constraint forces to model human-exoskeleton model contact with the chair) and lifting phase (when the Lagrangian multipliers equal 0). The objective function for the two phases are the same and consists of a weighted combination of minimization of joint torques squared, minimization of mechanical work in all joints, minimization of head angular velocity, and a regularization term to make the external forces slightly smoother. Without minimizing mechanical work, the resulting motion would be very dynamic, hence this objective function is crucial for generating trajectories suitable for the elderly. Although the scope of this paper is to determine the best way to exert external forces on an elderly person for STS assist, the approach described can be applied to human-exoskeleton STS transfer by declaring the external forces as zero.

Aller, Harant, and Mombaur applied optimal control in STS trajectory generation on the humanoid robot REEM-C (PAL Robotics), and successfully performed the motion in the physical system. The states defined in their optimal control problem include joint angles, joint velocities, and joint torques. The controls are the derivatives of joint torques and the duration of both STS phases are left free. For the optimizer to yield an optimal solution, they determined the minimum seat height to be 100% of the knee height and the furthest ankle placement to be 40% of the knee height away from the sitting contact [9].

Huo, Moon, Alouane, Bonnet, Huang, Amirat, Vaidyanathan, and Mohammed developed an impedance modulation control considering impedance compensation and balance reinforcement to assist STS motion of a person wearing the Angeleg Exoskeleton [40]. Taking a model-based approach, they simplified the human model to a triple inverted pendulum with 3 DOFs (lumped thighs, lumped shanks, and head, arms, and trunk lumped as one segment). Intended for users with partial mobility, their control method can account of the user's motor ability and follow the movement. In the event of the human-exoskeleton CoM's horizontal projection going beyond a set range with respect to the foot position, a "step" or "sit-back" strategy is deployed to prevent falls when standing up. This algorithm is implemented onto the Angelegs Exoskeleton and tested with four healthy adults in their mid-to-late 20s at a seat height of 0.7 m. EMG data is collected to analyze the influence of their algorithm on wearer's muscle activity.

This paper on impedance modulation control for assisting STS motions [40] and the

STS trajectory generation topic of thesis share a common goal of making a human perform crutch-less STS when wearing an exoskeleton, but the approaches are different. Huo et al. use the Angeleg exoskeleton (13 kg) and a simplified 3-DOF human model, when this thesis uses the TWIN exoskeleton (25 kg) and a 13-DOF human model with arm movements. The seat height considered in the optimal control problems presented in this thesis is lower than the one deployed in that paper (approximately 0.552 m vs 0.7 m in [40]). Huo et al. assume the target population to have partial mobility, whereas the optimal control problems solved in this thesis does not consider the level of lower-limb mobility in older adults nor the joint torque limits of the exoskeleton. Our rationale is to first obtain the minimum required torques for the lower limb joints to perform STS without crutches, with the torque exerted by the user being a percentage of the total torque calculated in the case of partial assistance.

The literature described above do not involve a human wearing an exoskeleton, and even if it does, arm movements are not considered. However, they have inspired the approach taken to generate an appropriate crutch-less STS trajectory in this thesis. Meanwhile, since lower-limb exoskeletons are mostly powered purely along the sagittal plane, a set of crutches must be used for safety and stability. Not only are crutches cumbersome and unnatural to the human gait [57], they can also induce stress in the upper-body and even introduce injuries after prolonged usage [66]. This calls for a need to generate crutch-less STS trajectories for a human-exoskeleton system, but we must first gain a better understanding by performing an experiment involving six STS conditions.

4.2   Motion Capture Experiment

A 25-year-old female participant, who has experience moving with the TWIN exoskeleton, was recruited to perform STS motions with the device under six cases. The motions analyzed, which are part of this larger data set, are listed below.

1. Active with crutches at seat height of approximately 100 % knee height / 0.46 m

2. Active with crutches at seat height of approximately 120 % knee height / 0.552 m

3. Passive with crutches at seat height of approximately 100 % knee height / 0.46 m

4. Passive with crutches at seat height of approximately 120 % knee height / 0.552 m

5. Passive without crutches at seat height of approximately 100 % knee height / 0.46 m

6. Passive without crutches at seat height of approximately 120 % knee height / 0.552 m

Active means the device is moving the human limbs, whereas passive means the motors are completely disengaged. These data are collected because there are no such data available particularly with the TWIN exoskeleton yet. Cases 1 and 2 can provide information on how much force is required in the crutches to successfully move with the TWIN's predefined STS motion. Cases 3 and 4 are collected to observe how a person would perform STS with crutches and wearing an exoskeleton without the influence of its predefined motion. Cases 5 and 6 are collected to analyze the biomechanics behind the motion to successfully perform crutch-less STS with TWIN. Please note that cases 5 and 6 do not demonstrate the intended use of this exoskeleton; they simply show that it is possible to do crutch-less STS with TWIN for feasibility reasons. Although each case was performed three times, some trials were affected by severe marker occlusions. Therefore, the trial with the least disruption from marker occlusions was chosen out of the three per case. The seat heights were inspired by the findings of the humanoid robot REEM-C performing STS, such that for an optimal STS trajectory to be generated, the minimum seat height should be at 100% knee height [9]. Although the structures of a humanoid robot and human wearing an exoskeleton are different in nature, it is assumed that it would also be easier for a person wearing an exoskeleton to stand up from a higher seat height. Therefore, two different seat heights are investigated.

Forces exerted by the crutches are collected separately on two Bertec force plates in cases 1 to 4. As depicted in Figure 3.1 from Chapter 3 Section 3.2, IIT's instruction on using the crutches to perform STS is to start with crutches as far back as possible, and then push up. To accommodate for this movement, the seat is placed between the force plates, as depicted in Figure 4.2. In cases 5 and 6, the forces exerted by the feet and seat are collected separately on the two force plates. Since crutches are not needed, the force plates are rearranged by placing next to each other (see Figure 4.3). A stool that is approximately 0.46 m tall is used for performing STS trials at a lower seat height. Five boards that are each 2 cm thick are added underneath the stool for higher seat height trials (see Figure 4.4).

Figure 4.2: Force plate setup for STS trials with crutches.

Figure 4.3: Force plate setup for STS trials without crutches.

Figure 4.4: Five boards each with 2-cm thickness underneath the stool for STS trials performed at a higher seat height.

Note that the five boards illustrated in Figure 4.4 do not fit within the force plate. For the crutch-less STS case performed at a higher seat height, where the boards are placed on a force plate, a smaller board with the same thickness of 2 cm replaces one of the five boards. Doing so ensures all forces during the sitting face are transmitted and recorded.

The VICON Vantage motion capture system is used for collecting motion capture data. The marker layout is based on two modified IOR marker sets. One is created by Giorgos Marinou from ORB Lab at the University of Heidelberg to accommodate the TWIN exoskeleton. Another one is created by Jonathan Lin from CERC HCRMI Lab at the University of Waterloo, where additional markers are added at some locations for asymmetry. Benefits of having an asymmetrical marker layout on the limb segments include reducing the chances of marker swapping on the software and easier marker identification during post processing. The full marker layout can be found in Appendix B. A Vicon skeleton model, VSK for short, is created based on the marker layout, and Procalc is a software used for modifying and creating new variables related to this VSK. Markers are placed superficially on the human, but the joint axis are beneath the skin. Therefore, it is necessary to redefine VSK variables so that the joint angles are more accurate. Figure 4.5 shows the VSK.
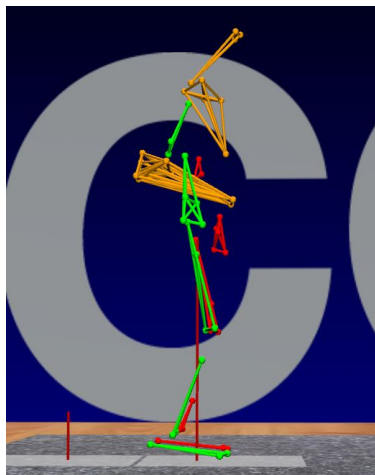
Figure 4.5: Vicon skeleton model of human-exoskeleton lumped.

4.3 Discoveries from Force Plate and Motion Capture Data

The STS cases involving active motors with crutches (cases 1 and 2) require significantly more time to complete STS, with a total duration of 11.36 s and 11.39 s respectively. This is because the default STS settings of the exoskeleton include 2 s to bend the trunk to prepare for STS, 2 s to pause between trunk bend and standing up, and 4 s to stand up from sitting. For the passive cases with crutches, the lower seat height takes 5.79 s and the higher seat height takes 5.58 s. The crutch-less passive cases have the shortest duration, with the lower seat height lasting 4.4 s and the higher seat height lasting 4.3 s. When discussing about findings on the kinematics, symmetry is assumed in the hips, knees, and ankles.

4.3.1 Force Plate

Under active conditions, the maximum combined peak force in the crutches at a higher seat height (case 2) is 8.14 % less than that at a lower seat height (case 1). In case 1, the peak combined force occurred after the seat-off. In case 2, the peak combined force happened at the seat-off. Under passive conditions with crutches, however, the maximum combined peak force in the crutches at a higher seat height (case 4) is 36 % higher than that at a lower seat height (case 3). In cases 3 and 4, the maximum peak combined force occurred before the seat-off. Under passive conditions without crutches, the peak force exerted at the feet at a higher seat height (case 6) is 3.31 % lower than that at a lower seat height (case 5). In cases 5 and 6, the peak force at the feet occurred after the seat-off. For the cases with crutches, it is possible to estimate the force at feet statically (Equation 4.1) or dynamically (Equation 4.2).

$$F_{crutches} + F_{feet} \approx M_{total} * g \qquad (4.1)$$

$$F_{crutches} + F_{feet} = M_{total} * (a_{COM} + g) \qquad (4.2)$$

The total mass of the human, exoskeleton, and crutches is 83.1 kg. Equation 4.2 is used, and the acceleration of the center of mass is approximated with the acceleration of the floating base origin. The location of the floating base origin is defined on Procalc and the acceleration values are exported from Vicon. To calculate the acceleration of the center of

mass with much higher accuracy, one can use software libraries, such as the Rigid Body Dynamics Library developed by Martin Felis [27]. Details of the results and estimations are illustrated in Table 4.1 and Figure 4.6.

Table 4.1: Forces exerted by crutches or feet in the six STS cases.

Case	Peak Combined Force in Crutches	Estimation of Force at Feet
1	330.3 N	484.9 N
2	303.4 N	531.0 N
3	274.0 N	556.1 N
4	373.2 N	447.5 N
	Peak Force At Feet	-
5	928.7 N	-
6	898.0 N	-
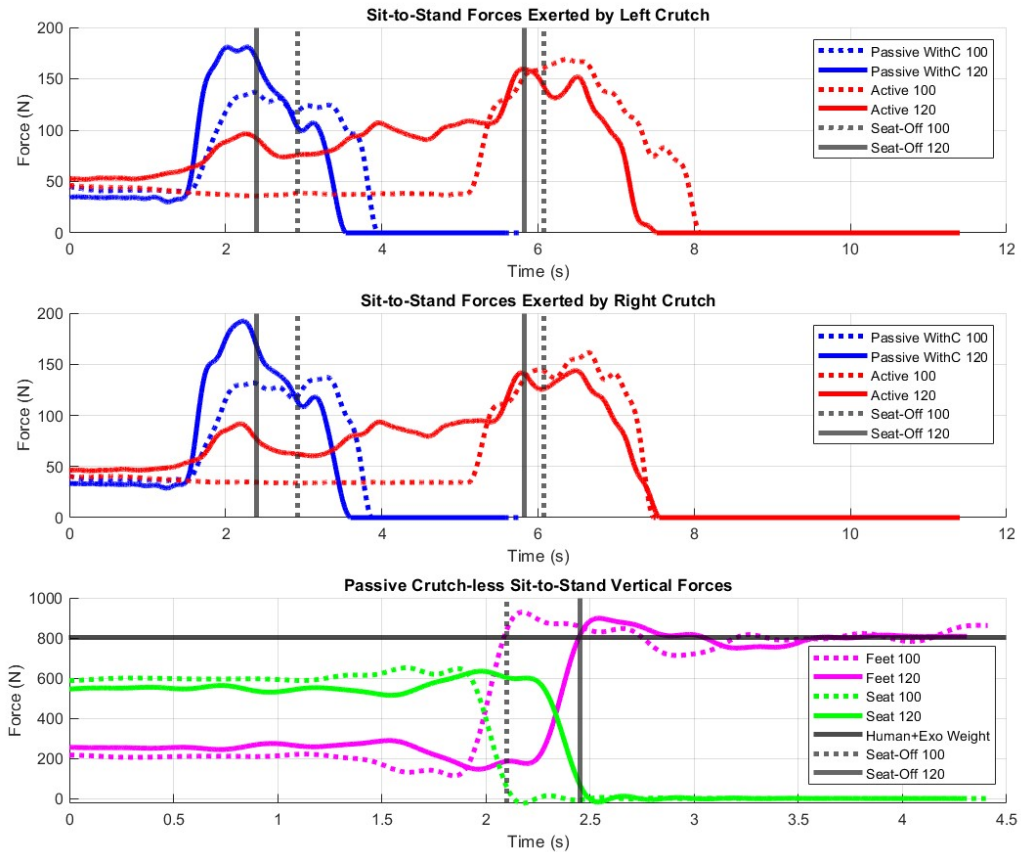
Figure 4.6: Vertical forces exerted by crutches or feet in all six STS cases.

Given the contradicting force value trends presented in cases 1 to 4, it is unknown whether the person exerts more or less force in the crutches at a higher seat height. That said, the lower force reading in case 3 could be caused by the person engaging their lower limb muscles to stand up. The user is relatively weaker in the upper limbs than lower limbs, so they perceived case 3 to be more challenging than case 4. Based on the estimation of the force in the feet, it is very likely that they also stood up with their legs and therefore relied less on the crutches. The force plate readings at the feet for crutch-less cases (5 & 6) exceed the total weight of the human wearing the exoskeleton, which is 804.4 N. This indicates that the user must accelerate upwards to stand up from sitting.

In the active cases, the peak combined force occurred at or after the seat-off moment, which is later than the passive cases involving crutches. This is likely caused by motor actuation in the predefined trajectory. In cases 3 and 4, the person must generate a large-enough force to push up with the crutches or with the feet. However, the active motors in cases 1 and 2 already make the person stand up regardless of how much crutch force is exerted in preparation for the lift. As for the passive cases without crutches (cases 5 and 6), it is difficult to explain why the peak force occurred after seat-off based on the data collected, but it could be related to the need for the user to accelerate upwards.

4.3.2 Kinematics

At a lower seat height, the subject exerts the largest forward bend at the xiphisternal and hip joints right before standing up from sitting without crutches. This phenomenon is also exhibited at a higher seat height, though the ROM is less than that at a lower seat height. This is likely because it is easier to perform STS at a taller chair, therefore the user does not need to bend their trunk as much to stand up from sitting. The duration of trunk bend in passive cases prior to lifting off the seat is less than the duration taken in the active cases, hinting that TWIN's predefined 2-s trunk-bend could be too long for the motion to be considered natural. These observations suggest that angular range and timing of trunk bend are crucial towards performing STS without crutches. Trajectories for the xiphisternal and hip joints can be found in Figures 4.8 and 4.9.

Compared against the passive cases, the active cases with crutches consistently have the largest ROM in the hip, knee, and ankle joints. It is because TWIN's predefined trajectory has pre-determined initial and final positions regardless of the user's size. However, this does not mean that the person is not standing straight in passive cases; it is instead caused by the lack of perfect fitting. Although this exoskeleton has customizable components, its thigh link does not allow for fine adjustments and instead fits a 2-cm range of length values. The error caused by this misalignment is propagated into the lower limb joints, which becomes more apparent when standing up since these angles do not reach 0 rad in the passive cases. Figure 4.7 contains a graphical explanation to support the reasoning. The lower limb joint trajectories are illustrated in Figures 4.8 and 4.9. The trajectories from active cases are data recorded from the Vicon Vantage motion capture system and they reflect the pre-programmed exoskeleton STS trajectory.
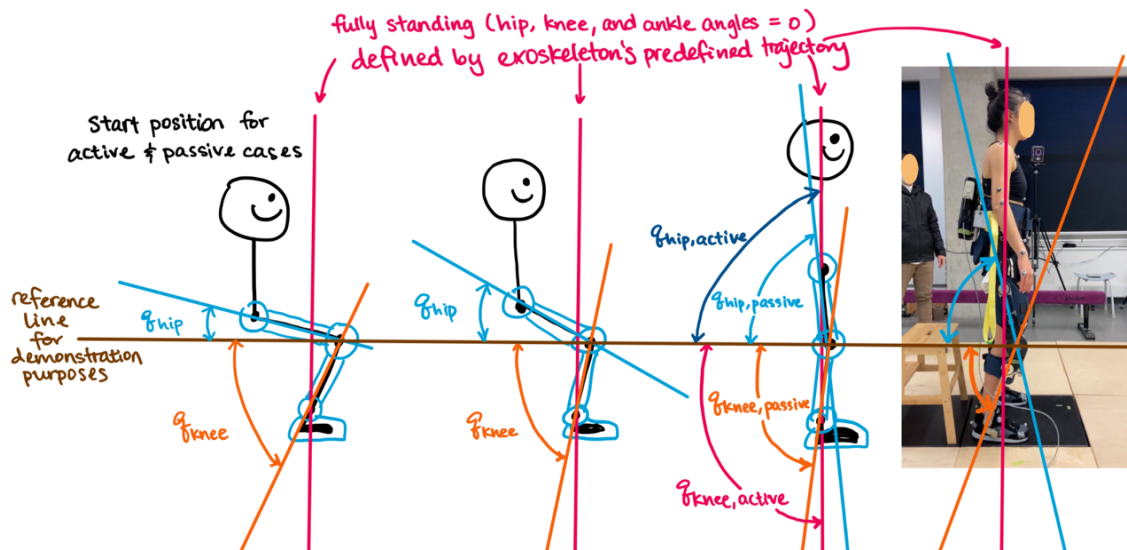
Figure 4.7: Graphical reasoning on why active cases have the largest ROM in the lower limbs.

Looking at the upper limb joint trajectories in Figures 4.10 and 4.11, the shoulders have the most sagittal movement in both seat heights. This could mean that swinging the arms back and forth can aid in performing crutch-less STS successfully. Note that the relatively smaller sagittal shoulder ROM in the passive crutch-less cases do not necessarily mean that a smaller shoulder ROM is associated to this method of performing STS. The other cases involving crutches have a higher shoulder sagittal ROM because the user must bring the crutches all the way back to push themselves up, which according to the subject, is uncomfortable. The ROM of all joints are summarized in Table 4.2.

The successful crutch-less STS motions from this investigation are considered feasible solutions since the subject can stand up without falling. So far, it is unknown whether they are optimal motions, let alone knowing the corresponding amount of torque exerted at the joints. Optimal control is able to determine the underlying actuation of the recorded motions and also generate an optimal trajectory. This allows us to determine if the feasible solution is optimal, and if it isn't, how it differs from the optimal solution. For the upcoming optimal control problems, only data from the passive crutch-less STS motion (i.e. case 6) is considered. The upcoming sections of this chapter will cover the background of optimal control.
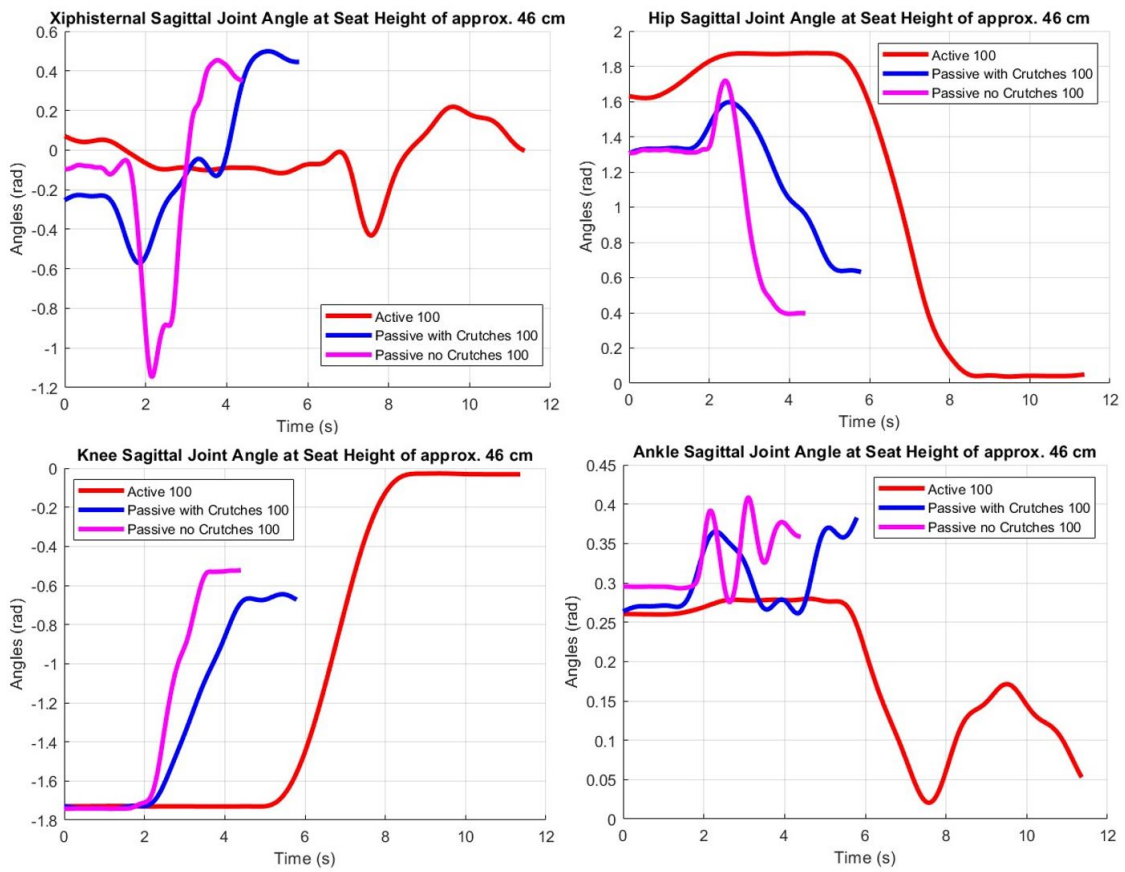
Figure 4.8: Joint angles of xiphisternal, hip, knee, and ankle at seat height of approx. 46 cm.
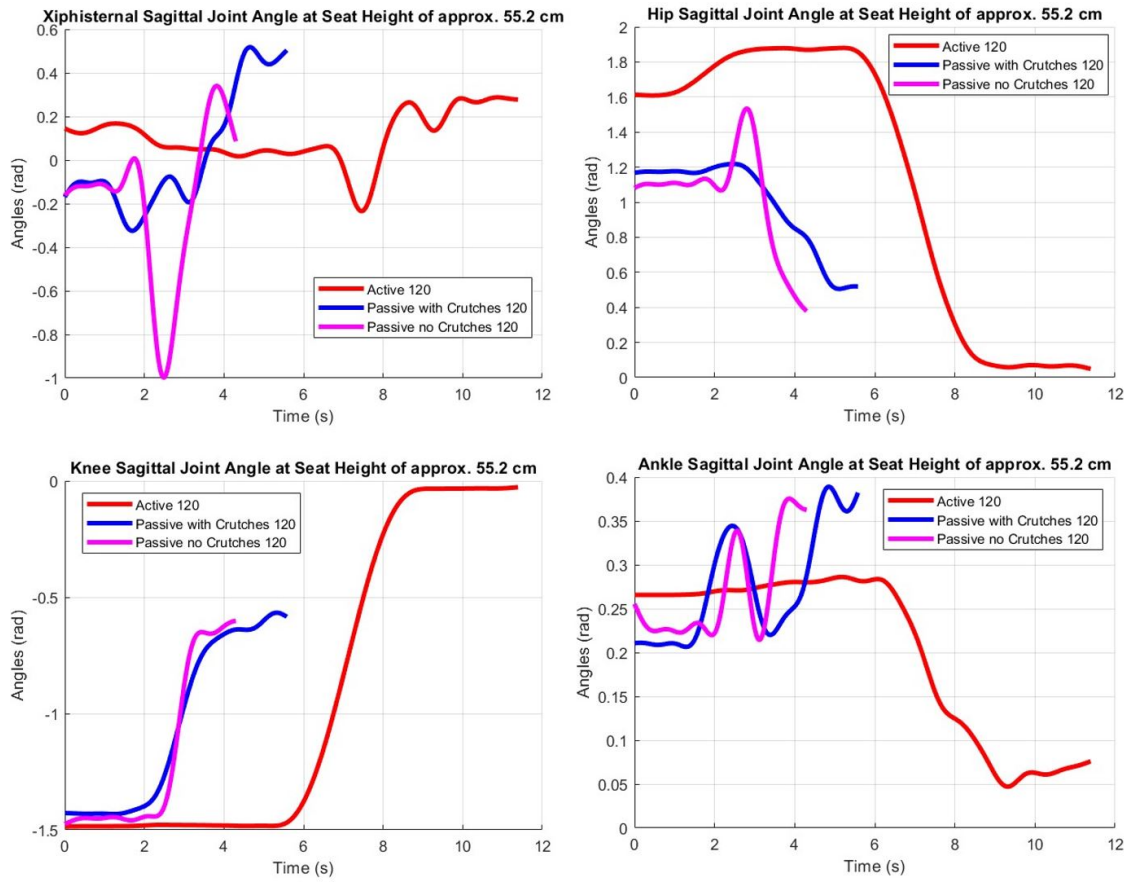
Figure 4.9: Joint angles of xiphisternal, hip, knee, and ankle at seat height of approx. 55.2 cm.
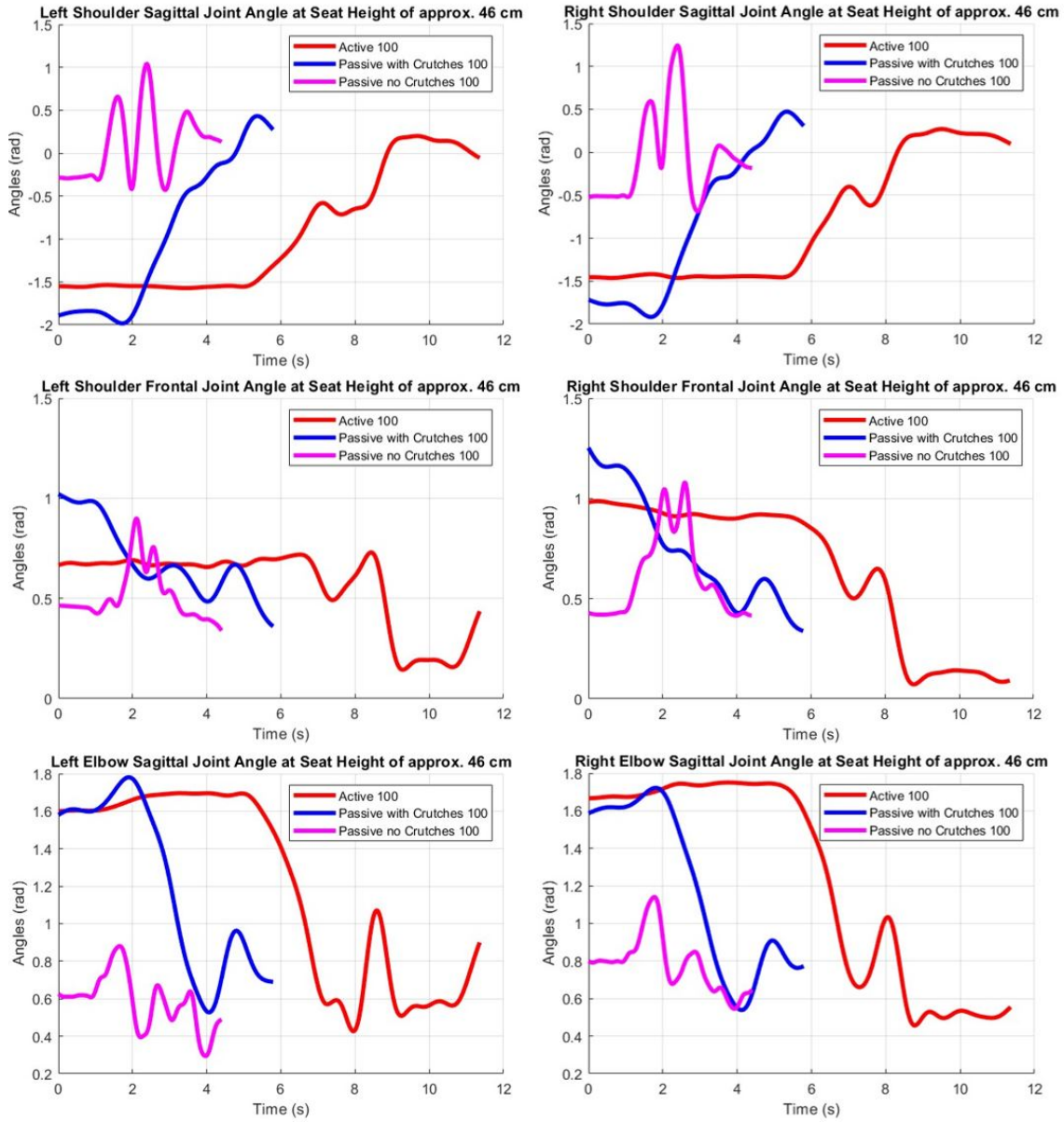
Figure 4.10: Joint angles of xiphisternal, hip, knee, and ankle at seat height of approx. 46 cm.
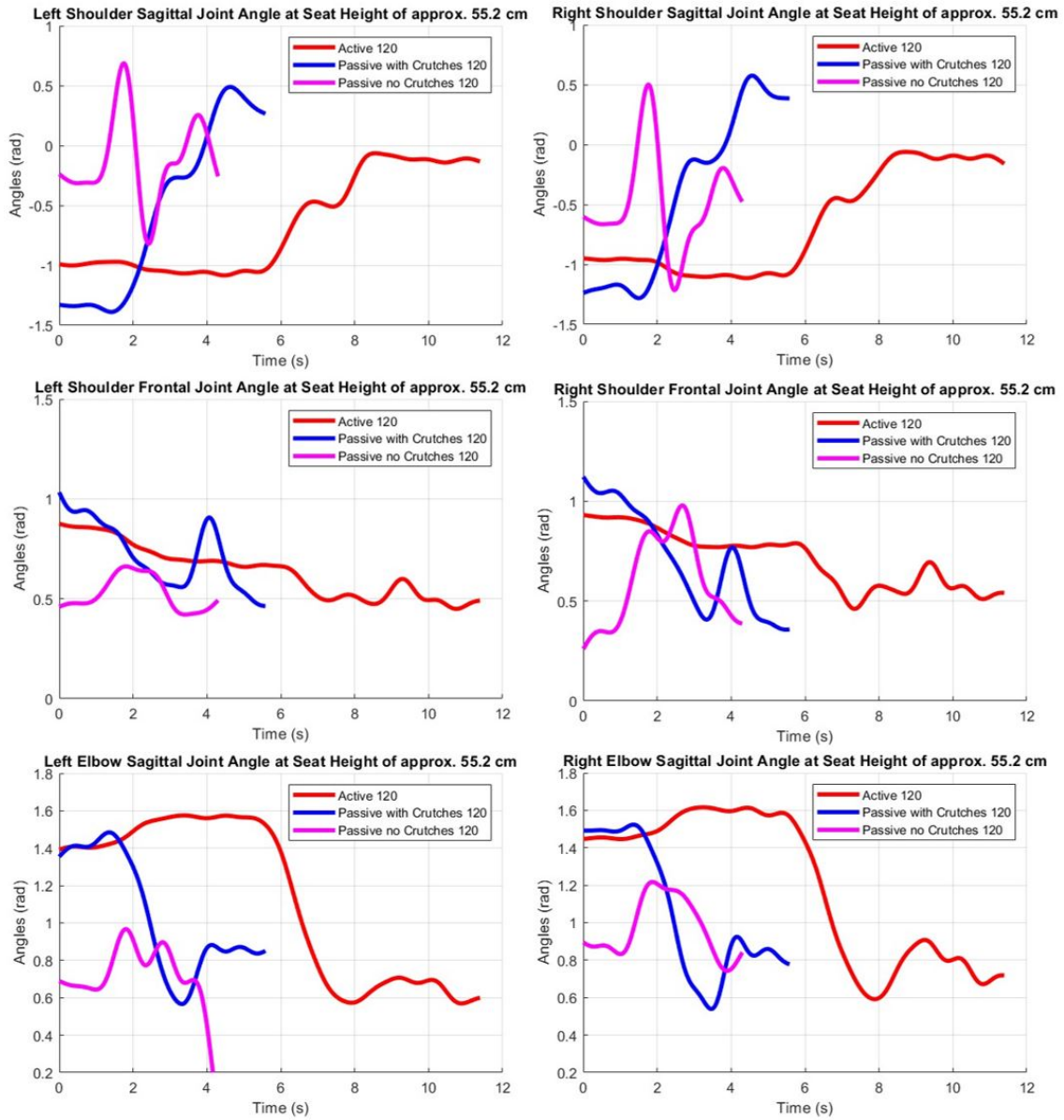
Figure 4.11: Joint angles of xiphisternal, hip, knee, and ankle at seat height of approx. 55.2 cm.

61

In Table 4.2, within each joint among all six cases, the dark and light orange cells represent the trials with the largest and second largest ROM respectively. As for cells in blue, a darker colour means that trial has a relatively larger ROM.

Table 4.2: Ranges of motion (ROM) in xiphisternal, hip, knee, ankle, shoulder, and elbow joints at both seat heights.

Joint	Case	100% h_{knee} ROM (rad)	120% h_{knee} ROM (rad)
Xiphisternal	Active, with crutches	[-0.4313, 0.2186]	[-0.2342, 0.2873]
	Passive, with crutches	[-0.5706, 0.4991]	[-0.3247, 0.5177]
	Passive, no crutches	[-1.1447, 0.4539]	[-0.9976, 0.3400]
Hip	Active, with crutches	[0.0378, 1.8744]	[0.0490, 1.8800]
	Passive, with crutches	[0.6318, 1.5956]	[0.5051, 1.2183]
	Passive, no crutches	[0.3942, 1.7176]	[0.3787, 1.5341]
Knee	Active, with crutches	[-1.7305, -0.0272]	[-1.4853, -0.0271]
	Passive, with crutches	[-1.7419, -0.6451]	[-1.4319, -0.5667]
	Passive, no crutches	[-1.7421, -0.5226]	[-1.4749, -0.6016]
Ankle	Active, with crutches	[0.0207, 0.2798]	[0.0472, 0.2861]
	Passive, with crutches	[0.2612, 0.3830]	[0.2065, 0.3889]
	Passive, no crutches	[0.2757, 0.4082]	[0.2144, 0.3754]
Left Shoulder (Sagittal)	Active, with crutches	[-1.5716, 0.2007]	[-1.0840, -0.0645]
	Passive, with crutches	[-1.9829, 0.4334]	[-1.3890, 0.4890]
	Passive, no crutches	[-0.4271, 1.0412]	[-0.8203, 0.6867]
Right Shoulder (Sagittal)	Active, with crutches	[-1.4635, 0.2710]	[-1.1140, -0.0610]
	Passive, with crutches	[-1.9185, 0.4739]	[-1.2812, 0.5754]
	Passive, no crutches	[-0.6870, 1.2461]	[-1.2140, 0.5006]
Left Shoulder (Frontal)	Active, with crutches	[0.1436, 0.7296]	[0.4495, 0.8759]
	Passive, with crutches	[0.3601, 1.0211]	[0.4637, 1.0335]
	Passive, no crutches	[0.3395, 0.8990]	[0.4211, 0.6621]
Right Shoulder (Frontal)	Active, with crutches	[0.0721, 0.9869]	[0.4613, 0.9307]
	Passive, with crutches	[0.3387, 1.2534]	[0.3570, 1.1225]
	Passive, no crutches	[0.4146, 1.0800]	[0.2601, 0.9789]
Left Elbow (Sagittal)	Active, with crutches	[0.4269, 1.6961]	[0.5698, 1.5750]
	Passive, with crutches	[0.5276, 1.7807]	[0.5670, 1.4844]
	Passive, no crutches	[0.2945, 0.8809]	[-0.0381, 0.9672]
Right Elbow (Sagittal)	Active, with crutches	[0.4570, 1.7502]	[0.5917, 1.6157]
	Passive, with crutches	[0.5389, 1.7219]	[0.5394, 1.5231]
	Passive, no crutches	[0.5454, 1.1403]	[0.7429, 1.2171]

Chapter 5

Sit-to-Stand Modeling

This chapter covers the concepts related to modeling multi-body rigid systems, the process of creating the simulation model, and ends with the mathematical formulation to model sit-to-stand.

5.1 Multi-body System Dynamics

Process dynamics can be deterministic, stochastic, discrete or continuous in time and contain discrete or continuous state variables. This thesis involves motions of a multi-body mechanical system, therefore only deterministic process dynamics with continuous time and states that can be expressed as ordinary or differential algebraic equations are described.

When forces and/or torques act on a multi-body system, its resultant motions are known as dynamics. Inverse dynamics calculates the generalized forces of the motion based on angular position, angular velocity, and angular acceleration. Forward dynamics calculates the angular acceleration based on angular position, angular velocities, and generalized forces [13]. As an example, forces and torques can originate from contacts and motor joints respectively.

A dynamic motion without contact forces acting on a multi-body system can be expressed with a set of ordinary differential equations (ODEs):

$$M(q, p)\ddot{q} + N(q, \dot{q}, p) = F(q, \dot{q}, p, \mathcal{M}) = \mathcal{T} + \mathcal{J}_g \mathcal{F}_g + \mathcal{J}_e \mathcal{F}_{ext} \qquad (5.1)$$

In Equation 5.1, q, $\dot{q}$, and $\ddot{q}$ each are a vector with the size of the degrees of freedom (DOF) in the multi-body system. They represent positions, velocities, and accelerations respectively. M is the inertia matrix that depends on q and system parameters p. N takes q, $\dot{q}$, and p into account for the Coriolis and centrifugal forces. $\mathcal{F}$ represents the total forces and torques acting on the system, which is characterized by a term involving joint torques $\mathcal{T}$, a second term involving gravity $\mathcal{F}_g$, and a third term involving external forces $\mathcal{F}_{ext}$.

When constraints are imposed on a multi-body system, the dynamic motions are instead described with a set of differential algebraic equations (DAEs):

$$\begin{pmatrix} \boldsymbol{M} & \boldsymbol{G^T} \\ \boldsymbol{G} & \boldsymbol{0} \end{pmatrix} \begin{pmatrix} \boldsymbol{\ddot{q}} \\ \boldsymbol{\lambda} \end{pmatrix} = \begin{pmatrix} \boldsymbol{-N + F} \\ \boldsymbol{\gamma} \end{pmatrix} \tag{5.2}$$

The M, $\mathcal{N}$, and $\mathcal{F}$ terms in Equation 5.2 are identical to those in Equation 5.1. The vector of Lagrange multipliers, λ, represents the contact forces from the constraints. With γ representing the contact Hessian, this set of DAEs become identical to the set of ODEs in Equation 5.1 when the contact forces from the constraints (λ) are zero.

5.2 Creation of Simulation Model

The model used in the simulations is a lumped model of an elderly woman and the TWIN exoskeleton. Originally written in Lua, the human, exoskeleton, and lumped models were visualized on RBDL-toolkit. This allows for fine manual adjustments to align the lower limb joints of the human and exoskeleton models, thereby making the lumped model as accurate as possible. Due to the library change from RBDL+MUSCOD-II to RBDL-CasADi then to biorbd/bioptim, a bioMod lumped model was constructed based on the Lua lumped model because only this file type can be supported in biorbd/bioptim.

This section is separated into three parts. It begins with the creation of the human model, then the exoskeleton model, and finally the lumped model.

5.2.1 Human Model

With 35 internal DOF, the original human model represents the 50th percentile 80-year-old elderly woman and the anthropometric data is based on de Leva with adjustments [37]. To simplify the model and also reflect the limited physical capabilities of wearing TWIN, a modified human model with less DOF is created. When a person wears the device,

its trunk brace wraps around the wearer's middle trunk and pelvis, meaning any sort of bending about the lumbo-sacral joint is highly restricted. As described in the exoskeleton state-of-the-art section, TWIN's lower limb joints only enable sagittal plane motion, so the hip and ankle movements of the wearer are limited to flexion/extension. The neck joint does not have any DOF because we are not interested in analyzing the ergonomics of doing STS without crutches with the TWIN. For joints with 0 DOF except the head, the two neighbouring segments are lumped as one segment. This means the forearm and hand segments are lumped as one segment, and the mid-trunk and pelvis are lumped as one segment. Since STS is a motion that is mainly along the sagittal plane, the DOF reductions in this modified human model are justifiable. Table 5.1 summarizes the joint locations and their respective DOF count in the original and modified human models.

Table 5.1: Total DOF-count in elderly woman (human-only) model.

Segment (Joint)	DOF count	
	Original Human	Modified Human
Head (Neck)	3	0
Upper arm (Shoulder)	3	2
Forearm (Elbow)	1	1
Hand (Wrist)	3	0
Upper trunk (Xiphisternal joint)	3	1
Mid trunk (Lumbo-Sacral)	3	0
Hip	3	1
Knee	1	1
Ankle	2	1
Floating base	6 (3D)	3 (2D)
Total DOF	**41**	**13**

5.2.2 Exoskeleton Model

As mentioned, TWIN has a total of six internal DOF in the sagittal plane – two at the hips (active), two at the knees (active), and two at the ankles (passive). Although the ankle joints are passive, the sagittal DOF on each side is still reflected in the model. The target geriatric user would still have mobility in their lower limbs, therefore it is reasonable to enable the ankle DOF. This means the box constraints on the ankle torque and range of motion (ROM) would need to be of the human user.

It is also reported in the state of the art section that TWIN comes in multiple sizes and can be customized to the user. The CAD meshes provided by the manufacturer ("default model") are of size Large and the lower limb dimensions do not fit the elderly human model described above. Table 5.2 describes the segment length discrepancy.

Table 5.2: Segment length difference between human and default exoskeleton models.

	Human	**TWIN Default Model**
Thigh length	0.344 m	0.405 m
Shank length	0.404 m	0.410 m
Foot height	0.0707 m	0.0924 m

For simulation purposes, TWIN is scaled down to fit the human model as accurately as possible, with its thigh length, shank length, and ankle height matching the human's lower-limb segment lengths. It is important to note that this assumption of perfectly-matching segment lengths may not reflect the real-life scenario. This is because the device's thigh link does not allow for fine adjustments and instead fits a 2-cm range of length values. The mass of each segment is scaled down based on the ratio between the new and old segment lengths, and the physical properties (center of mass (CoM) and inertia tensors) are recalculated based on these adjustments.

5.2.3 Lumped Model

When performing analysis on such system, one can construct a contact model or a lumped model. In a contact model, contact points are defined between the human and exoskeleton, thereby enabling analysis on force interactions between the two bodies during movement. Although the information obtained from a contact model can further evaluate the safety and efficacy of an exoskeleton motion, the mathematical formulation can become quite complex. A lumped model, as the name suggests, is one single model where the corresponding exoskeleton and human segments are lumped together as one component. This assumes the human is perfectly fitted in the device and no interaction force between the human and exoskeleton can be obtained, but it is simpler to create a lumped model. Therefore to keep the analysis simple, a lumped model was constructed and utilized. The equations used for calculating the lumped mass, lumped CoM, and lumped inertia matrices for each segment can be found in Equations 5.3, 5.4, and 5.5. d_{HL} stands for the distance between the human segment CoM and lumped segment CoM, whereas d_{EL} represents the distance between the exoskeleton segment CoM and lumped segment CoM. I stands for the inertia matrix.

$$m_{lumped} = m_{human} + m_{exo} \tag{5.3}$$

$$CoM_{lumped} = \frac{m_{human} * CoM_{human} + m_{exo} * CoM_{exo}}{m_{lumped}} \tag{5.4}$$

$$I_{human,atlumpedCoM} = I_{human,athumanCoM} + m_{human} * d_{HL}^2$$
$$I_{exo,atlumpedCoM} = I_{exo,atexoCoM} + m_{exo} * d_{EL}^2 \tag{5.5}$$
$$I_{lumped} = I_{human,atlumpedCoM} + I_{exo,atlumpedCoM}$$

The internal DOF available in the exoskeleton constraints movements in some human joints, so the DOF available in the lower limbs of the lumped model are equivalent to the exoskeleton's standalone model. The resulting lumped model with 10 internal DOF assumes symmetry in the lower limbs, has independent arms with 2 DOF in the shoulder joints (flexion/extension and abduction/adduction), and contains a xiphisternal joint that can perform bending motions along the sagittal plane. This dimensional configuration can allow for observations in arm movements when performing crutch-less STS while keeping the lower limb analysis simple. As mentioned earlier, the neck joint is fixed because the goal of this thesis is not to analyze the ergonomics of performing crutch-less STS with the exoskeleton. Table 5.3 details which segments of the human and exoskeletons are lumped together, and Table 5.4 lists the DOF of each joint of the lumped model. For the joints with lower DOF count than what a human can do, the movable direction is specified. Figure 5.1 shows the bioMod model visualized on bioViz.

Table 5.3: Lumped segments between human and exoskeleton.

Lumped Segments	Exoskeleton Segments	Human Segments
Lumped trunk	Trunk	Pelvis and mid-trunk
Lumped L&R thighs	L&R femur links	L&R thighs
Lumped L&R shank	L&R tibia links	L&R shanks
Lumped L&R feet	L&R foot links	L&R feet

Table 5.4: Details on internal DOF count of lumped model.

Joint	DOF	Direction (plane)
Neck	0 (fixed)	-
Shoulder	2	Sagittal and frontal
Elbow	1	Sagittal
Wrist	0 (fixed)	-
Xiphisternal	1	Sagittal
Lumbo-Sacral	0 (fixed)	-
Hip	1	Sagittal
Knee	1	Sagittal
Ankle	1	Sagittal
Total internal DOF	**10**	
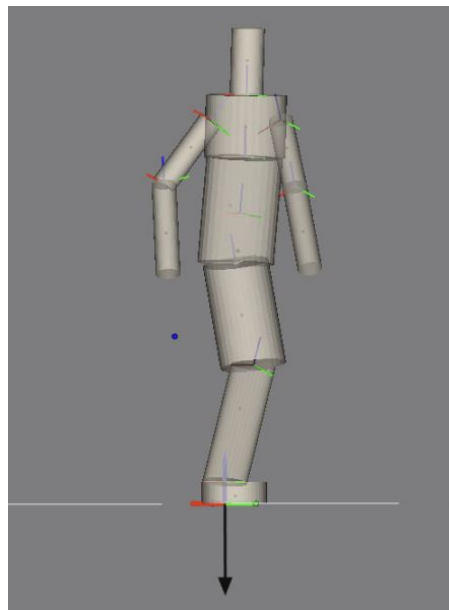
Figure 5.1: bioMod model used for optimal control problems.

5.3　Mathematical Model of STS Motion

5.3.1　Phase 1: Sitting

The sitting phase is defined as the period of time when the person is sitting on a chair with body movements at and above the hip joints already occurring. Since the floating base of the lumped model is defined at the pelvis-midtrunk segment, two sets of contact constraints are declared – one for feet on the ground and the other for the seat. The full mathematical formulation of the DAE and additional constraints is:

$$\dot{q} = v \tag{5.6}$$

$$\dot{v} = a \tag{5.7}$$

$$\begin{pmatrix} M & G^T \\ G & 0 \end{pmatrix} \begin{pmatrix} \ddot{q} \\ \lambda \end{pmatrix} = \begin{pmatrix} -N + F \\ \gamma \end{pmatrix} \tag{5.8}$$

$$g_{pos} = g(q(t), p) = 0 \tag{5.9}$$

$$g_{vel} = G(q(t), p) \cdot \dot{q} = 0 \tag{5.10}$$

5.3.2　Phase 2: Lifting

Recall from Section 4.2, a dynamic motion without contact forces acting on a multi-body system causes the DAE in Equation 5.2 to be equivalent to the ODE in Equation 5.1. In [64], the lifting phase of STS can be purely described by this ODE because the model used in their simulations has the floating base defined at the feet. This means that the feet position can be locked in space by simply fixing the floating base translation values, and once the seat contacts are absent, there are no more contact forces acting on the multi-body system.

In this thesis, however, the lifting phase cannot be described by the same ODE. This is because the model used in the simulations has the floating base defined at the pelvis-midtrunk segment, meaning that additional constraints must be added to the feet for them to stay in place. Therefore, the dynamic motion is represented by the same DAE as

Equation 5.8. The only difference is the size of λ and γ because these values relevant to the seat contact will be absent in the lifting phase.

5.3.3   Unilateral Constraints

To ensure the forces exerted do not pull the lumped model towards the ground nor the seat, unilateral constraints must be modeled. The main model difference between the sitting and lifting phases is the presence of seat contact. Coupled with the fact that bioptim requires one model per phase, the model for the sitting phase has both the feet-on-ground contact and seat contact constraints, whereas the model for the lifting phase only has the feet-on-ground contact constraints. The first step of enabling the unilateral constraints is to create the contact points in the bioMod files, which are specific model files native to bioptim and biorbd. After creating the contact points in the bioMod files, contacts must be enabled by setting `with_contact` to `True` in the python script when setting up the dynamics. Doing so calls the `ForwardDynamicsConstraintsDirect()` function of RBDL, which performs forward dynamics with contacts taken into account. If `with_contact` is not set to `True`, the contacts will not be considered in the calculations because `ForwardDynamics()` is used instead. Finally, when creating the constraints in bioptim, `ConstraintFcn.TRACK_CONTACT_FORCES` is added to create box constraints for all z components (i.e. up-down direction) of the contact points declared in the bioMod files. In both phases, the feet-on-ground contact force is bounded between 0 and positive infinity. As for the seat contact in phase 1, the contact force at all shooting nodes is bounded between 0 and positive infinity, but the contact force at the final node must equal 0 to denote the person leaving the seat to stand up.

Chapter 6

Sit-to-Stand Optimal Control

Optimal control is an approach that generates solutions to control dynamic systems such that the value of an objective function is minimized or maximized [77]. Two types of variables are involved in this method. The state variables describe the behaviour of a system at all time points, whereas the control variables manipulate the state variables [70]. Applications of optimal control include and are not limited to finance [73], resource management [73], and robotics [48, 64]. This thesis focuses on motion generation of a robotic system, so only relevant concepts are considered. Once the underlying process dynamics is determined, an optimal control problem can be formulated.

6.1   Objective Function

The objective function, which is also known as a cost function, is the function that is being optimized in this process. There are three types of objective functions: Lagrange type, Mayer type, or Bolza type. Lagrange type objective functions (see Equation 6.1) describe an entire process, and examples include integrals over torques and integrals over calculated values to reference values [63]. A Lagrange type objective function over calculated values to reference values is referred to as a tracking problem, and it is solved in the form of a least-squares optimal control problem. The difference between the calculated values and reference values is squared over a predefined duration, and the goal is to minimize said difference. Equation 6.2 shows an example of joint angle tracking in the form of least squares, with n_{DOF} and n_s representing the number of degrees of freedom and shooting nodes respectively. Mayer type objective functions (see Equation 6.3) only depend on values at the end of an interval, so they are used in scenarios that require minimizing or

maximizing total time or total distance [63]. Bolza type (see Equation 6.4) is a combination of Lagrange and Mayer type objective functions [63].

$$\Phi_L = \int_{t_0}^{t_f} L(t, \boldsymbol{x}(t), \boldsymbol{u}(t), \boldsymbol{p})dt \tag{6.1}$$

$$\min_{q} \quad \frac{1}{2} \sum_{j,i=0}^{n_{DOF}, n_s} |\boldsymbol{q}_{cal_j}(t_i) - \boldsymbol{q}_{ref_j}(t_i)|^2 \tag{6.2}$$

$$\Phi_E = E(t_f, \boldsymbol{x}(t_f), \boldsymbol{p}) \tag{6.3}$$

$$\Phi = E(t_f, \boldsymbol{x}(t_f)), \boldsymbol{p}) + \int_{t_0}^{t_f} L(t, \boldsymbol{x}(t), \boldsymbol{u}(t), \boldsymbol{p})dt \tag{6.4}$$

6.2 Boundary Value Problem

Boundary value problem is a set of ordinary differential equations (ODEs) with function and derivative values specified at two or more points [63]. It is a sub-problem of an optimal control problem and its formulation includes boundary conditions and/or constraints [63]. Solution methods for solving boundary value problems are also described in this sub-section.

6.2.1 Boundary Conditions and Constraints

Boundary conditions include initial value constraints, end value constraints, decoupled constraints, coupled constraints, and periodicity constraints. Initial value constraints are values that are fixed at the start of a phase t_0. It can be described as:

$$\boldsymbol{x}(t_0) - \boldsymbol{x}_0 = \boldsymbol{0} \qquad \text{Fixed initial values} \tag{6.5}$$
$$\boldsymbol{x}(t_0) - \boldsymbol{x}_0(\boldsymbol{p}) = \boldsymbol{0} \qquad \text{Parameter dependent initial values} \tag{6.6}$$

End value constraints are values that are fixed at the end of a phase t_f:

$$\boldsymbol{x}(t_f) - \boldsymbol{x}_f = \boldsymbol{0} \qquad \text{Fixed final values} \tag{6.7}$$

$$\boldsymbol{x}(t_f) - \boldsymbol{x}_f(\boldsymbol{p}) = \boldsymbol{0} \qquad \text{Parameter dependent final values} \tag{6.8}$$

Decoupled boundary constraints only concern one point at a time, which include and are not limited to initial point, end point, and phase-switch point. Phase-switch points occur in multi-phase models that are described by potentially different model equations. In the case of a sit-to-stand motion, the phase switching condition would be the moment the seat contact force equals zero. Below is an example for phase switching condition:

$$\boldsymbol{s}(\boldsymbol{x}(t_s), \boldsymbol{p}) = \boldsymbol{0} \tag{6.9}$$

Coupled boundary constraints relate states at different time points, and the general form can be expressed as:

$$\boldsymbol{r}(\boldsymbol{x}(t_0), \boldsymbol{x}(t_f), \boldsymbol{p}) = \boldsymbol{0} \tag{6.10}$$

Periodicity constraints are coupled boundary constraints where the end state equals the initial state. Running and walking motions are two of many examples that have periodicity constraints. Its general form is:

$$\boldsymbol{x}(t_0) - \boldsymbol{x}(t_f) = \boldsymbol{0} \tag{6.11}$$

Box constraints on all variables can be created to impose upper and lower limits. Its application include human joint range of motion, human joint torques, and time required to execute a motion.

$$\boldsymbol{x}_{min} \leq \boldsymbol{x}(t) \leq \boldsymbol{x}_{max} \tag{6.12}$$

$$\boldsymbol{u}_{min} \leq \boldsymbol{u}(t) \leq \boldsymbol{u}_{max} \tag{6.13}$$

$$\boldsymbol{p}_{min} \leq \boldsymbol{p} \leq \boldsymbol{p}_{max} \tag{6.14}$$

$$T_{min} \leq T = t_f - t_0 \leq T_{max} \tag{6.15}$$

6.2.2 Solution Methods for Boundary Value Problems

For multi-phase problems, the conditions and constraints must be specified for each phase and can be different depending on the motion of interest. Boundary value problems can be solved with the single-shooting method, multiple-shooting method, or collocation method. The difference between the first two methods lies in the number of intervals within a phase. Single-shooting involves a vector of initial values declared for the variable(s) of interest to solve the boundary value problem through iterative determination [63]. Multiple-shooting also solves the boundary value problem by iterating through the initial values, but the phase is divided into more than 1 node. In collocation method, an approximate optimal solution is computed at certain assumed locations, such that the governing differential equation at these locations is satisfied [87]. The controls are approximated as piece-wise linear interpolating functions, whereas the states are approximated as continuously differentiable and piece-wise cubic functions [87]. Compared to the collocation method, the multiple-shooting method has the advantage of allowing all sorts of constraints and yielding very accurate results. It also eliminates problems found in single-shooting methods, such as yielding unstable solutions and unable to converge with Newton's method if a bad starting point is given.

6.3 The Direct Multiple Shooting Method

In this thesis, we use the direct multiple-shooting method as implemented in the optimization tool Bioptim. Details about this tool can be found later in the Software Used section. The principles of this method, which are from the lecture notes of SYDE 750 Simulation and Optimization in Robotics and Biomechanics [63], are further described in this section.

Recall Equations 6.1, 6.3, and 6.4 that an optimal control problem is expressed in terms of continuous functions (states $\boldsymbol{x}(t)$ and controls $\boldsymbol{u}(t)$). In direct methods, a continuous problem is first discretized, then optimized.

6.3.1 Discretization of the Controls

The process begins with the discretization of the control functions, which are approximated by a grid on the time horizon $I_j = [t_0, t_f]$:

$$t_0 < t_1 < ... < t_{m-1} < t_m = tf \tag{6.16}$$

The discretized version of the control functions, $\boldsymbol{u}(t)$, is re-expressed with basis functions $\boldsymbol{\varphi}_j(t, \mathbf{q}_j)$, with $\mathbf{q}$ representing parameters. Equation 6.18 shows the formulation for piecewise constant basis functions, whereas Equation 6.19 shows the formulation for piecewise linear basis functions. Figure 6.1 is a visualization of a control function discretized as a piecewise constant basis function. Control functions can be discretized with higher order basis functions, such as splines, though one must be aware that this will increase the number of variables in the optimization. In this thesis, the control functions are represented by piecewise constant basis functions.

$$\boldsymbol{u}(t) = \boldsymbol{\varphi}(t, \boldsymbol{q}_j), \ \ \boldsymbol{q}_j \in \mathbb{R}^{k_j}, \ t \in I_j = [t_j, t_{j+1}] \text{ for } j = 0, 1, ..., m-1 \tag{6.17}$$

$$\boldsymbol{\varphi}(t, \boldsymbol{q}_j) = \boldsymbol{q}_j \tag{6.18}$$

$$\boldsymbol{\varphi}(t, \boldsymbol{q}_j) = \boldsymbol{q}_j^1 + \frac{t - t_j}{t_{j+1} - tj}(\boldsymbol{q}_j^2 - \boldsymbol{q}_j^1), \ \ \boldsymbol{q}_j = (\boldsymbol{q}_j^1 \boldsymbol{q}_j^2)^T \tag{6.19}$$
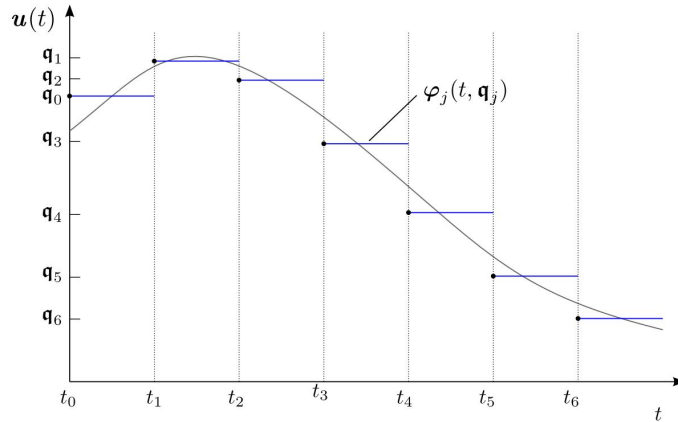
Figure 6.1: Visualization of piecewise constant controls discretization. Image obtained from Martin Felis' dissertation [28].

Discretization of the States

The discretization process begins with a time interval $[t_0, t_f]$ split into m sub-intervals, which are referred to as multiple shooting intervals. For simplicity, it is assumed that the

states are parameterized on a grid that is similarly-structured as the controls (see Equation 6.16). The intervals on this grid are called multiple shooting points, with integration and sensitivity generation performed separately on each interval:

$$\dot{\boldsymbol{x}} = \boldsymbol{f}(t, \boldsymbol{x}(t), \boldsymbol{\varphi}(t, \boldsymbol{q}_{j-1})), \qquad j = 1, ... m - 1, \qquad t \in I_j \tag{6.20}$$

$$\boldsymbol{x}(t_{j-1}) = \boldsymbol{s}_{j-1} \tag{6.21}$$

Solutions obtained from the direct multiple shooting method are not guaranteed to be continuous. To ensure that the states are continuous, the continuity condition in Equation 6.22 at the interval borders must be satisfied. Figures 6.2 and 6.3 compare the solutions without and with the continuity condition.

$$\boldsymbol{x}(t_{j+1}; t_j, \boldsymbol{s}_j) - \boldsymbol{s}_{j+1} = 0, \qquad j = 0, ..., m - 1 \tag{6.22}$$
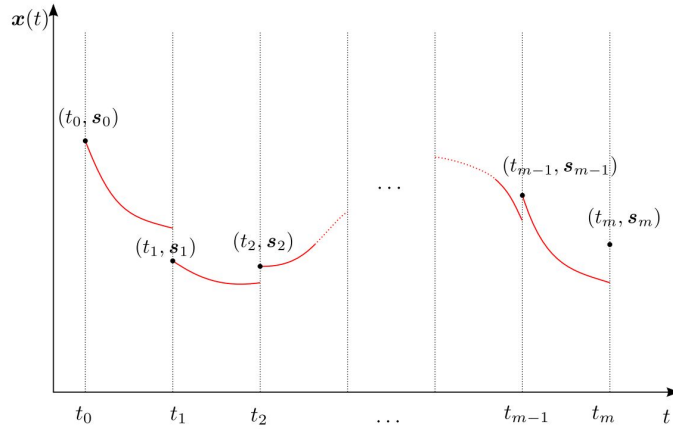
Figure 6.2: States without continuity condition satisfied. Image obtained from Martin Felis' dissertation [28].

Free Phase Duration

The phase duration introduced so far has a fixed value, though it is possible to leave the end time of each phase as a free optimization variable. Equation 6.3 can be expanded as:
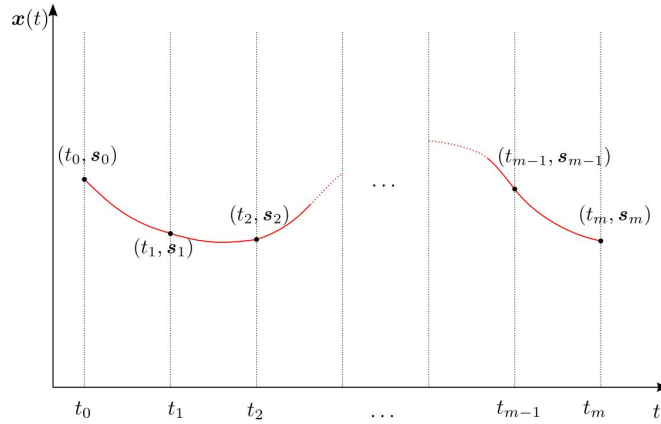
Figure 6.3: States with continuity condition satisfied. Image obtained from Martin Felis'
dissertation [28].

$$
\begin{aligned}
\min_{t, \boldsymbol{x}(t), \boldsymbol{u}(t)} \quad & E(t_f, \boldsymbol{x}(t_f), \boldsymbol{p}) \\
\text{s.t.} \quad & \dot{\boldsymbol{x}}(t_f) = \boldsymbol{f}(\boldsymbol{x}(t_f), \boldsymbol{u}(t_f), \boldsymbol{p}) \\
& \boldsymbol{g}(\boldsymbol{x}(t_f), \boldsymbol{u}(t_f), \boldsymbol{p}) \geq \boldsymbol{0} \\
& \boldsymbol{r}_{eq}(\boldsymbol{x}(t_f), \boldsymbol{p}) = \boldsymbol{0} \\
& \boldsymbol{r}_{ineq}(\boldsymbol{x}(t_f, \boldsymbol{p}) \geq \boldsymbol{0}
\end{aligned} \tag{6.23}
$$

Handling Discontinuities in Multiple Phases

The direct multiple shooting method can also solve optimal control problems with multiple
phases. Similar to the interval borders within a phase, the following condition for phase
transition must be satisfied:

$$
\boldsymbol{x}(t_i^+) = \boldsymbol{x}(t_i^-) + \boldsymbol{J}(t_i^-, \boldsymbol{x}_i^-, \boldsymbol{p}) \qquad \text{for } i = 1, ..., n_{ph} \tag{6.24}
$$

6.3.2 Discretized Optimal Control Problem

Combining the discretized controls, discretized states, free phase duration, and phase
transition continuity condition, the discretized optimal control problem is:

$$
\begin{aligned}
\min_{\boldsymbol{y}} \quad & \tilde{\boldsymbol{\Phi}}(\boldsymbol{y}) \\
\text{s.t.} \quad & \boldsymbol{x}(t_{j+1}, \boldsymbol{s}_j, \boldsymbol{q}_j) - \boldsymbol{s}_{j+1} = \boldsymbol{0} \qquad \text{for } j = 0, ..., m-1 \\
& \tilde{\boldsymbol{r}}_{eq,j}(\boldsymbol{s}_0, ..., \boldsymbol{s}_m) = \boldsymbol{0} \qquad \text{for } j = 0, ..., m \\
& \tilde{\boldsymbol{r}}_{ineq,j}(\boldsymbol{s}_0, ..., \boldsymbol{s}_m) \geq \boldsymbol{0} \qquad \text{for } j = 0, ..., m \\
& \boldsymbol{y}^T = (\boldsymbol{s}_0, \boldsymbol{q}_0, \boldsymbol{s}_1, \boldsymbol{q}_1, ..., \boldsymbol{s}_{m-1}, \boldsymbol{q}_{m-1}, \boldsymbol{s}_m, \boldsymbol{p}, T_1, ..., T_{ph})^T
\end{aligned}
\tag{6.25}
$$

The first condition represents the continuity condition at the shooting nodes in state discretization from Equation 6.22. The second and third conditions describe the equality and inequality constraints at the shooting and final nodes. $\boldsymbol{y}^T$ describes a vector of all discretized variables at all nodes, free parameters $\boldsymbol{p}$, and the duration of ph number of phases.

The size of $\boldsymbol{y}$ depends on the problem to be tackled, the number of variables, the number of parameters, the number of phases, and the control discretization. It is calculated with Equation 6.26, with the first term representing the number of state variables across all degrees of freedom and nodes, the second term representing the number of control variables in all shooting nodes, the third term being the number of free parameters, and the fourth being the number of phases. Note that Equation 6.26 is only applicable to piecewise constant control discretization.

$$
n_y = n_x(m+1) + n_u m + n_p + n_{ph} \tag{6.26}
$$

6.3.3 Solution of the Discretized Optimal Control Problem

Equation 6.25 is a result of the discretization process and is a nonlinear programming problem (NLP). Sequential quadratic programming (SQP) is an efficient method for solving nonlinear programs. The general idea is to apply Newton's method to solve the first-order necessary conditions (Karush-Kuhn-Tucker (KKT) conditions) in an iterative manner:

$$
\boldsymbol{y}_{k+1} = \boldsymbol{y}_k + \Delta \boldsymbol{y}_k \tag{6.27}
$$

The step direction, $\Delta \boldsymbol{y}_k$, can be calculated by solving Equation 6.28, which is the quadratic model of the Lagrangian function $\boldsymbol{L}(\boldsymbol{x}, \boldsymbol{\lambda}, \boldsymbol{\mu}) := \boldsymbol{f}(\boldsymbol{x}) - \sum \lambda_i g_i(\boldsymbol{x}) - \sum \mu_i h_i(\boldsymbol{x})$. Note that $\boldsymbol{y} = (\boldsymbol{x}, \boldsymbol{\lambda})^T$ and $\boldsymbol{x}$ represents the state variables.

$$\min_{\Delta \boldsymbol{x}} \quad (\nabla \boldsymbol{f}^k)^T \Delta \boldsymbol{x} + \frac{1}{2}\Delta \boldsymbol{x}^T \boldsymbol{H}^k \Delta \boldsymbol{x}$$
$$\text{s.t.} \quad \boldsymbol{g}(\boldsymbol{x}^k) + \nabla \boldsymbol{g}(\boldsymbol{x}^k)^T \Delta \boldsymbol{x} = \boldsymbol{0} \tag{6.28}$$
$$\boldsymbol{h}(\boldsymbol{x}^k) + \nabla \boldsymbol{h}(\boldsymbol{x}^k)^T \Delta \boldsymbol{x} \geq \boldsymbol{0}$$

$\boldsymbol{H}$ is the Hessian of the Lagrange function. In practice, it is computationally very expensive to evaluate the numerical derivatives numerically, so the Hessian is approximated with the matrix $\boldsymbol{B}$ and the method used for solving the discretized optimal control problem would involve Quasi-Newton or inexact Newton methods [63]. With the computed derivatives, they are integrated to compute the states and trajectories within the shooting intervals. For example, one can use a Runge-Kutta scheme of fourth order with 15 steps each, which is also the integration method adopted in this thesis. One can find the details on SQP methods and KKT conditions in [50].

6.4 Automatic Differentiation

A derivative can be obtained by performing numerical differentiation, symbolic differentiation, or automatic differentiation. Numerical differentiation can be done via external numerical differentiation (derivatives are approximated with the finite difference formula [17]), or internal numerical differentiation (derivatives are approximated using a single discretization scheme with details described in [50]). Symbolic differentiation calculates a function's derivative as a mathematical expression involving symbolic variables using chain rule, product rule etc. [43]. Automatic differentiation combines concepts of numerical differentiation and symbolic differentiation, such that it evaluates the function and its derivatives at given points [16].

Automatic differentiation is known to be an efficient technique for computing derivatives and has two implementation methods. Based on chain rule and other differentiation rules, forward mode separates a mathematical expression into a sequence of differentiable elementary operations, such that derivative and intermediate variable computations are performed in a single forward pass [41]. The second method is the reverse mode, which is separated into two phases. It first populates intermediate variables and stores the dependencies in memory via forward pass, and once the forward pass is complete, the derivatives are computed with respect to the intermediate variables obtained in the first phase [41].

6.5 Software Explored and Used

Developed by Martin Felis from the Optimization, Robotics, and Biomechanics (ORB) Lab in Heidelberg University, the Rigid Body Dynamics Library (RBDL) can perform modeling and dynamics simulation of constrained rigid multi-body systems [27]. It is implemented in C++ and based on Roy Featherstone's 6-D Spatial Algebra, and the highly efficient computation is done through recursive methods. This model-based package can also be utilized with optimization software libraries such as MUSCOD-II to solve an optimal control problem [51].

The original intent was to use RBDL and MUSCOD-II to solve the sit-to-stand optimal control problem involving an elderly woman and the TWIN exoskeleton. RBDL reads model files in Lua, therefore a significant amount of time and effort was spent on creating a Lua file on a lumped model of an elderly woman and TWIN. RBDL-toolkit is the software used for visualizing and animating the Lua model. Given MUSCOD-II's licensing details, this software was not readily available at the time, so other libraries were explored.

RBDL-CasADi is a library available on GitHub that can also perform optimal control on rigid-body dynamics systems. CasADi is an open-source tool that performs nonlinear optimization using a symbolic framework with automatic differentiation (forward and reverse modes implemented) [10]. Although RBDL+MUSCOD-II and RBDL-CasADi can load Lua models and are in C++, the biggest difference lies in the differentiation method since MUSCOD-II performs numerical differentiation. At that time, another MASc candidate was also exploring RBDL-CasADi. We encountered challenges related to syntax implementation (from numerical differentiation to automatic differentiation) and Lua reader errors. Given thesis time constraints, we decided to explore other libraries to seek for alternatives.

Biorbd is a C++ library based on RBDL that can perform rigid body dynamics on multi-body musculoskeletal systems for biomechanics analysis [62]. Bioptim implements the direct multiple-shooting method and can either utilize IPOPT [89] or acados [85] to solve optimal control problems. It utilizes biorbd and CasADi to perform optimization problems through a Python interface [60], and uses Python libraries such as Matplotlib [39], SciPy [86], and NumPy [32]. Bioviz is a Python visualizer that can animate the results generated from bioptim [61]. These three tools are developed by researchers from the Laboratoire de Simulation et Modélisation du Mouvement at Université de Montréal. For the optimal control portion of this thesis, bioptim with the IPOPT backend and bioviz are used.

6.6 Optimal Control Problem Formulation

In this thesis, optimal control is used for motion analysis and motion synthesis. The purpose of motion analysis is to obtain the required kinematics and actuation from the motion capture data, whereas the purpose of motion synthesis is to generate an optimal trajectory. Kinematics and joint torques of the feasible solution (motion analysis) and optimal solution (motion synthesis) are compared.

6.6.1 Motion Analysis

Motion analysis is done via state tracking and is expressed in the context of least-squares tracking. q_d is the joint angular positions generated by the optimal control problem, whereas y_d is the joint angular positions from the reference data. The weight for this least-squares term, σ, is set to 1. A very small minimize torque-squared Lagrange-type objective term, which acts as a regularization term, is added to maintain smooth controls. To ensure this term does not affect the optimizer's ability to track the positional reference data, this term must be very small, and in this thesis, the weight (ψ) is set to 10^{-8}. The first summation refers to the two phases (sitting and lifting), and the inner summation refers to the number of shooting nodes in each phase. Equation 6.29 shows the full OCP formulation for motion analysis.

$$
\begin{aligned}
\min_{x(\cdot)} \quad & \frac{1}{2} \sum_{ph=1}^{n_{ph}=2} \left(\sum_{s_{ph}=1}^{ns_{ph}} \left(\psi ||q_d(t_{s_{ph}}) - y_d(t_{s_{ph}})||^2 + \sum_{i=1}^{n_{act}=10} \int_{t_{s_{ph}-1}}^{t_{s_{ph}}} \sigma \tau_i^2 dt \right) \right) \\
\text{s.t.} \quad & \dot{x}(t) = f_{ph}(t, x(t), u(t), p) \qquad \text{for } t \in [t_{s_{ph}-1}, t_{s_{ph}}] \\
& r_{eq}(x(0), ..., x(t_{s_{ph}}), p) = 0, \qquad \text{for } t \in [t_{s_{ph}-1}, t_{s_{ph}}] \text{ and } s_{ph} \in [1, ns_{ph}] \\
& r_{ineq}(x(0), ..., x(t_{s_{ph}}), p) \geq 0, \qquad \text{for } t \in [t_{s_{ph}-1}, t_{s_{ph}}] \text{ and } s_{ph} \in [1, ns_{ph}] \\
& g_{ph}(t, x(t), u(t), p) \geq 0 \qquad \text{for } t \in [t_{ph-1}, t_{ph}] \text{ and } s_{ph} \in [1, ns_{ph}] \\
& t_0 = 0, t_2 = T
\end{aligned}
\tag{6.29}
$$

The first constraints is the system dynamics and it is the DAE that describes the STS motion in Equation 5.8. r_{eq} and r_{ineq} are the equality and inequality boundary constraints for all shooting nodes in both phases. g_{ph} are the box constraints on system states $[q, \dot{q}, \tau]^T$.

The floating base velocities are bounded at $\pm$ 4 m/s and the joint velocities are bounded at $\pm$ 4 rad/s. The box constraints on position and joint torque bounds can be found in Tables 6.1 and 6.2. The minimum and maximum position values in the recording data are considered in the construction of the position bounds. Since the crutch-less STS motion is performed by the human with motors disengaged, and the intent for MA is to analyze the torque exerted to perform the recorded motion, the torque bounds do not reflect the torque limits of the TWIN exoskeleton.

Table 6.1: Joint position bounds for lumped model in motion analysis.

Joint	DOF	Description	Min	Max
Lumbo-Sacral	transY	Midtrunk-Pelvis forward translation [m]	-0.7	0.7
	transZ	Midtrunk-Pelvis vertical translation [m]	-0.4	0
	rotX	Midtrunk-Pelvis flexion/extension [rad]	-1.0	1.0
Xiphisternal	rotX	Upper trunk flexion/extension [rad]	-1.2	1.0
Lumped Hips	rotX	Left & right hip flexion/extension [rad]	-0.02	2.474
Lumped Knees	rotX	Left & right knee flexion/extension [rad]	-1.807	0.02
Lumped Ankles	rotX	Left & right ankle flexion/extension [rad]	-0.02	0.4
L Shoulder	rotX	Left shoulder flexion/extension [rad]	-1.5	1.5
	rotY	Left shoulder abduction/adduction [rad]	0	1.5
R Shoulder	rotX	Right shoulder flexion/extension [rad]	-1.5	1.5
	rotY	Right shoulder abduction/adduction [rad]	-1.5	0
L Elbow	rotX	Left elbow flexion/extension [rad]	-1.5	1.5
R Elbow	rotX	Right elbow flexion/extension [rad]	-1.5	1.5

Table 6.2: Joint torque bounds for lumped model in motion analysis.

Joint	DOF	Description	Min	Max
Xiphisternal	rotX	Upper trunk flexion/extension [Nm]	-50.0	50.0
Lumped Hips	rotX	Left & right hip flexion/extension [Nm]	-250.0	250.0
Lumped Knees	rotX	Left & right knee flexion/extension [Nm]	-300.0	300.0
Lumped Ankles	rotX	Left & right ankle flexion/extension [Nm]	-250.0	100.0
L Shoulder	rotX	Left shoulder flexion/extension [Nm]	-50.0	50.0
	rotY	Left shoulder abduction/adduction [Nm]	-50.0	50.0
R Shoulder	rotX	Right shoulder flexion/extension [Nm]	-50.0	50.0
	rotY	Right shoulder abduction/adduction [Nm]	-50.0	50.0
L Elbow	rotX	Left elbow flexion/extension [Nm]	-50.0	50.0
R Elbow	rotX	Right elbow flexion/extension [Nm]	-50.0	50.0

6.6.2 Motion Synthesis

The objective function for motion synthesis involves a minimize torque-squared term. This is because joint torque-squared plays a key role in motion optimization [64]. α is the weight for the minimize torque-squared term and is set to value of 10. The first summation refers to the sitting and lifting phases, and the inner summation refers to the number of actuated joints in the model. The full OCP formulation for motion synthesis is shown in Equation 6.30.

$$
\min_{x(\cdot)} \quad \sum_{ph=1}^{n_{ph}=2} \int_{t_{ph-1}}^{t_{ph}} \left(\sum_{i=1}^{n_{act}=10} \alpha \tau_i^2 \right) dt
$$

$$
\begin{aligned}
\text{s.t.} \quad & \dot{x}(t) = f_{ph}(t, x(t), u(t), p) && \text{for } t \in [t_{ph-1}, t_{ph}] \\
& r_{eq}(x(0), ..., x(T), p) = 0 \\
& r_{ineq}(x(0), ..., x(T), p) \geq 0 \\
& g_{ph}(t, x(t), u(t), p) \geq 0 && \text{for } t \in [t_{ph-1}, t_{ph}] \\
& t_0 = 0, t_2 = T
\end{aligned}
\tag{6.30}
$$

Similar to the boundary value problem for motion analysis, the first three constraints represent the system dynamics of the STS motion (DAE from Equation 5.8), equality boundary constraints, and inequality boundary constraints respectively, for all shooting nodes in both phases. g_{ph} are the box constraints formulation on system states and the

velocity bounds are also bounded at ± 4 m/s for floating base and ± 4 rad/s for joints (same as MA). As for joint position and torque bounds, details can be found in Tables 6.3 and 6.4. The torque bounds do not reflect the torque limits of the TWIN exoskeleton because the intent for MS is to provide a baseline on the minimum torque required by the motors to perform an optimal crutch-less STS. The results will then reveal the torque required and provide insight on the type of motors needed.

Table 6.3: Joint position bounds for lumped model in motion synthesis.

Joint	DOF	Description	Min	Max
Lumbo-Sacral	transY	Midtrunk-Pelvis forward translation [m]	-0.7	0.7
	transZ	Midtrunk-Pelvis vertical translation [m]	-0.4	0
	rotX	Midtrunk-Pelvis flexion/extension [rad]	-1.0	1.0
Xiphisternal	rotX	Upper trunk flexion/extension [rad]	-1.0	0.3
Lumped Hips	rotX	Left & right hip flexion/extension [rad]	0	2.474
Lumped Knees	rotX	Left & right knee flexion/extension [rad]	-1.807	0
Lumped Ankles	rotX	Left & right ankle flexion/extension [rad]	0	0.785
L Shoulder	rotX	Left shoulder flexion/extension [rad]	-0.785	3.142
	rotY	Left shoulder abduction/adduction [rad]	0	1.5
R Shoulder	rotX	Right shoulder flexion/extension [rad]	-0.785	3.142
	rotY	Right shoulder abduction/adduction [rad]	-1.5	0
L Elbow	rotX	Left elbow flexion/extension [rad]	0	2.618
R Elbow	rotX	Right elbow flexion/extension [rad]	0	2.618

Table 6.4: Joint torque bounds for lumped model in motion synthesis.

Joint	DOF	Description	Min	Max
Xiphisternal	rotX	Upper trunk flexion/extension [Nm]	-50.0	50.0
Lumped Hips	rotX	Left & right hip flexion/extension [Nm]	-200.0	200.0
Lumped Knees	rotX	Left & right knee flexion/extension [Nm]	-200.0	200.0
Lumped Ankles	rotX	Left & right ankle flexion/extension [Nm]	-100.0	100.0
L Shoulder	rotX	Left shoulder flexion/extension [Nm]	-50.0	50.0
	rotY	Left shoulder abduction/adduction [Nm]	-50.0	50.0
R Shoulder	rotX	Right shoulder flexion/extension [Nm]	-50.0	50.0
	rotY	Right shoulder abduction/adduction [Nm]	-50.0	50.0
L Elbow	rotX	Left elbow flexion/extension [Nm]	-50.0	50.0
R Elbow	rotX	Right elbow flexion/extension [Nm]	-50.0	50.0

6.7 Results

6.7.1 Motion Analysis

In MA, we are solving a least-squares optimization problem with a regularization term. Since the primary goal is analysis, the weights for both objective terms must reflect the importance and size of the quantity. In this thesis, it is decided that the regularization term be at least a factor of 100 smaller than the least-squares term. Fixed to the duration breakdown of the motion capture data, the sitting and lifting phases last 2.45 s and 1.85 s respectively. A frame-by-frame animation of the position tracking results is illustrated in Figure 6.4.
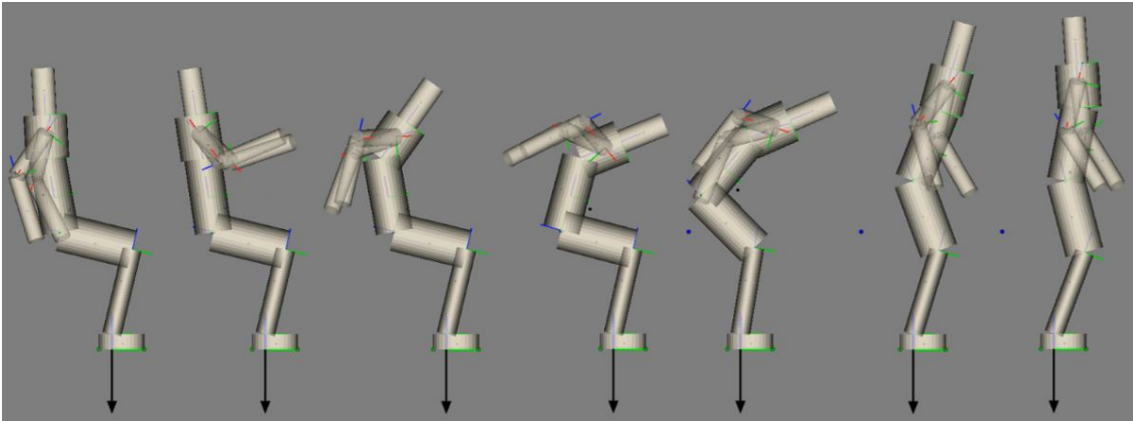
Figure 6.4: Animation frames of feasible solution obtained from MA.

The optimizer is able to closely track upper limb, with minor tracking differences in the floating base DOFs and lower limb joints. Given the way the bioMod model is created, a value of 0 in the floating base's Z direction means the lumped model is standing upright. The time taken to perform the forward trunk-bend prior to lifting is 1.05 s, accounting for 24.4% of the full STS duration of 4.3 s. The largest range of motion (ROM) within this time frame is 0.52 rad. Figures 6.5, 6.6, and 6.7 show the joint position tracking results.
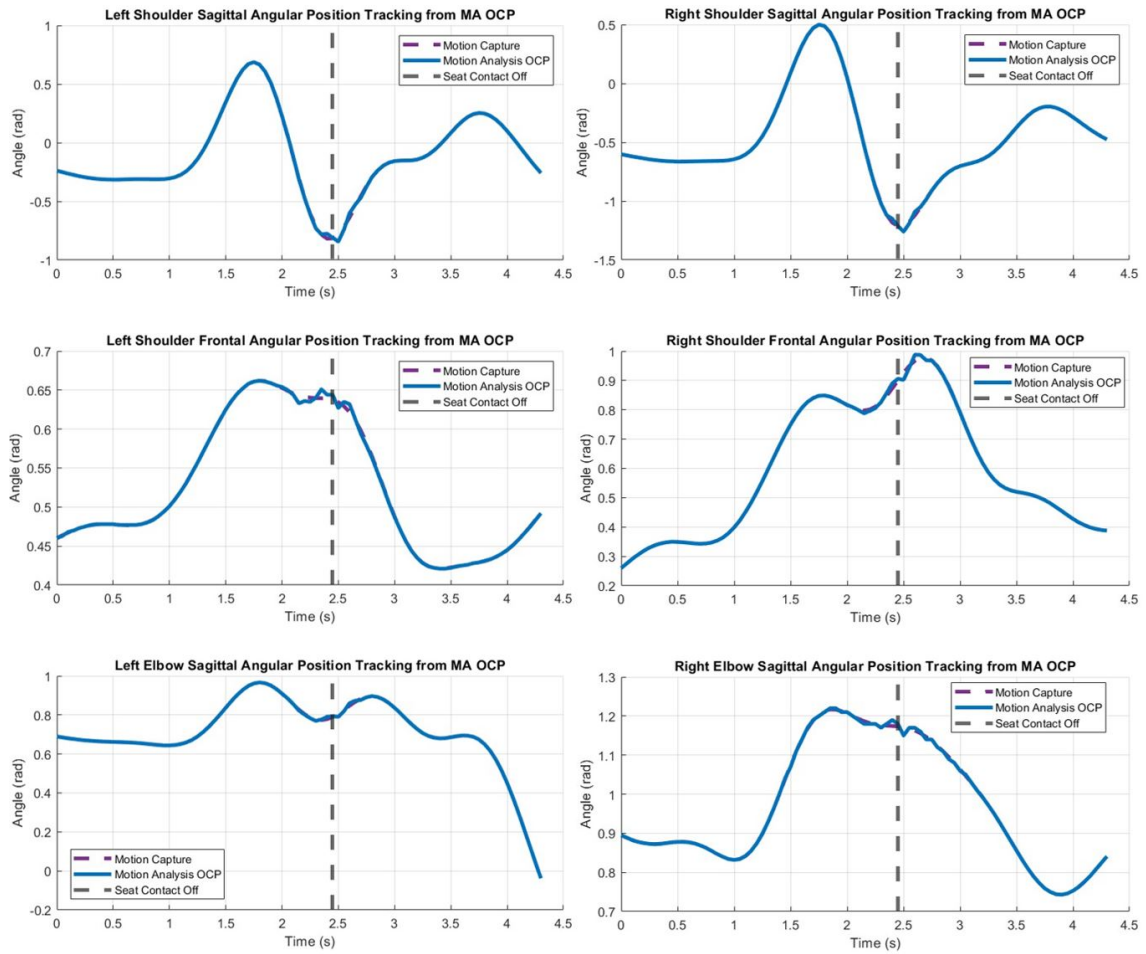
Figure 6.5: Motion analysis OCP results: Joint position tracking at upper limb DOFs.
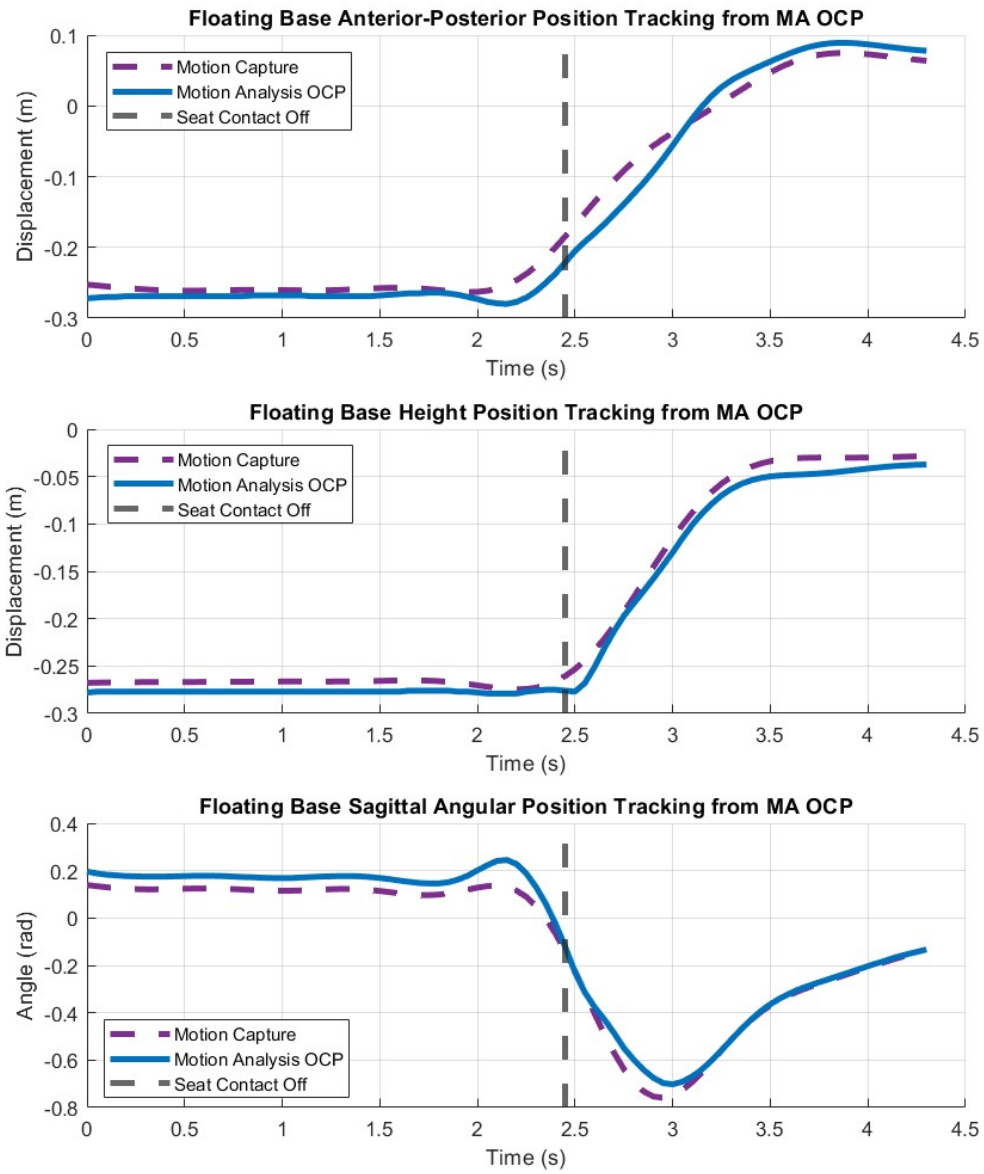
Figure 6.6: Motion analysis OCP results: Position tracking at floating base DOFs.
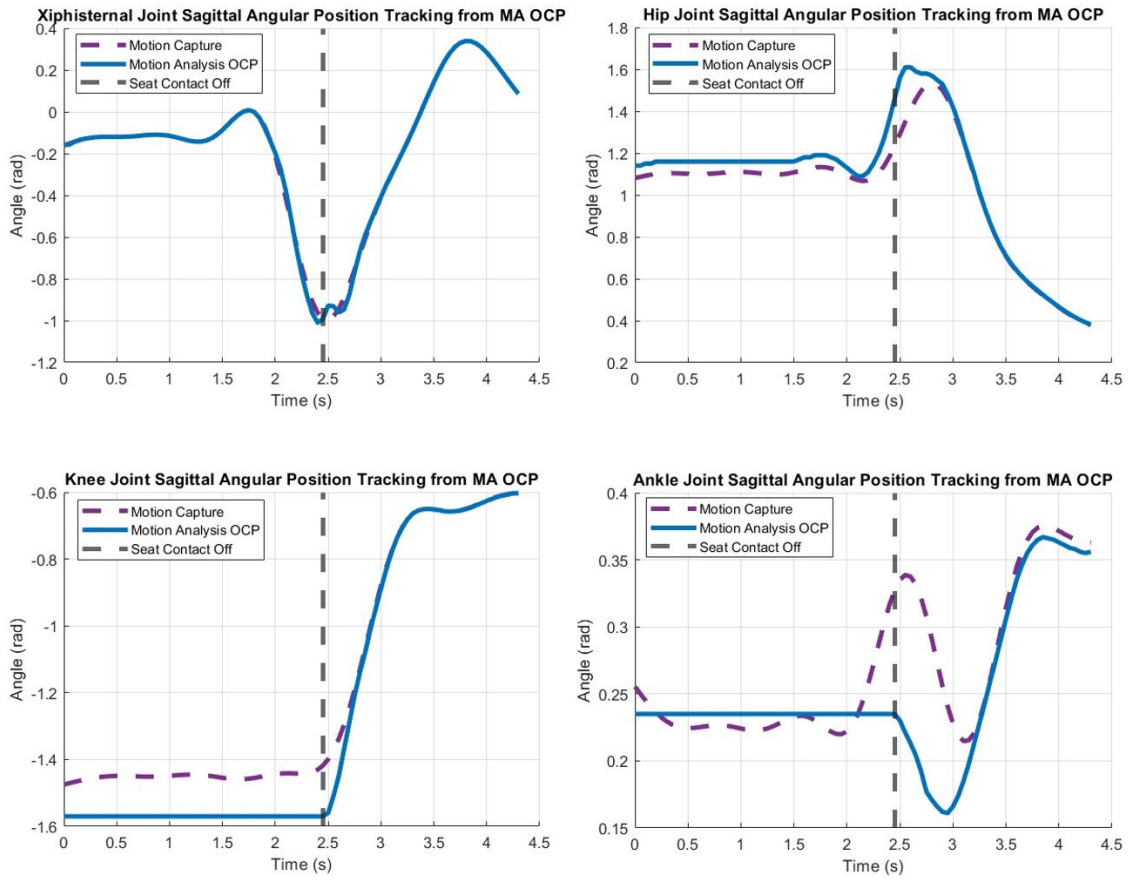
Figure 6.7: Motion analysis OCP results: Joint position tracking at xiphisternal joint and lower limb DOFs.

Looking at the corresponding joint velocity trajectories, the STS motion starts with lifting up the shoulder joints, with activity beginning at around 1 s (see Figure 6.8). The upper trunk then bends forward, with activity beginning at around 1.25 s, followed by the upper body bending about the hip at 2 s (see Figure 6.9). For completeness, the floating base velocities are illustrated in figure 6.10.
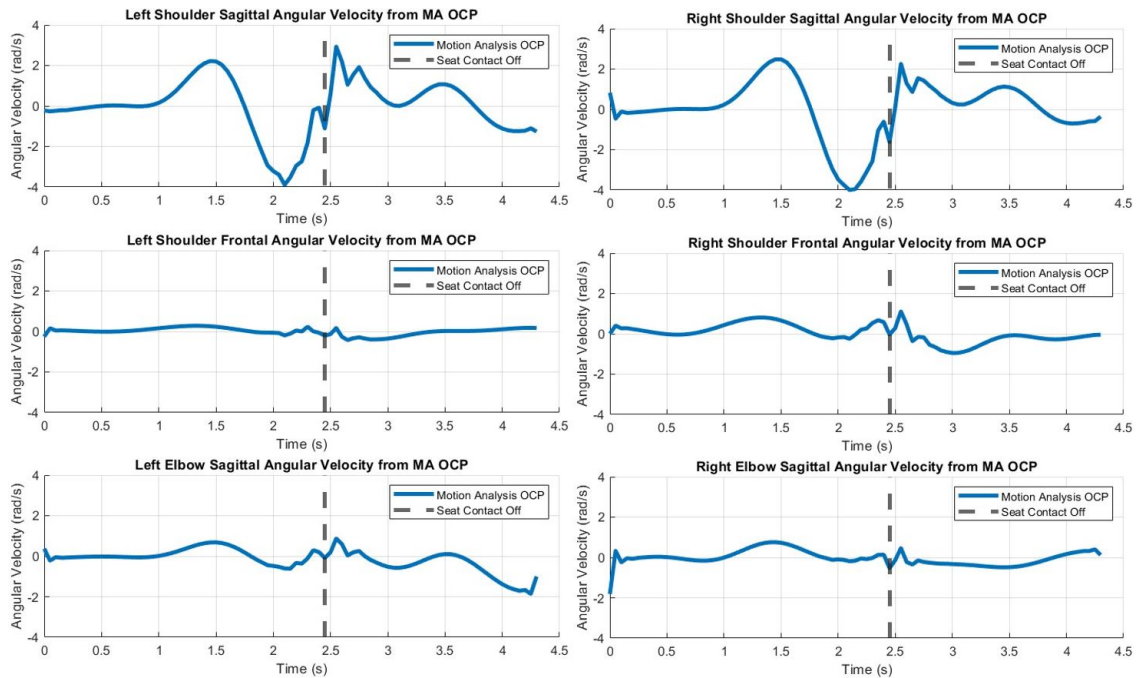
Figure 6.8: Motion analysis OCP results: Upper limb joint velocities.
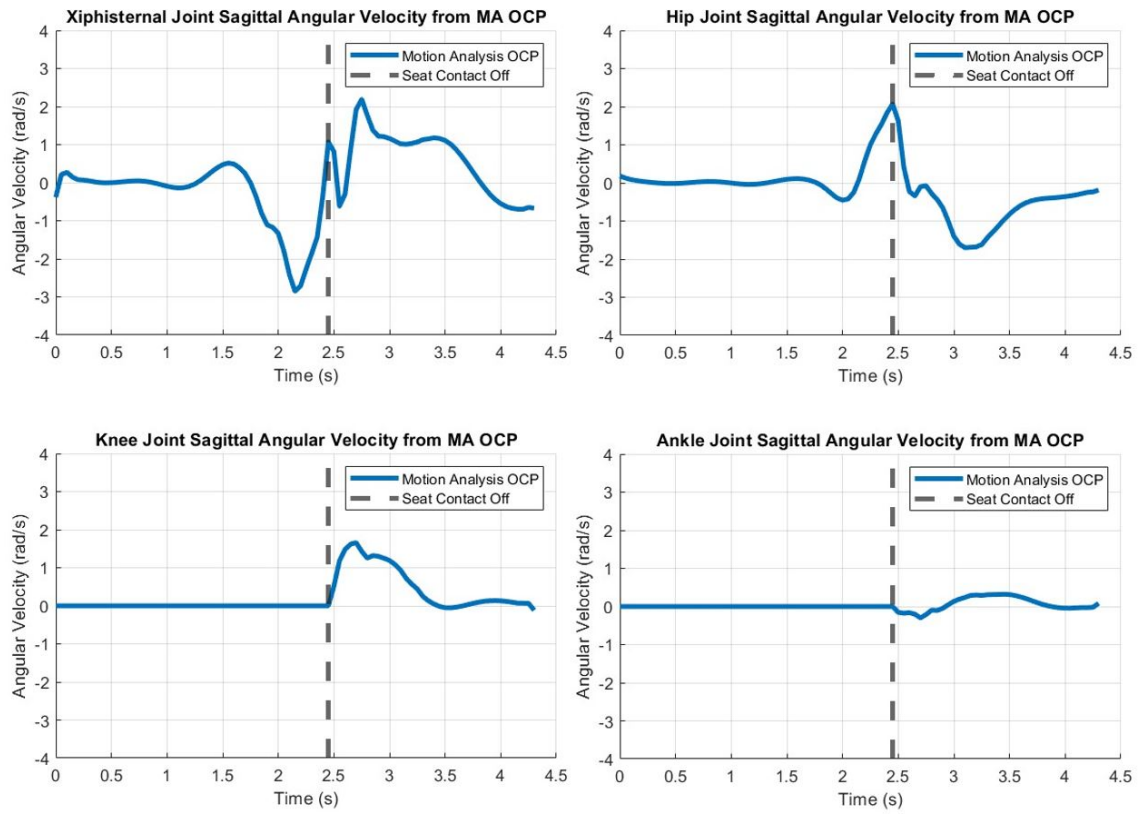
Figure 6.9: Motion analysis OCP results: Xiphisternal and lower limb joint velocities.
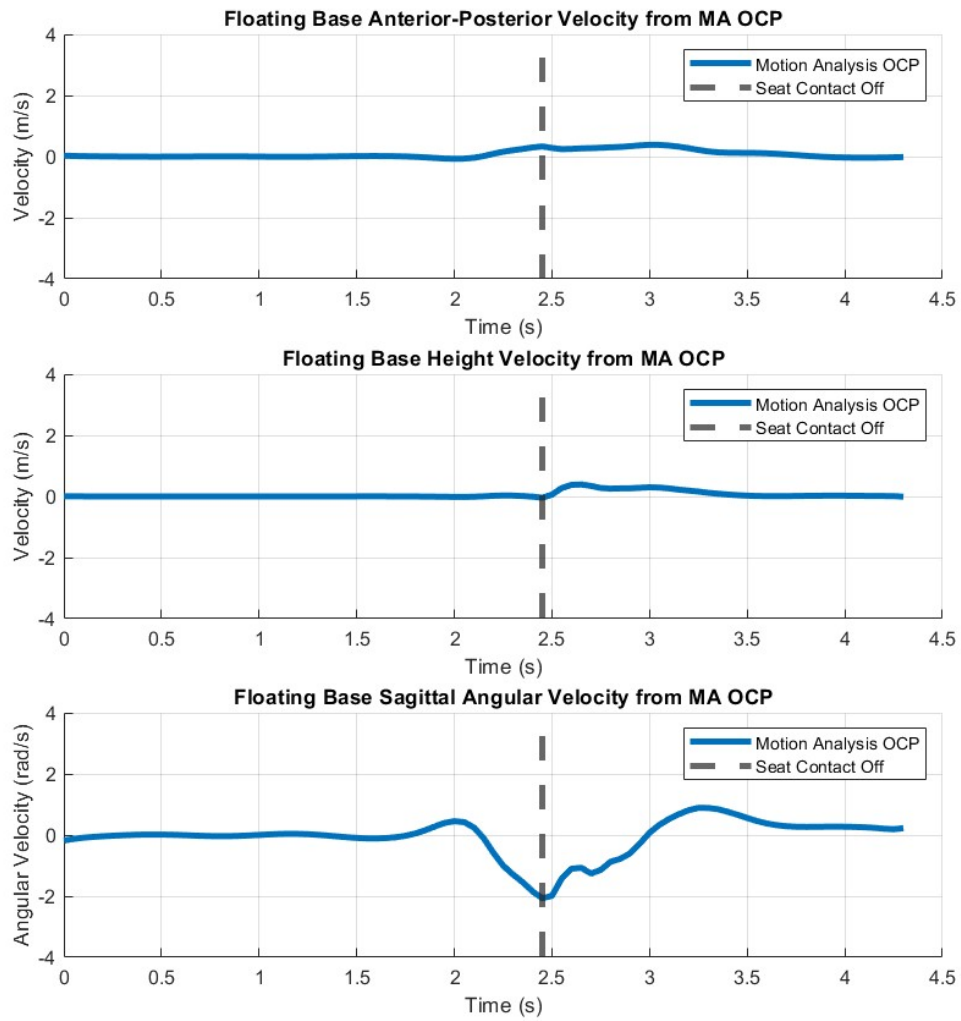
Figure 6.10: Motion analysis OCP results: Floating base velocities.

The required actuation in the joint torques are generated and the trajectories can be seen in Figures 6.11 and 6.12. It is verified that the unilateral constraints are satisfied. The upper and lower limb joints have the most torque activity between 2 s and 3 s, which corresponds to approximately 0.5 s before and after the transition from sitting to lifting. The maximum magnitude of the torques at the xiphisternal joint, lumped hips, lumped knees, and lumped ankles are 40.4 Nm, 120 Nm, 193 Nm, and 120 Nm respectively.
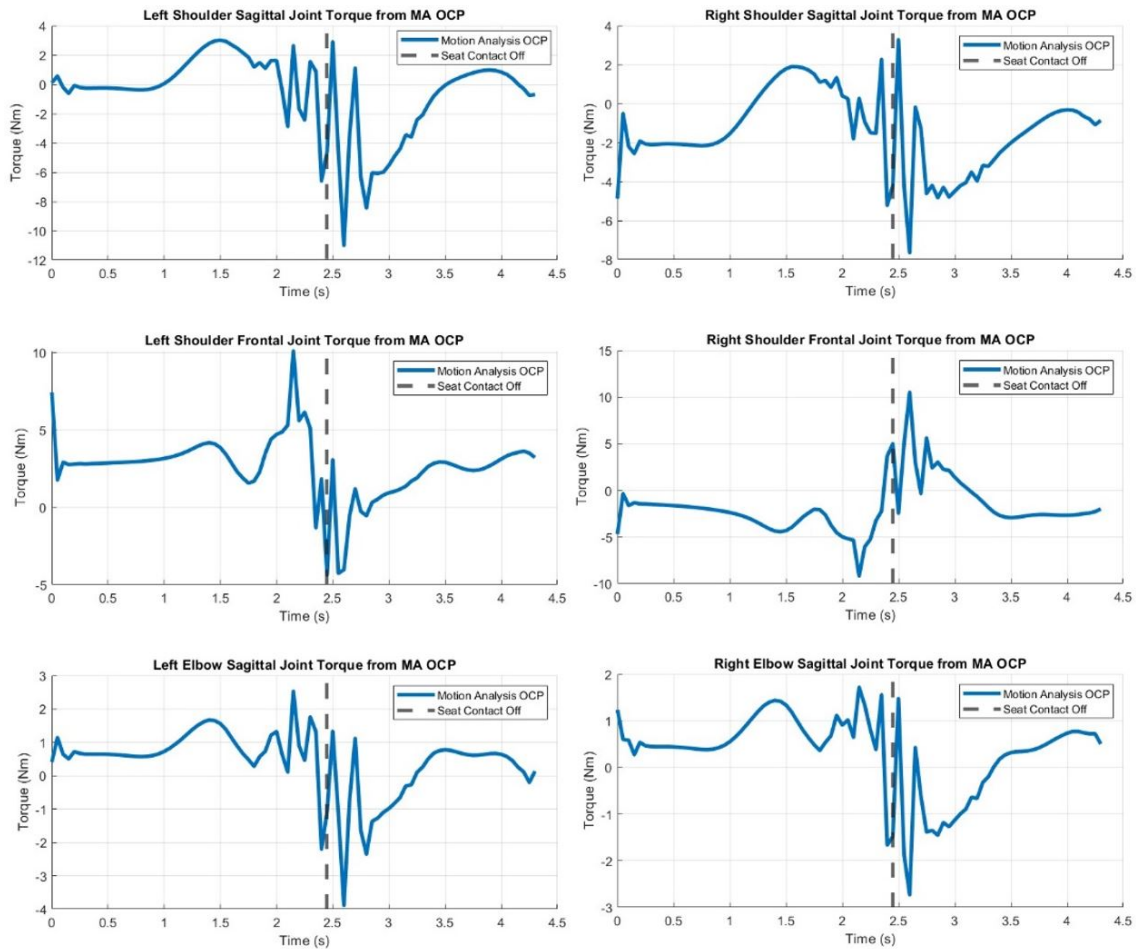
Figure 6.11: Motion analysis OCP results: Upper limb joint torques.
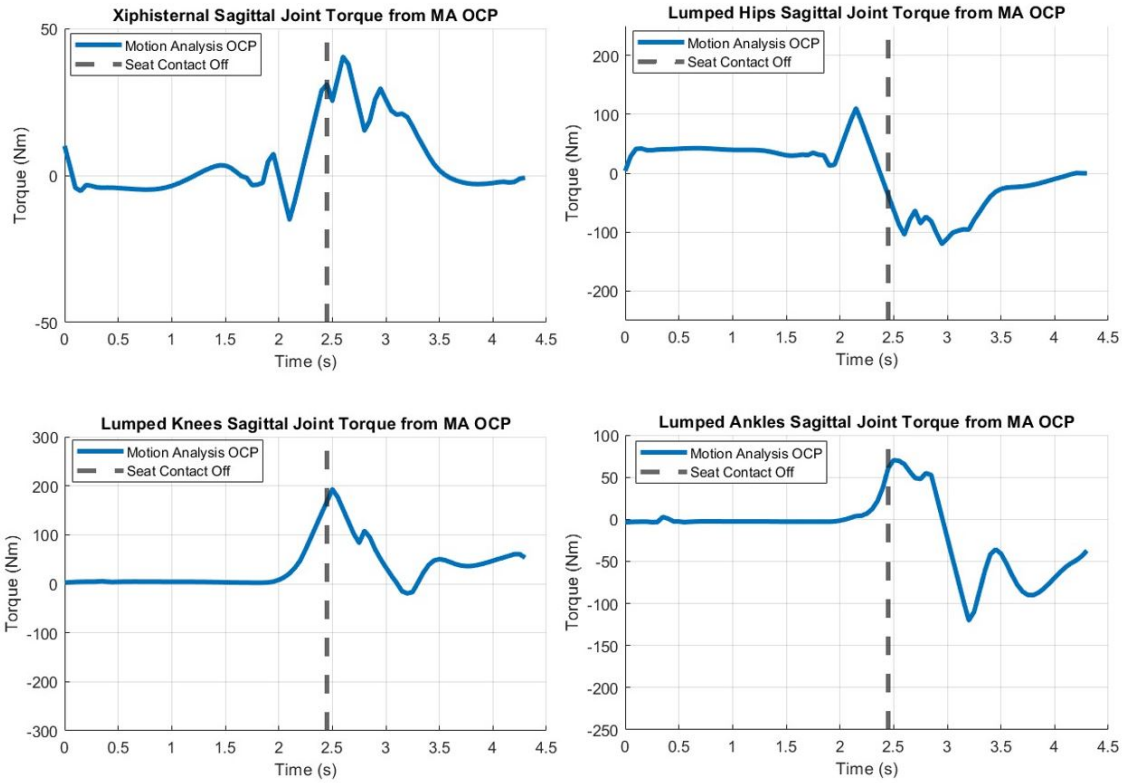
Figure 6.12: Motion analysis OCP results: Xiphisternal and lower limb joint torques.

In the torque plots above, positive is hip extension, knee extension, and ankle plantarflexion. The sum of the cost functions from both phases come to a value of 0.0903, with Table 6.5 lists the breakdown of cost function values per objective term per phase.

Table 6.5: Cost function break-down in motion analysis OCP results.

	Least Squares	Minimize Torque-squared
Phase 1 (Sitting)	$5.95 * 10^{-2}$	$9.33 * 10^{-5}$
Phase 2 (Lifting)	$3.04 * 10^{-2}$	$2.80 * 10^{-4}$

6.7.2 Motion Synthesis

An optimal solution was found and each phase of the full motion lasts 1 s, which is the lower bound set for time since this variable is left free. 1 s for sitting and 1 s for lifting

could be too fast for the elderly. The sudden change in blood flow is likely more pronounced in the geriatric population and possibly making them dizzy. Details in the timing and older adults will be further discussed. A sequence of frames of the resulting animation with scaled time comparing the feasible and optimal solutions are illustrated in Figure 6.13. The upper limb motions from the motion synthesis OCP are symmetrical between left and right. The shoulder flexion/extension and abduction/adduction ROMs are smaller in the optimal solution. In fact, the optimal solution does not suggest any shoulder abduction/adduction movement (see Figure 6.14). Meanwhile, the elbow flexion/extension ROM suggested by the optimal solution is larger than the ROM performed in the feasible solution. The minimum shoulder flexion/extension and maximum elbow flexion/extension occur once the person leaves the seat and enters the lifting phase. The xiphisternal joint's trajectory is different between the optimal and feasible solutions. Throughout the lifting phase, the optimal solution suggests the person to keep their upper trunk as upright as possible, whereas the subject in the feasible solution hunches forward instead. There is also a difference in maximum magnitude of the torque exerted at the xiphisternal joint: 40.4 Nm in the feasible solution and 9.34 Nm in the optimal solution.

As for the lower limb joints, the motion synthesis brings the model to a fully standing position (see Figures 6.15 and 6.16), with the trunk bent slightly forward. Given the way the bioMod model is constructed, a value of 0 in the floating base's Z direction means the lumped model is standing upright. Regarding the forward trunk-bend that occurs immediately before the lifting, the optimal solution's ROM is 0.48 rad lasting 0.4 s (20% of the full duration of 2 s), compared against 0.52 rad ROM and 1.05 s (24.4% of full 4.3 s-duration) in the feasible solution. The maximum magnitude of the torques exerted by the lumped hips, lumped knees, and lumped ankles are 109 Nm (less than MA's), 200 Nm (larger than MA's), and 73 Nm (less than MA's) respectively.

According to the upper body joint velocity plots, the xiphisternal joint, shoulder frontal and elbow sagittal patterns suggest different behaviours. Although MA and MS exhibit a similar pattern in the second half of the duration in the shoulder sagittal DOF, the first half looks different. Particularly, the velocity range of the shoulder in the sagittal direction is slightly smaller in MS compared to MA, whereas the velocity range of the elbow in the sagittal direction is much larger in MS compared to MA. The troughs and crests in the xiphisternal joint between MA and MS are almost opposite of each other. Looking at the lower limb joint velocity plots, the hips and knees in MS share a similar pattern with larger amplitudes in the second half of the motion compared to MA, and the ankles in MS have an opposite pattern than in MA. The slope changes in all three DOFs in MS also seem smoother than the slope changes in MA.

The joint velocity graphs are illustrated in Figures 6.17, 6.18, and 6.19. The joint

torques are shown in Figures 6.20 and 6.21. In all the figures illustrated in this subsection, the grey lines represent the motion analysis OCP trajectories, whereas the black lines represent the motion synthesis OCP trajectories. The times are scaled, with Figure 6.22 reflecting the time differences. Tables 6.6, 6.7, and 6.8 summarize the position, velocity, and torque ranges between motion analysis OCP and motion synthesis OCP. Darker cells represent the results with a larger value range.
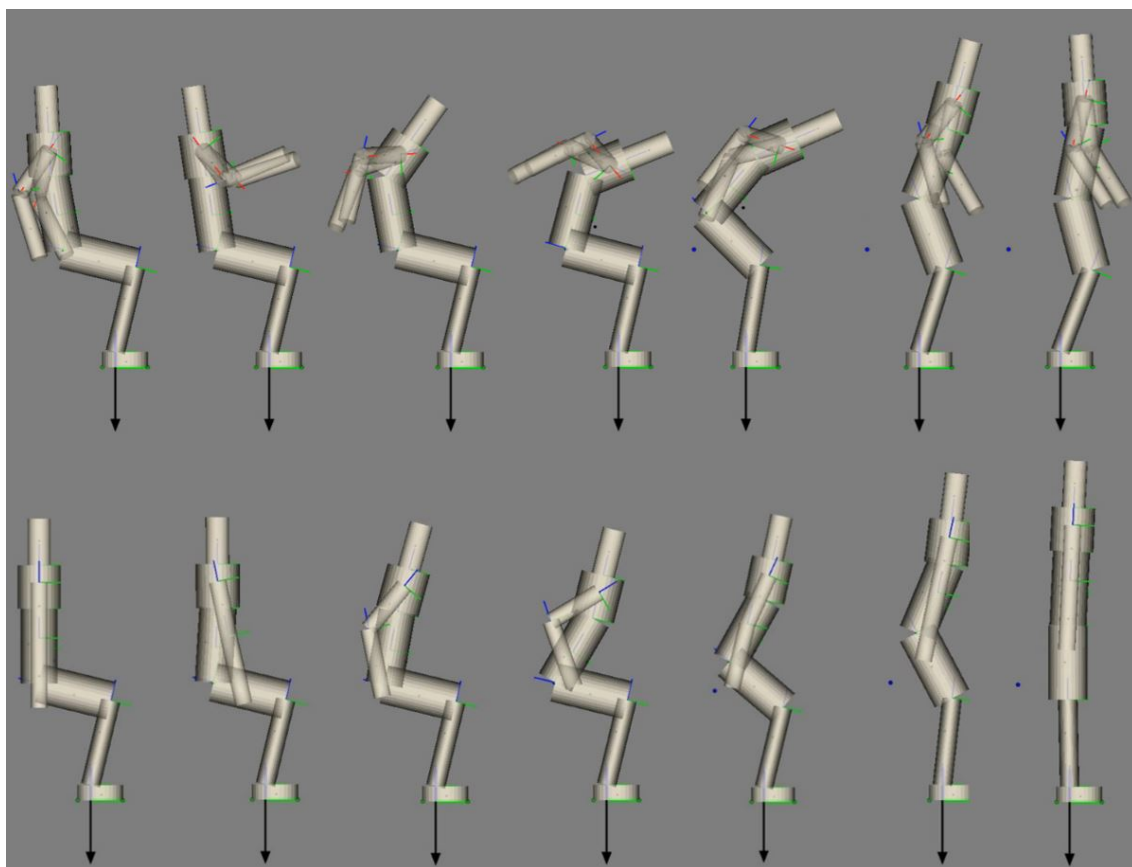
Figure 6.13: Animation frames of feasible solution obtained from MA (top) and optimal solution obtained from MS (bottom).
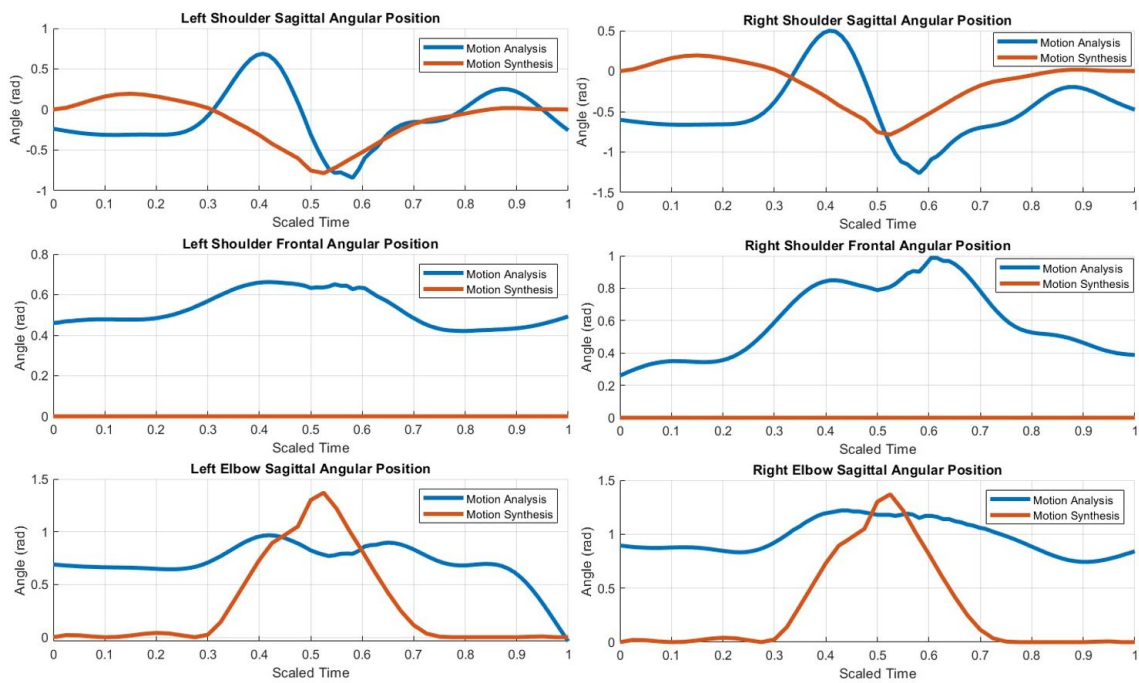
Figure 6.14: Motion synthesis OCP results: Upper limb joint positions.
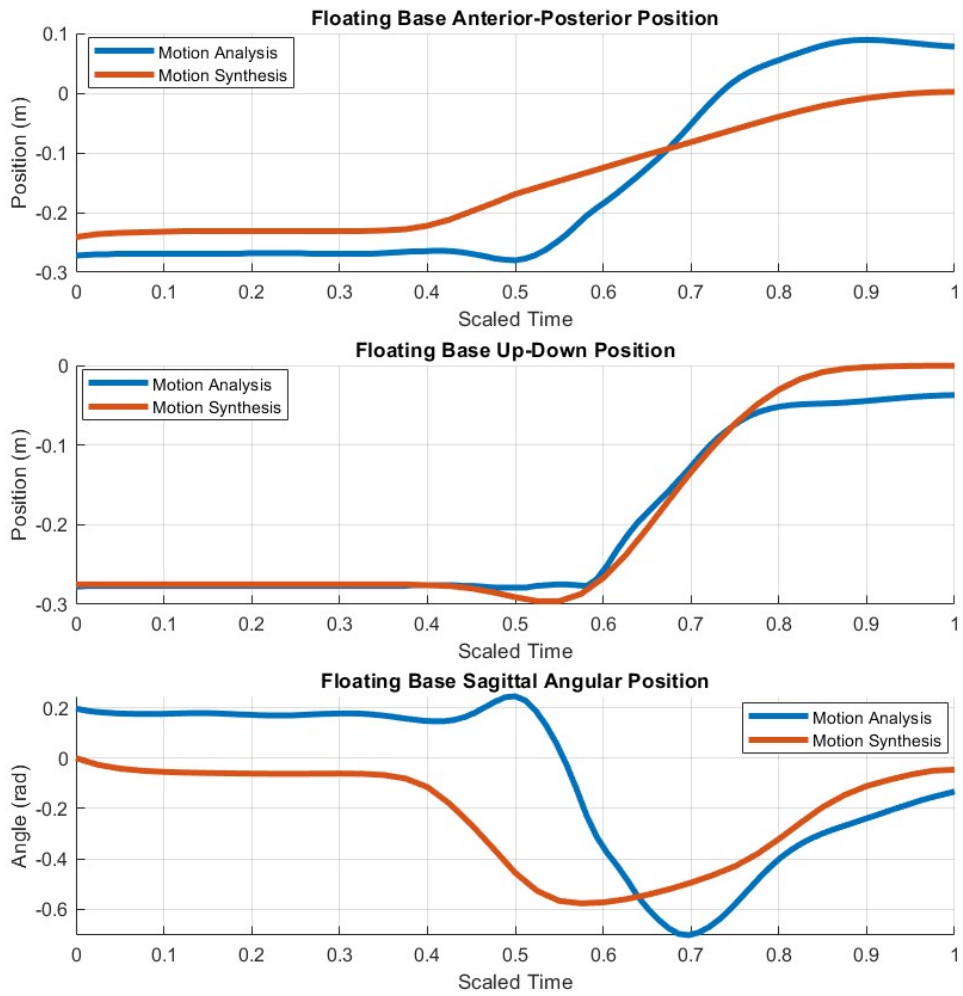
Figure 6.15: Motion synthesis OCP results: Floating base positions.
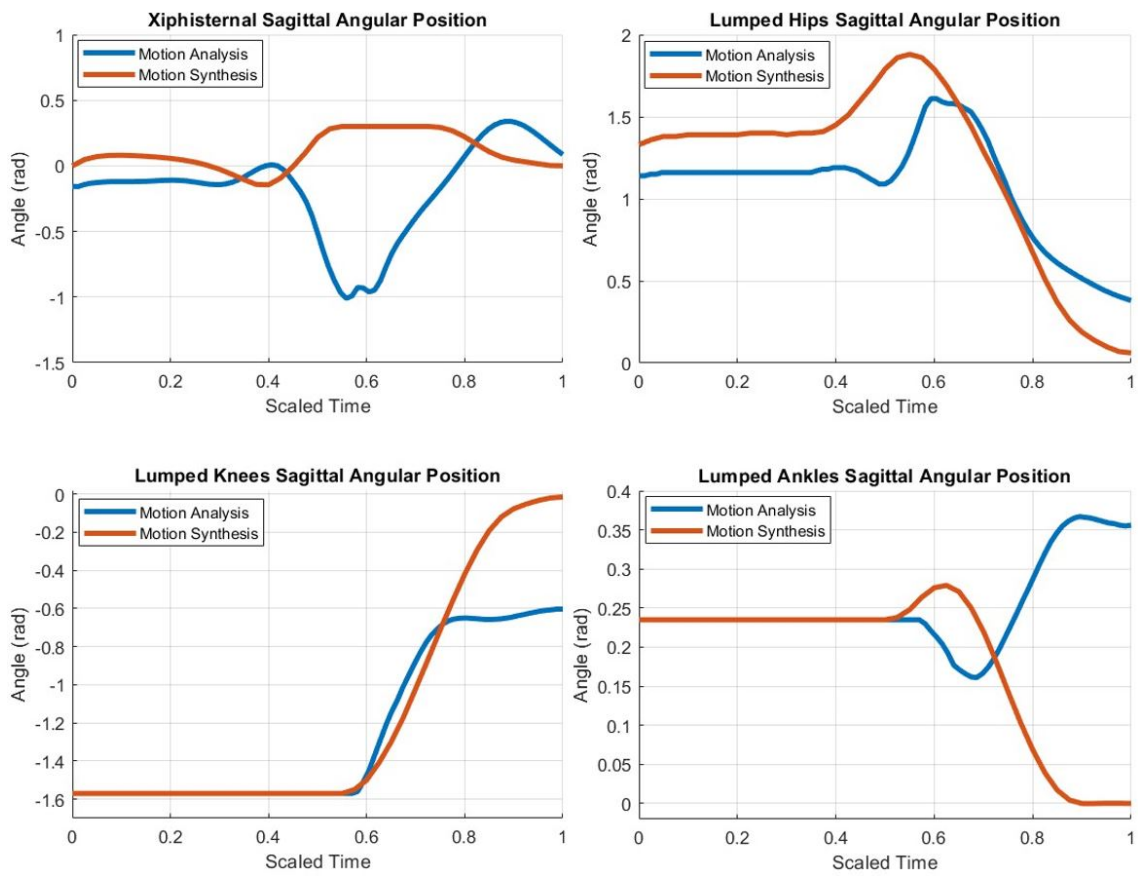
Figure 6.16: Motion synthesis OCP results: Xiphisternal and lower limb joint positions.
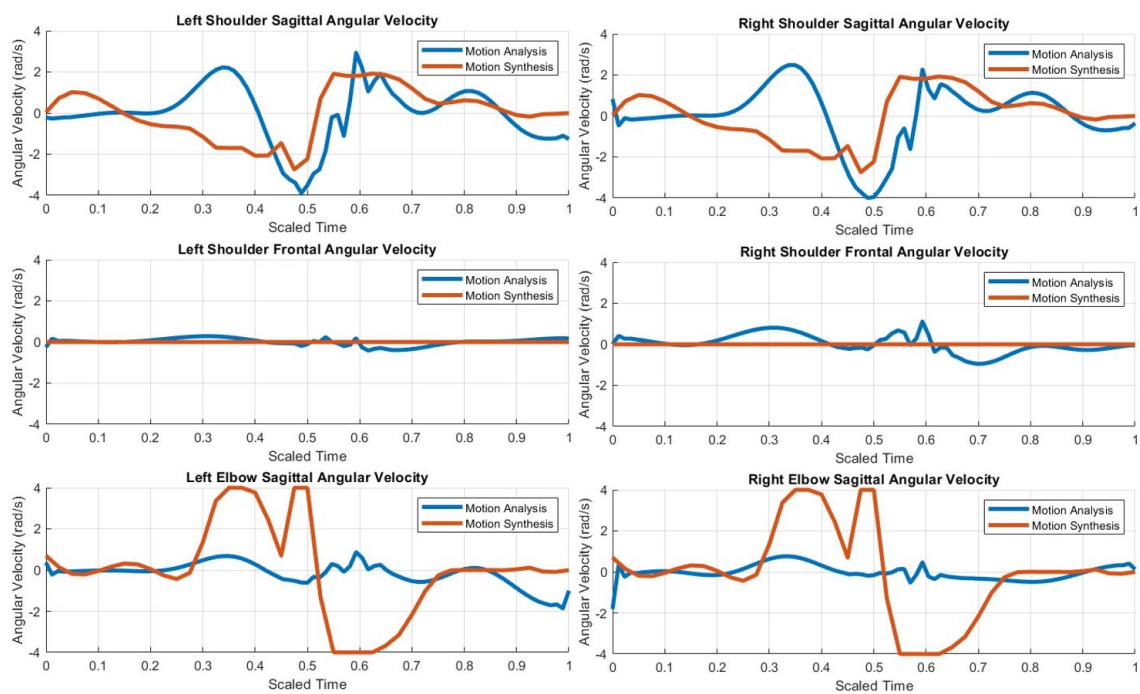
Figure 6.17: Motion synthesis OCP results: Upper limb joint velocities.
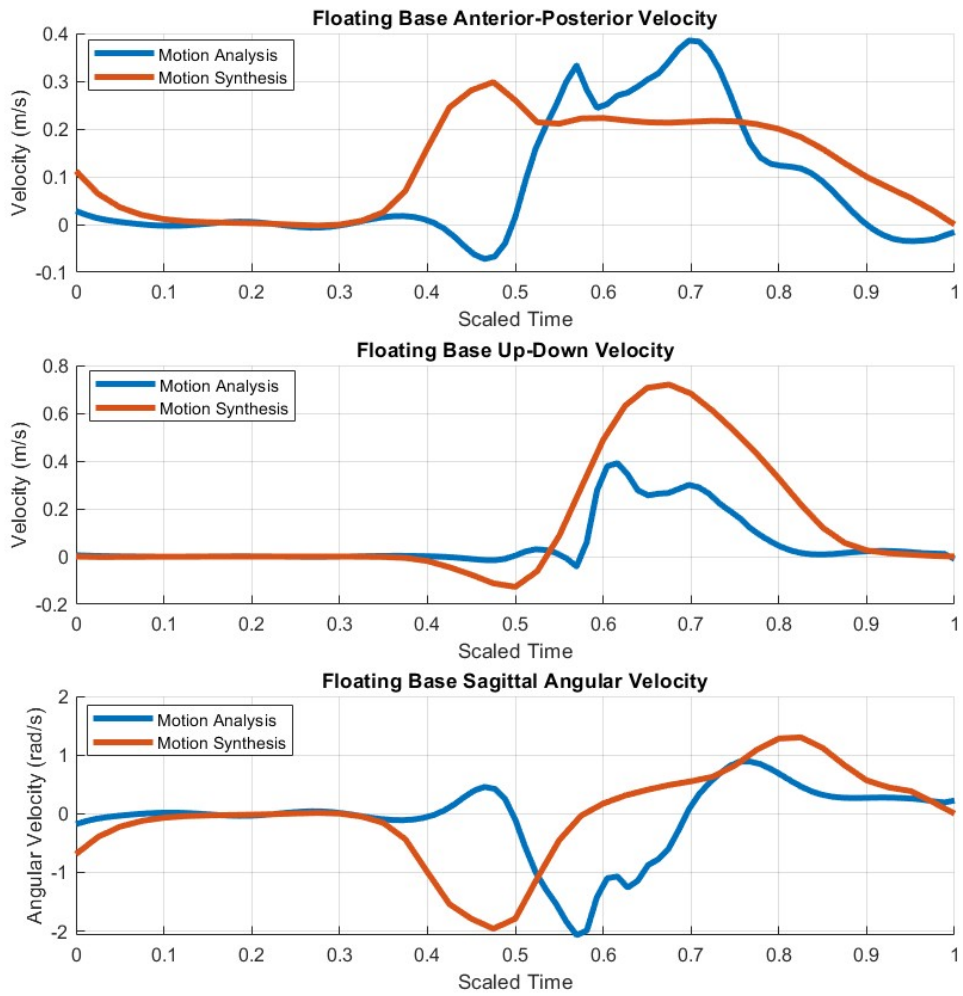
Figure 6.18: Motion synthesis OCP results: Floating base velocities.
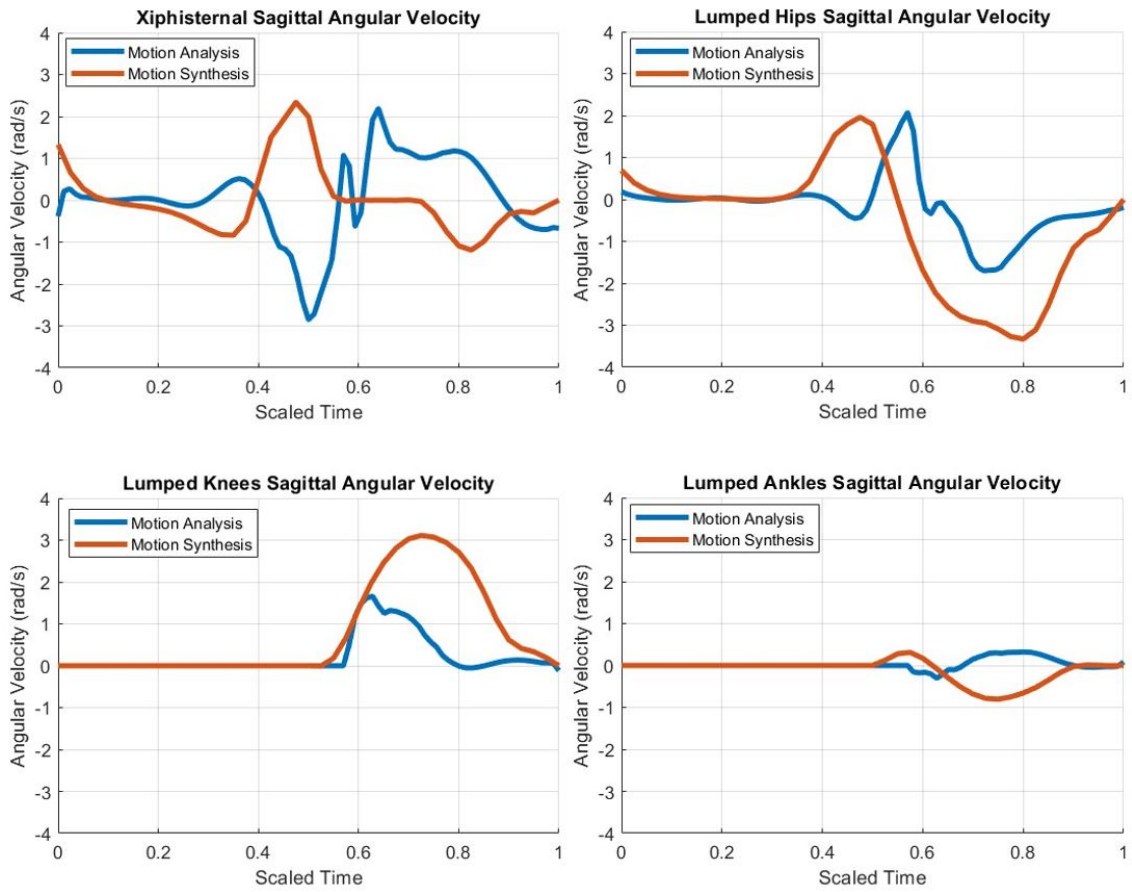
Figure 6.19: Motion synthesis OCP results: Xiphisternal and lower limb joint velocities.
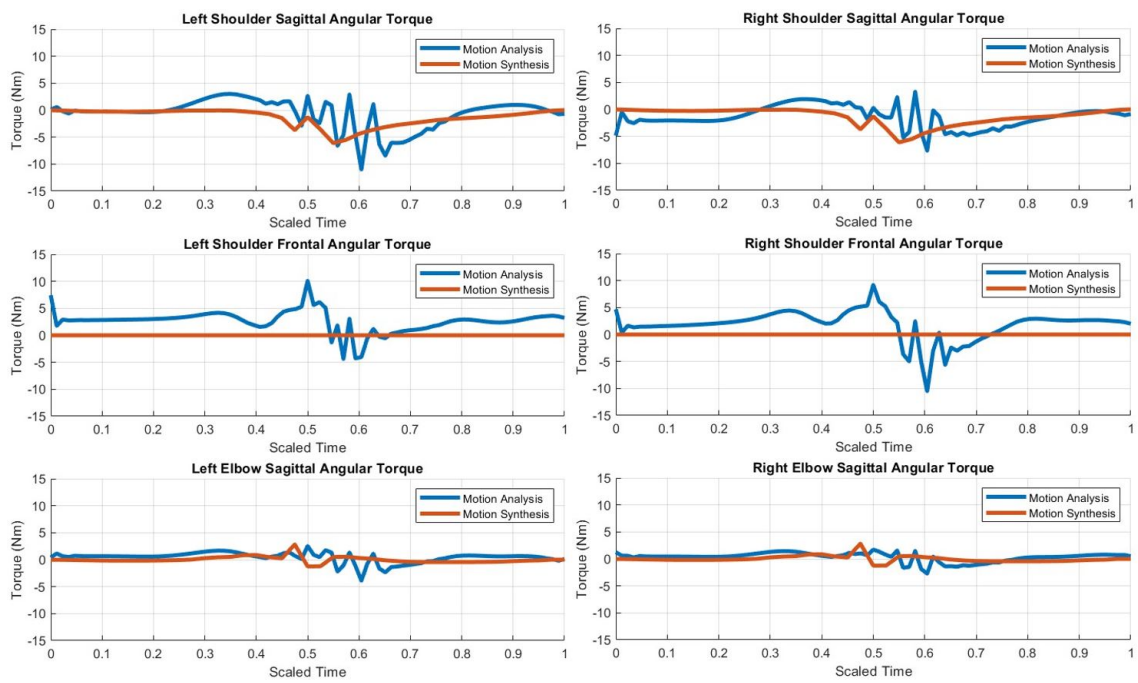
Figure 6.20: Motion synthesis OCP results: Upper limb joint torques.
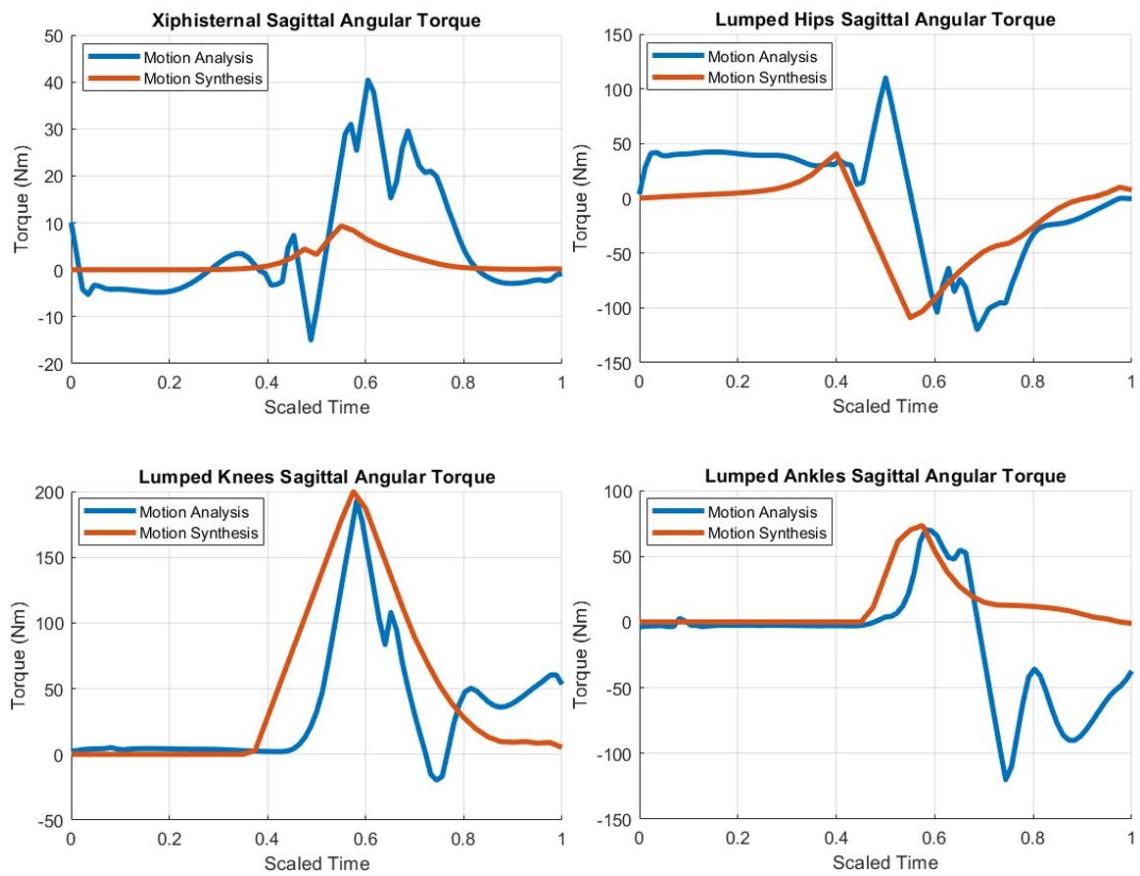
Figure 6.21: Motion synthesis OCP results: Xiphisternal and lower limb joint torques.
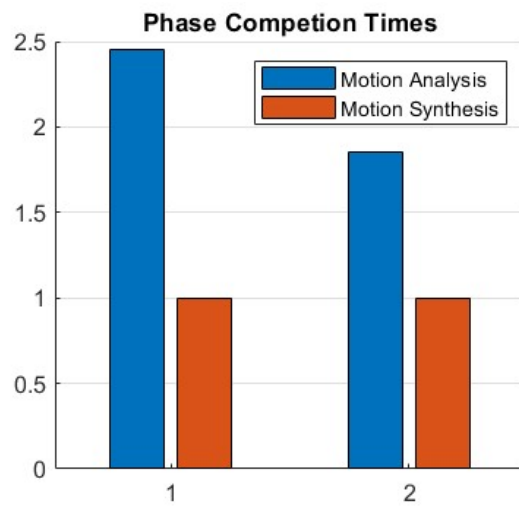
Figure 6.22: Phase completion times for motion analysis and motion synthesis.

Table 6.6: Position range between motion analysis OCP and motion synthesis OCP results.

	Position Range	
	Motion Analysis	Motion Synthesis
Floating base transY (m)	[-0.28, 0.0891]	[-0.241, 0.0022]
Floating base transZ (m)	[-0.279, -0.0373]	$[-0.296, -2.81 * 10^{-4}]$
Floating base rotX (rad)	[-0.702, 0.245]	$[-0.576, 1.34 * 10^{-14}]$
Xiphisternal joint rotX (rad)	[-1.01, 0.339]	[-0.145, 0.3]
Lumped Hips rotX (rad)	[0.381, 1.61]	[0.0612, 1.88]
Lumped Knees rotX (rad)	[-1.57, -0.603]	[-1.57, -0.0153]
Lumped Ankles rotX (rad)	[0.161, 0.367]	$[-9.85 * 10^{-9}, 0.279]$
L Shoulder rotX (rad)	[-0.842, 0.687]	[-0.785, 0.194]
L Shoulder rotY (rad)	[0.421, 0.662]	$[0, 4.75 * 10^{-5}]$
L Elbow rotX (rad)	[0.038, 0.967]	$[-3.01 * 10^{-9}, 1.37]$
R Shoulder rotX (rad)	[-1.26, 0.5]	[-0.785, 0.194]
R Shoulder rotY (rad)	[-0.988, -0.26]	$[-4.76 * 10^{-5}, 0]$
R Elbow rotX (rad)	[0.743, 1.22]	$[-3.01 * 10^{-9}, 1.37]$

Table 6.7: Velocity range between motion analysis OCP and motion synthesis OCP results.

	Velocity Range	
	Motion Analysis	Motion Synthesis
Floating base transY (m/s)	[-0.0722, 0.385]	[-0.0022, 0.298]
Floating base transZ (m/s)	[-0.0412, 0.391]	[-0.127, 0.72]
Floating base rotX (rad/s)	[-2.07, 0.889]	[-1.96, 1.3]
Xiphisternal joint rotX (rad/s)	[-2.85, 2.19]	[-1.19, 2.34]
Lumped Hips rotX (rad/s)	[-1.7, 2.07]	[-3.33, 1.96]
Lumped Knees rotX (rad/s)	[-0.118, 1.66]	[-0.0062, 3.11]
Lumped Ankles rotX (rad/s)	[-0.302, 0.321]	[-0.805, 0.31]
L Shoulder rotX (rad/s)	[-3.89, 2.93]	[-2.74, 1.92]
L Shoulder rotY (rad/s)	[-0.419, 0.281]	$[-1.1 * 10^{-4}, 2.38 * 10^{-4}]$
L Elbow rotX (rad/s)	[-1.86, 0.87]	[-4, 4]
R Shoulder rotX (rad/s)	[-4, 2.48]	[-2.74, 1.92]
R Shoulder rotY (rad/s)	[-1.11, 0.951]	$[-2.38 * 10^{-4}, 1.1 * 10^{-4}]$
R Elbow rotX (rad/s)	[-1.81, 0.759]	[-4, 4]

Table 6.8: Torque range between motion analysis OCP and motion synthesis OCP results.

	Torque Range (Nm)	
	Motion Analysis	Motion Synthesis
Xiphisternal joint rotX	[-15, 40.4]	[-0.0125, 9.35]
Lumped Hips rotX	[-120, 110]	[-109, 40.7]
Lumped Knees rotX	[-19.7, 193]	$[2.61 * 10^{-8}, 200]$
Lumped Ankles rotX	[-120, 70.3]	[-1.14, 73.5]
L Shoulder rotX	[-11, 3.01]	[-6.12, 0]
L Shoulder rotY	[-4.38, 10.1]	$[-2.21 * 10^{-5}, 0]$
L Elbow rotX	[-3.89, 2.53]	[-1.25, 2.82]
R Shoulder rotX	[-7.65, 3.28]	[-6.12, 0]
R Shoulder rotY	[-9.19, 10.5]	$[-3.56 * 10^{-4}, -2.21 * 10^{-5}]$
R Elbow rotX	[-2.73, 1.72]	[-1.25, 2.82]

Table 6.9 shows a breakdown of cost function values per objective term per phase.

Table 6.9: Cost function break-down in motion synthesis OCP results.

	Lower Limb Joints	Upper Body Joints
Phase 1 (Sitting)	$2.349164 * 10^3$	$5.055541 * 10^2$
Phase 2 (Lifting)	$1.544919 * 10^4$	$3.248029 * 10^3$

6.8 Discussion

The second approach taken to improve human-exoskeleton interaction in this thesis uses optimal control to compare the feasible STS motion (via MA) against the optimal STS motion (via MS). The seat height chosen is approximately 120% of the knee height. With both results being able to reach an optimal solution, it shows promise and marks an important first step in creating a crutch-less STS trajectory appropriate for geriatric users wearing the TWIN lower-limb exoskeleton. It makes sense for the cost functions for both OCPs to be consistently higher in the lifting phase than in the sitting phase, since more torque is required to stand up than sitting.

In motion analysis OCP, the upper limb, floating base, and xiphisternal joint position trajectories almost perfectly track the reference data. Some minor differences can be observed in the hip and knee joints during the sitting phase, with an offset of 0.06 rad and

0.095 rad respectively. This could stem from a slight model difference between VSK and bioMod. Although the floating base translation values are scaled to the lumped model's segment lengths, the VSK and bioMod model are not exactly the same. The segments declared in the VSK are highly dependent on the motion capture marker layout. With the presence of TWIN, certain markers in the original IOR marker layout must be relocated to accommodate the device while avoiding occlusion. Although one can redefine variables on Procalc to obtain more accurate translation and position values, there will always be some error from perfectly reflecting the bioMod model, thus introducing offset between reference data and output trajectories. Another option is to completely redesign the human-exoskeleton marker layout to reflect segments that are even more similar to the ones exhibited in the bioMod file. However, the new marker locations must situate on rigid / bony landmarks to avoid displacement from movements, and they must not create occlusion issues. Figure 6.23 illustrates the difference.
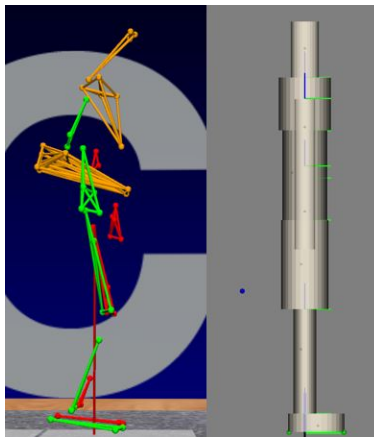
Figure 6.23: VSK (left) and bioMod model (right) standing upright.

As for the ankle joint in MA, the OCP is unable to perfectly track the reference data, with the largest difference of 0.118 rad occurring at 2.55 s. It is possible that the influence of the small minimization of torque-squared objective function causes the joint positions to not track the reference data perfectly. On the other hand, the corresponding joint torque trajectories do not look entirely smooth for all DOFs, thereby indicating the objective function weight for this function is too small. One suggestion is to add a minimization of torque-derivative-squared as a third objective function in the future. Although increasing the weight for minimization of torque-squared is an option for improvement, its consequence can be longer computation time with no optimal solution found. One suggestion is to add a minimization torque-derivative-squared term ($\dot{\tau}^2$). Since this objective function minimizes

the rate of change in the torque, it is hypothesized that including it may eliminate noise and generate smoother torque trajectories.

Sensitivity analysis determines how the output changes based on the input. In the motion analysis OCP, some parameter exploration on the weight of the minimization of torque-squared term has been performed. When increasing this objective term's weight from 10^{-8} to 10^{-7} while keeping the weight of the least-squares term unchanged, the torque trajectories became slightly smoother, though this came at the expense of longer computation time, such that no solution was found even after 2000 iterations (which took 28 hours). These two phenomena can be justified by two reasons. Increasing the weight of an objective term increases its influence in the overall objective function, and minimization of torque squared is known to smoothen motions. Given that the system involved is rather complex with 13 DOFs, one small change in the formulation can vastly change the problem space and influence the capability of reaching an optimal solution. That said, sensitivity analysis is beyond the scope of this thesis.

The larger range in lower limb joints and floating base up-down translation in MS OCP does not mean that the person is not fully standing up in MA OCP/reference data. As mentioned in the section describing the STS biomechanics experiment, TWIN is unable to perfectly fit a subject due to the lack of fine adjustments in the modules. Therefore, the kinematic data shows that the person is not fully standing up when in reality they are. Since MA OCP involves position tracking to the reference data, the error is propagated. This also explains why the knee and ankle torques from MA OCP do not reach 0. From the optimizer's perspective, these angles must remain bent at the end of the motion, therefore a nonzero torque is exerted. Meanwhile, the CoM of the pelvis-midtrunk segment is located posterior to the centre since it is lumped with TWIN's battery pack, which is placed on the back of the trunk module. To ensure the person does not fall backwards when standing, it is likely that the optimal solution ensures the trunk is slightly bent forward at the end of the second phase. That said, more analysis is required to determine the stability of the system. Although there were thoughts of adding an objective term to ensure the total CoM is situated inside the support polygon of the feet, this stability criterion for static motions is not applicable for dynamic motions such as STS. A suggestion would be to investigate how instability can be incorporated in crutch-less STS motion with an exoskeleton in the future.

Immediately before lifting from sitting at a seat height of approximately 120% knee height, the forward trunk-bend behaviour in the optimal and feasible solutions only have a 0.04 rad ROM and 4.4% duration difference. This suggests that the subject's forward trunk-bend motion in preparation for the lifting phase is rather optimal, and hints that the trunk-bend duration for a human-like STS motion should account for between 20% and

25% of the full STS duration. However, this only holds true provided that the full STS duration lasts between 2 s and 5 s.

One reason for the upper body joint behaviours to be different in the feasible solution is the fact that the human is moving the exoskeleton. When standing up immediately after sitting, the upper trunk bend behaviour in MA is to hunch forward, whereas the upper trunk behaviour in MS is to keep as upright as possible. This difference could stem from the absence of motor friction in the MS OCP formulation. Recall that MA reconstructs motion capture data, which is a feasible solution performed by a human wearing the TWIN exoskeleton in the real world. When the motors are disengaged, the user had to exert more torque to overcome the motor friction to make any movements in the lower limbs. When the person was standing up, minimizing joint torque was not a requirement in their mind because their priority is to successfully stand up without falling when wearing the device. Therefore, they hunched their back forward to generate as much momentum as possible. In MS, the trajectory is purely based on the bioMod file, which does not include any information about motor friction. The optimal solution likely assumed that motor friction won't be an issue as illustrated in the feasible solution, so the optimal solution suggests to keep the upper trunk as upright as possible instead. Therefore, the torques presented in this thesis are technically net torques. Meanwhile, this also explains why the xiphisternal joint angular velocity patterns are different between MA and MS.

The difference in upper limb joint velocity behaviours are likely to be influenced by their larger "torque-squared minimization" objective function weight in the MS OCP formulation, such that the amount of torque in these joints have a higher contribution to the objective value. For instance, the elbow joints have a higher joint velocity range due to the low elbow torque exerted.

The opposite joint velocity plot patterns in the ankles is likely linked to its position tracking results, which follows a different trend than the motion capture data. The smoother and larger amplitudes in the hips, knees, and ankles in MS is likely linked to the absence of motor friction consideration in the bioMod model, which is described in the discussion paragraph about the xiphisternal joint behaviours.

Similar to the MA OCP torque results, some sharp turns can be observed in the MS OCP torque trajectories, so it is recommended to test different weights on the minimization of torque-squared objective function. The optimal solution suggests that the crutch-less STS motion can be performed by exerting more torque in the knees and less torque in the xiphisternal and lower limb joints. However, TWIN's motors are unable to perform the optimal solution with full assistance to the user because the maximum combined motor torques at the hips and knees are 112 Nm and 88 Nm respectively [84] The torque required

110

to stand up in both OCPs are similar: almost 110 Nm for the hips, almost 200 Nm for the knees, and around 70 Nm for the ankles. This means TWIN can only provide partial assistance to aid the user performing crutch-less STS. The amount of assistance would depend on the level of lower limb mobility and/or strength in the wearer. Although TWIN already has two assistance modes, current and prospective researchers working with this device can further the development by incorporating the torque values generated from the optimal solution.

Although time is left as a free variable in MS, the OCP formulation does not include an objective function term to minimize time. That said, the optimal solution suggests both phases to be executed with the shortest amount of time declared in 1-4s range. It is possible that more torque is needed as the motion duration lasts longer. Coupled with the lower limb joint torque derivative bounds set to $\pm$ 500 Nm/s, this could explain why the optimal solution took the least time allowed to execute the full STS motion. As mentioned earlier, the 1s-sitting and 1s-lifting in the optimal solution might not be suitable for elderly users. With the cardiovascular system being more affected as a person ages, any sudden change in blood flow can be more pronounced and cause dizziness in the older adult. Suggestions on making the trajectory duration be suitable for older adults include increasing the lower bound of the free time variable, adding an objective function that can represent the change in blood flow of the geriatric cardiovascular system during STS, and reducing the torque-derivative bounds.

6.9 Limitations

Given the use of CasADi for the OCPs presented in this thesis, its symbolic framework has imposed limitations. A symbolic expression is not a vector. Unless there is an explicit function implemented, it is impossible to access individual scalar components within a vector and perform further mathematical operations with the current structure of automatic differentiation in CasADi.

One of the consequences caused by CasADi's limitation is including minimization of mechanical work in the objective function. In [64], minimizing mechanical work in the joints is crucial for generating motions appropriate for the geriatric population, and this value is calculated by summing all products of torque and angular velocity at each actuated joints, i.e. $\sum \tau_i \dot{q}_i$. Although the minimization of torque-squared generates a smooth trajectory, the resulting motions with this objective function alone can look very dynamic. Multiple attempts have been made to include the minimization of mechanical work, which must be added as a custom objective function on bioptim. Not only did the optimizer not yield any

solution, there have been scenarios where the sagittal shoulder and elbow joint torques are oscillating. CasADi's symbolic framework does not allow one to sum all products of torque and angular velocity at each actuated joints. Therefore, in the attempts made on including this objective function, mechanical work was obtained with this operation: $|\boldsymbol{\tau}| \cdot |\dot{\boldsymbol{q}}|$ using $fabs()$. According to a GitHub issue on CasADi [7], one shall use $fabs()$ in CasADi as if they would use $abs()$ in Python, therefore applying $fabs()$ on a vector (τ and $\dot{q}$ in this case) yields a component-wise absolute instead of the vector norm. Although this method of calculating mechanical work yields the same result mathematically, it is unknown if there are other underlying problems of this approach. It is recommended to probe deeper into bioptim's formulation on constructing a custom objective function and implementation with CasADi. This is because the strange motions observed could be caused by hidden and unaddressed factors. In both MA and MS OCP, sensitivity analysis can be explored in the future to investigate how a change in the input can affect the output.

6.10   Future Improvements and Conclusion

Despite the limitations encountered, we have successfully determined the lower-limb joint torques required and the optimal trajectories to perform crutch-less STS. The works covered are considered as a foundation towards generating an appropriate crutch-less STS trajectory for elderly TWIN users.

The research done in the STS trajectory generation portion of this thesis can expand into multiple directions. Based on the lower limb joint torques from the results, one can implement it into existing exoskeletons by adjusting the values to better reflect the human height and lumped segment masses. The implementation can be done in the form of full or partial exoskeleton assistance. In the latter case, the user can decide the level of assistance based on their capabilities. Not only can STS motions from different seat heights be generated, one can also develop a STS controller that automatically deploys the appropriate trajectory by detecting the seat height of the person via the knee angle.

Within the scope of STS, one possibility is to perform MS with a 3D lumped model. The purpose is to obtain an optimal solution for crutch-less STS in 3D space. Involving lower-limb exoskeletons that can only perform flexion/extension, one option is to investigate how other 3D DOFs behave to compensate for the purely-sagittal lower-limb movements. Another option is to evaluate the movement and amount of net torque needed in all human lower limb joint DOFs by setting 6 DOFs in each leg (3 in the hip, 1 in the knee, and 2 in the ankles). Stability evaluation can also be applied on both options, and one can also incorporate stability in the OCP formulation. Another possibility is to re-run the

optimal control problems with a contact model. This can provide information on how the exoskeleton braces maintain contact with the user throughout the motion, and the work can expand further into movement ergonomics.

As covered in the literature review, optimal control is not limited to STS. It can be applied to crutch-less flat-ground walking, sloped walking, rough-terrain walking, stair ascent, stair descent, active self-balancing, and perturbation recovery. With most exoskeletons currently only able to perform STS and flat-ground walking, adding more capabilities can support more activities of daily living and therefore increase the value of exoskeletons.

The ultimate goal is to have exoskeletons provide partial support for elderly persons. The ideal scenario would be the geriatric user initiating and leading the movement, so the exoskeleton would only follow and provide support. The ideal range of assistance is 0% to 75% of the person's body weight since the target elderly population are older adults living with very mild or mild frailty. In other words, motor support would still be present in the 0% assistance case, but the torques exerted would only be responsible for the exoskeleton segments. The amount of assistance would depend on user's strength. One can consider implementing real-time EMG detection, phase detection with joint angles, and time-independent impedance control into the exoskeleton for this kind of support. In a less ideal case, such as the motions are driven by the exoskeleton instead of the user, the timing must be slower than the results presented in this thesis. To generate trajectories, the minimum time must be more than 2 s to avoid sudden change in blood flow. If using the same MS OCP method presented, one should add objective functions to describe geriatric motion and cardiovascular behaviour and increase the lower bound of the free time variable.

Chapter 7

Summary and Future Prospects

7.1   Summary of Results

The experiences of two graduate students from the lab wearing the TWIN exoskeleton for the first time indicate that an exoskeleton's motions can be intimidating to first-time users. There are little-to-no instructions available to teach people how to move with such a device, nor is there research done in this area so far. Therefore, we developed a novel tutorial and evaluated its effectiveness with a small group of lab members. Due to COVID-19 restrictions, external members are not allowed for recruitment. According to the preliminary results, the participants view the tutorial as beneficial, though the group who received it experienced higher mental demands, higher physical demands, and poorer perceived performance. This is likely caused by the constant need to recall concepts learned in the tutorial, a longer experiment duration (the tutorial and walking trials occur within one session), and the exoskeleton demonstrations unintentionally created an expectation for the users to meet. Various suggestions on making the tutorial appropriate for older adults are identified, such as dedicating free interaction time with the device, spanning the experiment over multiple sessions, including biomechanics measurements, making the tutorial safer by creating an "acquaintance mode" in the exoskeleton, and increasing study sample size.

Optimal control has shown promise in generating more natural and human-like trajectories, and this thesis has demonstrated the possibility of analyzing a motion capture recording of crutch-less STS and generating an optimal crutch-less STS trajectory. Considering a lumped model of an elderly woman with TWIN that allows for upper body movements, the net lower limb joint torques required to perform the feasible and optimal solutions are determined. Comparisons between the solutions are also made. The optimal solution

suggests to perform STS with less arm abduction/adduction movement. The optimal solution also suggests the person to keep their upper trunk as upright as possible, which is opposite of what is performed in the feasible solution. In preparation for the lifting motion, the forward trunk-bend behaviour is similar in the feasible and optimal solutions. To make the crutch-less STS motion more natural, the forward trunk-bed should last between 20% and 25% of the entire duration with a ROM between 0.48 rad and 0.52 rad, given that the full duration lasts between 2 s and 5 s. The results presented are considered preliminary works towards an elderly-friendly STS motion with the exoskeleton, so further improvements on making the optimal trajectory suitable for the target population are identified. Despite the limitations faced, the optimal control work presented lays the groundwork for future related development.

7.2   Future Prospects

The preliminary study on the exoskeleton tutorial features an aspect that is often overlooked in wearable robots, but more work still must be done to evaluate its true effectiveness and for it to be suitable for the geriatric population. Details on future improvements specific to the preliminary study can be found in Chapter 3. In general, it is beneficial to have the target population interact with an exoskeleton first-hand. Any misconceptions related to the device can be clarified through conversations and real-life demonstrations, so it is possible to reduce/eliminate the older adult's pre-existing bias against robotic interventions. As they share their experience with friends and family, more people would be informed about what an exoskeleton really is, and possibly improving exoskeleton acceptance in the geriatric population. The tutorial introduced is transferable to any lower-limb exoskeletons with any control methods. After all, it is a tool made for a new user to get acquainted with the device, so the tutorial is applicable to the device and movement modes of interest by undergoing minor modifications.

The optimal control approaches covered in this thesis are preliminary works towards generating STS trajectories suitable for the geriatric population. Details on how to improve the OCP formulation for this target population can be found in Chapter 6. Optimal control is versatile because not only can it be expanded to other motions like human-exoskeleton perturbation recovery and stair walking without crutches, it is also transferable to any lower-limb exoskeletons by simply changing the model definition of the system. This method of trajectory generation further enables the possibility of modifying existing lower-limb exoskeletons in the market, and possibly making them more inclusive towards a larger number of target populations. The output optimal trajectories are not limited to time-

dependent control methods, meaning they can also be utilized as reference trajectories in the time-independent control methods described in Chapter 2.

Although the novel tutorial and optimal control are two vastly different approaches in nature, they complement each other to improve the interaction between the human and exoskeleton. Once the exoskeleton is programmed with the assistance modes suitable for older adults living with very mild or mild frailty, researchers and healthcare professionals can work together to teach the target population how to move with the device with the improved tutorial. Biomechanics measurements can also be utilized to evaluate the performance and analyze what further improvements can be made in the exoskeleton behaviours. Therefore, researchers are recommended to investigate methods of helping target users get acquainted with the device to improve device acceptance, and not solely focus on algorithm development.

References

[1] Easywalk. Accessed: 2023-04-24.

[2] Myosuit. Accessed: 2023-04-24.

[3] Restore. Accessed: 2023-04-24.

[4] Restore exo-suit faqs. Accessed: 2023-04-24.

[5] Restore exo-suit robotic system. Accessed: 2023-04-24.

[6] Soft lower rehabilitation exoskeleton. Accessed: 2023-04-24.

[7] abs/fabs in python not functional. *https://github.com/casadi/casadi/issues/60*, 2012.

[8] Twin, l'esoscheletro. dai robot all'uomo, la ricerca iit per la salute - lorenzo de michieli al wmf (youtube video), 2019.

[9] Felix Aller, Monika Harant, and Katja Mombaur. Optimization of dynamic sit-to-stand trajectories to assess whole-body motion performance of the humanoid robot reem-c. *Frontiers in Robotics and AI*, 9, 2022.

[10] Joel A. E. Andersson, Joris Gillis, Greg Horn, James B. Rawlings, and Moritz Diehl. Casadi: a software framework for nonlinear optimization and optimal control. *Mathematical Programming Computation*, 11, 2019.

[11] Narong Aphiratsakun, Kittipat Chairungsarpsook, and M. Parnichkun. Zmp based gait generation of ait's leg exoskeleton. *2010 The 2nd International Conference on Computer and Automation Engineering, ICCAE 2010*, 5:886–890, 02 2010.

[12] Narong Aphiratsakun and Manukid Parnichkun. Balancing control of ait leg exoskeleton using zmp based flc. *International Journal of Advanced Robotic Systems*, 6(4):34, 2009.

[13] Arash Arami. Human movement neuromechanics lecture notes on force-torque relation and articulated system dynamics, January 2021.

[14] Aaron Bangor, Philip T. Kortum, and James T. Miller. An empirical evaluation of the system usability scale. *International Journal of Human–Computer Interaction*, 24(6):574–594, 2008.

[15] Romain Baud, Ali Reza Manzoori, Auke Ijspeert, and Mohamed Bouri. Review of control strategies for lower-limb exoskeletons to assist gait. *Journal of NeuroEngineering and Rehabilitation*, 18, 2021.

[16] Atilim Gunes Baydin. Automatic differentiation (or differentiable programming). *https://gbaydin.github.io/assets/pdf/slides-baydin-ad-atipp16.pdf*, 2016.

[17] Hans Georg Bock. Recent advances in parameteridentification techniques for o.d.e. In Peter Deuflhard and Ernst Hairer, editors, *Numerical Treatment of Inverse Problems in Differential and Integral Equation*, pages 95–121, Heidelberg, Fed. Rep. of Germany, 1982. Springer.

[18] John Brooke. Sus: A retrospective. *Journal of Usability Studies*, 8:29–40, 2013.

[19] Carlos Jose Calleja, Hadassah Drukarch, and Eduard Fosch-Villaronga. Diversity observations in an exoskeleton experiment. In *Workshop DEI HRI 2022*, 2022.

[20] Adam Carlan. Eksonr - the next step in neurorehabilitation. 2021.

[21] Jose L Contreras-Vidal, Nikunj A Bhagat, Justin Brantley, Jesus G Cruz-Garza, Yongtian He, Quinn Manley, Sho Nakagome, Kevin Nathan, Su H Tan, Fangshi Zhu, and Jose L Pons. Powered exoskeletons for bipedal locomotion after spinal cord injury. *Journal of Neural Engineering*, 13(3):031001, 2016.

[22] Maria del Rio Carral, Vanlisa Bourqui, Noémie Vuilleumier, Amalric Ortieb, and Mohamed Bouri. Are functional measures sufficient to capture acceptance? a qualitative study on lower limb exoskeleton use for older people. *International Journal of Social Robotics*, 2021.

[23] United Nations Population Division. *World population ageing, 2019: highlights*. New York, 2019.

[24] Alexis Duburcq, Yann Chevaleyre, Nicolas Bredeche, and Guilhem Boéris. Online trajectory planning through combined trajectory optimization and function approximation: Application to the exoskeleton atalante. In *2020 IEEE International Conference on Robotics and Automation (ICRA)*, pages 3756–3762, 2020.

[25] Alexander Duschau-Wicke, Joachim Zitzewitz, Andrea Caprez, Lars Lünenburger, and Robert Riener. Path control: A method for patient-cooperative robot-aided gait rehabilitation. *IEEE transactions on neural systems and rehabilitation engineering : a publication of the IEEE Engineering in Medicine and Biology Society*, 18:38–48, 02 2010.

[26] Ryan J. Farris. *Design of a powered lower-limb exoskeleton and control for gait assistance in paraplegics*. PhD thesis, 2012. Copyright - Database copyright ProQuest LLC; ProQuest does not claim copyright in the individual underlying works; Last updated - 2022-01-10.

[27] Martin L. Felis. Rbdl: an efficient rigid-body dynamics library using recursive algorithms.

[28] Martin Leonhard Felis. *Modeling Emotional Aspects in Human Locomotion*. PhD thesis, Heidelberg University, 2015.

[29] Eduard Fosch-Villaronga, Carlos Calleja, and Hadassah Drukarch. D1.1 report on the identified areas for regulatory improvement for lower-limb exoskeletons. Technical report, eLaw, Leiden University, January 2022.

[30] C. Dominik Güss. What is going through your mind? thinking aloud as a method in cross-cultural psychology. *Frontiers in Psychology*, 9, 2018.

[31] Omar Harib, Ayonga Hereid, Ayush Agrawal, Thomas Gurriet, Sylvain Finet, Guilhem Boeris, Alexis Duburcq, M. Eva Mungai, Matthieu Masselin, Aaron D. Ames, Koushil Sreenath, and Jessy Grizzle. Feedback control of an exoskeleton for paraplegics: Toward robustly stable hands-free dynamic walking, 2018.

[32] Charles R. Harris, K. Jarrod Millman, Stéfan J. van der Walt, Ralf Gommers, Pauli Virtanen, David Cournapeau, Eric Wieser, Julian Taylor, Sebastian Berg, Nathaniel J. Smith, Robert Kern, Matti Picus, Stephan Hoyer, Marten H. van Kerkwijk, Matthew Brett, Allan Haldane, Jaime Fernández del Río, Mark Wiebe, Pearu Peterson, Pierre Gérard-Marchant, Kevin Sheppard, Tyler Reddy, Warren Weckesser, Hameer Abbasi, Christoph Gohlke, and Travis E. Oliphant. Array programming with NumPy. *Nature*, 585(7825):357–362, September 2020.

[33] Sandra G. Hart. *NASA Task Load Index (TLX)*. 1986.

[34] Sandra G. Hart. Nasa-task load index (nasa-tlx); 20 years later. In *Proceedings of the Human Factors and Ergonomics Society Annual Meeting*, pages 904–908, 2006.

[35] Florian Leander Haufe, Kai Schmidt, Jaime Enrique Duarte, Peter Wolf, Robert Riener, and Michele Xiloyannis. Activity-based training with the myosuit: a safety and feasibility study across diverse gait disorders. *Journal of NeuroEngineering and Rehabilitation*, 17:135–145, 2020.

[36] T. Hayashi, H. Kawamoto, and Y. Sankai. Control method of robot suit hal working as operator's muscle using biological and dynamical information. In *2005 IEEE/RSJ International Conference on Intelligent Robots and Systems*, pages 3063–3068, 2005.

[37] KL Ho Hoang and Mombaur K. Adjustments to de leva-anthropometric regression data for the changes in body proportions in elderly humans. *Journal of Biomechanics*, 48:3732–3736, 2015.

[38] Yue Hu and Katja Mombaur. Optimal control based push recovery strategy for the icub humanoid robot with series elastic actuators. In *2017 IEEE/RSJ International Conference on Intelligent Robots and Systems (IROS)*, pages 5846–5852, 2017.

[39] J. D. Hunter. Matplotlib: A 2d graphics environment. *Computing in Science & Engineering*, 9(3):90–95, 2007.

[40] Weiguang Huo, Huiseok Moon, Mohamed Amine Alouane, Vincent Bonnet, Jian Huang, Yacine Amirat, Ravi Vaidyanathan, and Samer Mohammed. Impedance modulation control of a lower-limb exoskeleton to assist sit-to-stand movements. *IEEE Transactions on Robotics*, 38(2):1230–1249, 2022.

[41] Maximilian Jalea. On the suitability of automatic differentiation for direct optimal control with a focus on the usability for non experts. Master's thesis, Ruprecht-Karls Universitaet Heidelberg, Grabengasse 1, 69117 Heidelberg, Germany, 2023.

[42] Sergey Jatsun, Sergei Savin, Andrey Yatsun, and Ruslan Turlapov. Adaptive control system for exoskeleton performing sit-to-stand motion. In *2015 10th International Symposium on Mechatronics and its Applications (ISMA)*, pages 1–6, 2015.

[43] Gordon S. Novak Jr. Cs 381k: Symbolic differentiation. 2007.

[44] Merel M. Jung and Geke D. S. Ludden. What do older adults and clinicians think about traditional mobility aids and exoskeleton technology? *ACM Transactions on Human-Robot Interaction*, 8:1–17, 2019.

[45] Takahiro Kagawa and Yoji Uno. Gait pattern generation for a power-assist device of paraplegic gait. In *RO-MAN 2009 - The 18th IEEE International Symposium on Robot and Human Interactive Communication*, pages 633–638, 2009.

[46] Rita Rastogi Kalyani, Mark Corriere, and Luigi Ferrucci. Age-related and disease-related muscle loss: the effect of diabetes, obesity, and other diseases. *The Lancet Diabetes Endocrinology*, 2:819–829, 2014.

[47] Akim Kapsalyamov, Prashant K. Jamwal, Shahid Hussain, and Mergen H. Ghayesh. State of the art lower limb robotic exoskeletons for elderly assistance. *IEEE Access*, 7:95075–95086, 2019.

[48] Henning Koch and Katja Mombaur. Exoopt - a framework for patient centered design optimization of lower limb exoskeletons. In *2015 IEEE International Conference on Rehabilitation Robotics (ICORR)*, pages 113–118, 2015.

[49] Charles Lambelet, Damir Temiraliuly, Marc Siegenthaler, Marc Wirth, Daniel G. Woolley, Olivier Lambercy, Roger Gassert, and Nicole Wenderoth. Characterization and wearability evaluation of a fully portable wrist exoskeleton for unsupervised training after stroke. *Journal of NeuroEngineering and Rehabilitation*, 17(132):9–11, 2020.

[50] Daniel B Leineweber. *Analyse und Restrukturierung Eines Verfahrens Zur Direkten Lösung Von Optimal-Steuerungsproblemen:(the Theory of MUSCOD in a Nutshell)*. PhD thesis, IWR, 1996.

[51] Daniel B. Leineweber, Andreas Schäfer, Hans Georg Bock, and Johannes P. Schlöder. An efficient multiple shooting based reduced sqp strategy for large-scale dynamic process optimization: Part ii: Software aspects and applications. *Computers Chemical Engineering*, 27(2):167–174, 2003.

[52] James R. Lewis. The system usability scale: Past, present, and future. *International Journal of Human–Computer Interaction*, 34(7):577–590, 2018.

[53] Jin Li, Qiang Xue, Shuo Yang, Xiaolong Han, Shouwei Zhang, Min Li, and Jingchen Guo. Kinematic analysis of the human body during sit-to-stand in healthy young adults. *Medicine*, 100(22):e26208, 2021.

[54] Vasundhara Mahajan, Pramod Agarwal, and Hari Om Gupta. Chapter 3 - power quality problems with renewable energy integration. In P. Sanjeevikumar, C. Sharmeela, Jens Bo Holm-Nielsen, and P. Sivaraman, editors, *Power Quality in Modern Power Systems*, pages 105–131. Academic Press, 2021.

[55] Anas Mahdi, Jonathan Feng-Shun Lin, and Katja Mombaur. Maintaining mobility in older age - design and initial evaluation of the robot skywalker for walking sit-to-stand assistance. In *2022 9th IEEE RAS/EMBS International Conference for Biomedical Robotics and Biomechatronics (BioRob)*, pages 01–08, 2022.

[56] Patricia J. Manns, Caitlin Hurd, and Jaynie F. Yang. Perspectives of people with spinal cord injury learning to walk using a powered exoskeleton. *Journal of NeuroEngineering and Rehabilitation*, 16(94), 2019.

[57] Maria M. Martins, Cristina P. Santos, Anselmo Frizera-Neto, and Ramón Ceres. Assistive mobility devices focusing on smart walkers: Classification and review. *Robotics and Autonomous Systems*, 60(4):548–562, 2012.

[58] Andrés Martínez, Brian Lawson, Christina Durrough, and Michael Goldfarb. A velocity-field-based controller for assisting leg movement during walking with a bilateral hip and knee lower limb exoskeleton. *IEEE Transactions on Robotics*, 35(2):307–316, 2019.

[59] Andrés Martínez, Brian Lawson, and Michael Goldfarb. A controller for guiding leg movement during overground walking with a lower limb exoskeleton. *IEEE Transactions on Robotics*, 34(1):183–193, 2018.

[60] Benjamin Michaud, François Bailly, Eve Charbonneau, Amedeo Ceglia, Léa Sanchez, and Mickael Begon. Bioptim, a python framework for musculoskeletal optimal control in biomechanics. *IEEE Transactions on Systems, Man, and Cybernetics: Systems*, pages 1–12, 2022.

[61] Benjamin Michaud and Mickael Begon. bioviz: A vizualization python toolbox for biorbd. Web page, 2018.

[62] Benjamin Michaud and Mickaël Begon. biorbd: A c++, python and matlab library to analyze and simulate the human body biomechanics. *Journal of Open Source Software*, 6(57):2562, 2021.

[63] Katja Mombaur. Lecture notes in syde 750 simulation & optimization in robotics and biomechanics, January to April 2021.

[64] Katja Mombaur and Khai-Long Ho Hoang. How to best support sit to stand transfers of geriatric patients: Motion optimization under external forces for the design of physical assistive devices. *Journal of Biomechanics*, 58:131–138, 2017.

[65] Rezvan Nasiri, Mohammad Shushtari, Hossein Rouhani, and Arash Arami. Virtual energy regulator: A time-independent solution for control of lower limb exoskeletons. *IEEE Robotics and Automation Letters*, 6(4):7699–7705, 2021.

[66] KA Opila, AC Nicol, and JP Paul. Upper limb loadings of gait with crutches. 109(4):285–290, 1987.

[67] A. Ortlieb, M. Bouri, R. Baud, and H. Bleuler. An assistive lower limb exoskeleton for people with neurological gait disorders. In *2017 International Conference on Rehabilitation Robotics (ICORR)*, pages 441–446, 2017.

[68] Robert L. Herron Phillip A. Bishop. Use and misuse of the likert item responses and other ordinal measures. *International Journal of Exercise Science*, 8(3):297–302, 2015.

[69] Hugo A. Quintero, Ryan J. Farris, and Michael Goldfarb. A method for autonomous control of lower limb exoskeletons for persons with paraplegia. *Journal of Medical Devices*, 6:041003–1 – 041003–6, 2012.

[70] Singiresu S. Rao. *Engineering Optimization: Theory and Practice*. John Wiley Sons Inc., 4 edition, 2009.

[71] Kilian Rapp, Clemens Becker, Ian D. Cameron, Hans-Helmut König, and Gisela Büchele. Epidemiology of falls in residential aged care: Analysis of more than 70,000 falls from residents of bavarian nursing homes. *Journal of the American Medical Directors Association*, 13:187.e1 – 187.e6, 2012.

[72] Sergei Savin, SergeyJatsun, Andrey Yatsun, and A. Malchikov. Study of controlled motion of exoskeleton moving from sitting to standing position. 08 2015.

[73] Suresh P. Sethi. *Optimal Control Theory: Applications to Management Science and Economics*. Springer International Publishing, 2021.

[74] Linda Shore, Adam de Eyto, and Leonard O'Sullivan. Technology acceptance and perceptions of robotic assistive devices by older adults – implications for exoskeleton design. *Disability and Rehabilitation: Assistive Technology*, 0(0):1–9, 2020.

[75] Mohammad Shushtari, Hannah Dinovitzer, Jiacheng Weng, and Arash Arami. Ultra-robust real-time estimation of gait phase. *IEEE Transactions on Neural Systems and Rehabilitation Engineering*, 30:2793–2801, 2022.

[76] Mohammad Shushtari, Rezvan Nasiri, and Arash Arami. Online reference trajectory adaptation: A personalized control strategy for lower limb exoskeletons. *IEEE Robotics and Automation Letters*, 7(1):128–134, 2022.

[77] Bruno Siciliano, Lorenzo Sciavicco, Luigi Villani, and Giuseppe Oriolo. Optimal trajectories. In *Robotics: Modelling, Planning and Control*, pages 499–500. Springer London, 2009.

[78] José Fernando Silva and Sónia F. Pinto. 35 - linear and nonlinear control of switching power converters. In Muhammad H. Rashid, editor, *Power Electronics Handbook (Fourth Edition)*, pages 1141–1220. Butterworth-Heinemann, fourth edition edition, 2018.

[79] Kenta Suzuki, Gouji Mito, Hiroaki Kawamoto, Yasuhisa Hasegawa, and Yoshiyuki Sankai. Intention-based walking support for paraplegia patients with robot suit hal. *Advanced Robotics*, 21(12):1441–1469, 2007.

[80] Francesca Sylos-Labini, Valentina La Scaleia, Andrea d'Avella, Iolanda Pisotta, Federica Tamburella, Giorgio Scivoletto, Marco Molinari, Shiqian Wang, Letian Wang, Edwin van Asseldonk, Herman van der Kooij, Thomas Hoellinger, Guy Cheron, Freygardur Thorsteinsson, Michel Ilzkovitz, Jeremi Gancet, Ralf Hauffe, Frank Zanov, Francesco Lacquaniti, and Yuri P. Ivanenko. Emg patterns during assisted walking in the exoskeleton. *Frontiers in Human Neuroscience*, 8, 2014.

[81] Candy Tefertiller, Kaitlin Hays, Janell Jones, Arun Jayaraman, Clare Hartigan, Tamara Bushnik, and Gail F. Forrest. Initial Outcomes from a Multicenter Study Utilizing the Indego Powered Exoskeleton in Spinal Cord Injury. *Topics in Spinal Cord Injury Rehabilitation*, 24(1):78–85, 2017.

[82] Atsushi Tsukahara, Yasuhisa Hasegawa, Kiyoshi Eguchi, and Yoshiyuki Sankai. Restoration of gait for spinal cord injury patients using hal with intention estimator for preferable swing speed. *IEEE Transactions on Neural Systems and Rehabilitation Engineering*, 23(2):308–318, 2015.

[83] Ozer Unluhisarcikli, Maciej Pietrusinski, Brian Weinberg, Paolo Bonato, and Constantinos Mavroidis. Design and control of a robotic lower extremity exoskeleton for gait rehabilitation. pages 4893–4898, 2011.

[84] Christian Vassallo, Samuele De Giuseppe, Chiara Piezzo, Stefano Maludrottu, Giulio Cerruti, Maria Laura D'Angelo, Emanuele Gruppioni, Claudia Marchese, Simona Castellano, Eleonora Guanziroli, Franco Molteni, Matteo Laffranchi, and Lorenzo De Michieli. Gait patterns generation based on basis functions interpolation for the twin lower-limb exoskeleton. In *2020 IEEE International Conference on Robotics and Automation (ICRA)*, pages 1778–1784, 2020.

[85] Robin Verschueren, Gianluca Frison, Dimitris Kouzoupis, Jonathan Frey, Niels van Duijkeren, Andrea Zanelli, Branimir Novoselnik, Thivaharan Albin, Rien Quirynen, and Moritz Diehl. acados: a modular open-source framework for fast embedded optimal control, 2019.

[86] Pauli Virtanen, Ralf Gommers, Travis E. Oliphant, Matt Haberland, Tyler Reddy, David Cournapeau, Evgeni Burovski, Pearu Peterson, Warren Weckesser, Jonathan Bright, Stéfan J. van der Walt, Matthew Brett, Joshua Wilson, K. Jarrod Millman, Nikolay Mayorov, Andrew R. J. Nelson, Eric Jones, Robert Kern, Eric Larson, C J Carey, İlhan Polat, Yu Feng, Eric W. Moore, Jake VanderPlas, Denis Laxalde, Josef Perktold, Robert Cimrman, Ian Henriksen, E. A. Quintero, Charles R. Harris, Anne M. Archibald, Antônio H. Ribeiro, Fabian Pedregosa, Paul van Mulbregt, and SciPy 1.0 Contributors. SciPy 1.0: Fundamental Algorithms for Scientific Computing in Python. *Nature Methods*, 17:261–272, 2020.

[87] O von Stryk and R Bulirsch. Direct and indirect methods for trajectory optimization. *Ann Oper Res*, 37:357–373, 1992.

[88] Sheryl F. Vondracek and Sunny A. Linnebur. Diagnosis and management of osteoporosis in the older senior. *Clinical interventions in aging*, 4:121–135, 2009.

[89] Andreas Waechter and Lorenz T. Biegler. On the implementation of an interior-point filter line-search algorithm for large-scale nonlinear programming. *Math. Program.*, 106:25–57, 2006.

[90] X Xue, X Yang, H Tu, W Liu, D Kong, Z Fan, Z Deng, and N Li. The improvement of the lower limb exoskeletons on the gait of patients with spinal cord injury: A protocol for systematic review and meta-analysis. *Medicine (Baltimore)*, 101(4), 2022.

[91] Takayoshi Yamada and Shin ichi Demura. Relationships between ground reaction force parameters during a sit-to-stand movement and physical activity and falling risk of the elderly and a comparison of the movement characteristics between the young and the elderly. *Archives of Gerontology and Geriatrics*, 48(1):73–77, 2009.

[92] Hiroshi R. Yamasaki, Hiroyuki Kambara, and Yasuharu Koike. Dynamic optimization of the sit-to-stand movement. *Journal of Applied Biomechanics*, 27(4):306–313, 2011.

[93] Binwei Zhou, Qiang Xue, Shuo Yang, Huaiqiang zhang, and Tongtong Wang. Design and control of a sit-to-stand assistive device based on analysis of kinematics and dynamics. *Journal for Control, Measurement, Electronics, Computing and Communications*, 62(3):353–364, 2021.

APPENDICES

Appendix A

SUS, RTLX, and Custom Survey Statements

A.1 SUS Survey

This is a System Usability Scale. Please answer the following questions based on your experience after wearing Twin Exoskeleton.

1. Please enter your participant number.

2. For each of the following statements, please mark one box that best describes your reactions to Twin Exoskeleton today.

    (a) I think that I would like to use Twin Exoskeleton frequently.

    - Strongly Disagree / Disagree / Neutral / Agree / Strongly Agree

    (b) I found Twin Exoskeleton unnecessarily complex.

    - Strongly Disagree / Disagree / Neutral / Agree / Strongly Agree

    (c) I thought Twin Exoskeleton was easy to use.

    - Strongly Disagree / Disagree / Neutral / Agree / Strongly Agree

    (d) I think that I would need the support of a technical person to be able to use Twin Exoskeleton.

    - Strongly Disagree / Disagree / Neutral / Agree / Strongly Agree

(e) I found the various functions in Twin Exoskeleton were well integrated.

- Strongly Disagree / Disagree / Neutral / Agree / Strongly Agree

(f) I thought there was too much inconsistency in Twin Exoskeleton.

- Strongly Disagree / Disagree / Neutral / Agree / Strongly Agree

(g) I would imagine that most people would learn to use Twin Exoskeleton very quickly.

- Strongly Disagree / Disagree / Neutral / Agree / Strongly Agree

(h) I found Twin Exoskeleton very cumbersome (awkward) to use.

- Strongly Disagree / Disagree / Neutral / Agree / Strongly Agree

(i) I felt very confident using Twin Exoskeleton.

- Strongly Disagree / Disagree / Neutral / Agree / Strongly Agree

(j) I needed to learn a lot of things before I could get going with Twin Exoskeleton.

- Strongly Disagree / Disagree / Neutral / Agree / Strongly Agree

A.2   RTLX Survey

Five RTLX surveys were used for the five tasks (sit-to-stand, stand-to-sit, turning, MWM, and AWM), but the questions are the same (see Figure A.1).

Figure 8.6

NASA Task Load Index

Hart and Staveland's NASA Task Load Index (TLX) method assesses work load on five 7-point scales. Increments of high, medium and low estimates for each point result in 21 gradations on the scales.

Participant Number	Task	Date

Mental Demand — How mentally demanding was the task?

Very Low — Very High

Physical Demand — How physically demanding was the task?

Very Low — Very High

Temporal Demand — How hurried or rushed was the pace of the task?

Very Low — Very High

Performance — How successful were you in accomplishing what you were asked to do?

Perfect — Failure

Effort — How hard did you have to work to accomplish your level of performance?

Very Low — Very High

Frustration — How insecure, discouraged, irritated, stressed, and annoyed wereyou?

Very Low — Very High

Figure A.1: RTLX Survey

130

A.3 Custom Surveys on Measuring User's Comfort Level

A.3.1 [No Tutorial] Before-Session Questionnaire

This questionnaire is to be completed by the user before the start of the exoskeleton session.

1. Please enter your participation number.

2. Please answer the following questions by selecting the option that truly reflects your opinion.

   (a) I am excited to wear the Twin Exoskeleton.
       - Strongly Disagree / Disagree / Neutral / Agree / Strongly Agree
   (b) I think I am comfortable with wearing the Twin Exoskeleton.
       - Strongly Disagree / Disagree / Neutral / Agree / Strongly Agree
   (c) I am nervous to wear the Twin Exoskeleton.
       - Strongly Disagree / Disagree / Neutral / Agree / Strongly Agree
   (d) I am scared to wear the Twin Exoskeleton.
       - Strongly Disagree / Disagree / Neutral / Agree / Strongly Agree

3. Additional Comments (feel free to add as many details as you like!):

A.3.2 [Tutorial] Before-Session Questionnaire

This questionnaire is to be completed by the user before the start of the tutorial session.

1. Please enter your participation number.

2. Please answer the following questions by selecting the option that truly reflects your opinion.

   (a) I am excited to wear the Twin Exoskeleton.
       - Strongly Disagree / Disagree / Neutral / Agree / Strongly Agree

(b) I think I am comfortable with wearing the Twin Exoskeleton.

- Strongly Disagree / Disagree / Neutral / Agree / Strongly Agree

(c) I am nervous to wear the Twin Exoskeleton.

- Strongly Disagree / Disagree / Neutral / Agree / Strongly Agree

(d) I am scared to wear the Twin Exoskeleton.

- Strongly Disagree / Disagree / Neutral / Agree / Strongly Agree

(e) I think receiving a tutorial on how to use the Exoskeleton would be helpful for wearing the Twin Exoskeleton for the first time.

- Strongly Disagree / Disagree / Neutral / Agree / Strongly Agree

3. Additional Comments (feel free to add as many details as you like!):

A.3.3   [No Tutorial] After-Session Questionnaire

This questionnaire is to be completed by the user after the end of the exoskeleton session.

1. Please enter your participation number.

2. Please answer the following questions by selecting the option that truly reflects your opinion.

(a) I am excited to wear the Twin Exoskeleton.

- Strongly Disagree / Disagree / Neutral / Agree / Strongly Agree

(b) I felt comfortable wearing the Twin Exoskeleton.

- Strongly Disagree / Disagree / Neutral / Agree / Strongly Agree

(c) I am nervous to wear the Twin Exoskeleton.

- Strongly Disagree / Disagree / Neutral / Agree / Strongly Agree

(d) I am scared to wear the Twin Exoskeleton.

- Strongly Disagree / Disagree / Neutral / Agree / Strongly Agree

(e) I think having a tutorial on getting acquainted with the Twin Exoskeleton would better prepare my first time wearing the device.

- Strongly Disagree / Disagree / Neutral / Agree / Strongly Agree

132

(f) I prefer to be supported by the lift than a person when wearing the Twin Exoskeleton. (If you are indifferent, select Neutral.)

- Strongly Disagree / Disagree / Neutral / Agree / Strongly Agree

(g) I am comfortable with wearing the Twin Exoskeleton in the future.

- Strongly Disagree / Disagree / Neutral / Agree / Strongly Agree

3. Please rank the following tasks that were performed **with** the Twin Exoskeleton from 1 to 5. 1 means the easiest, 5 means the most difficult.

Sit-to-stand

Stand-to-sit

Turning

Manual Walk Mode (each step triggered manually)

Automatic Walk Mode (each step triggered by incline)

4. Additional Comments (feel free to add as many details as you like!): E.g. What other exercises do you think would be helpful for the preparation?

A.3.4 [Tutorial] After-Session Questionnaire

This questionnaire is to be completed by the user after the end of the exoskeleton session.

1. Please enter your participation number.

2. Please answer the following questions by selecting the option that truly reflects your opinion.

(a) I am excited to wear the Twin Exoskeleton.

- Strongly Disagree / Disagree / Neutral / Agree / Strongly Agree

(b) I am comfortable wearing the Twin Exoskeleton.

- Strongly Disagree / Disagree / Neutral / Agree / Strongly Agree

(c) I am nervous to wear the Twin Exoskeleton.

- Strongly Disagree / Disagree / Neutral / Agree / Strongly Agree

(d) I am scared to wear the Twin Exoskeleton.

- Strongly Disagree / Disagree / Neutral / Agree / Strongly Agree

(e) I like the idea of having a tutorial to prepare myself for the Twin Exoskeleton.

- Strongly Disagree / Disagree / Neutral / Agree / Strongly Agree

(f) The tutorial helped preparing me for the Twin Exoskeleton.

- Strongly Disagree / Disagree / Neutral / Agree / Strongly Agree

(g) The tutorial is easy to follow.

- Strongly Disagree / Disagree / Neutral / Agree / Strongly Agree

(h) The tutorial should be improved before I wear the Twin Exoskeleton in the future.

- Strongly Disagree / Disagree / Neutral / Agree / Strongly Agree

(i) I prefer to be supported by the lift than a person when wearing the Twin Exoskeleton. (If you are indifferent, select Neutral.)

- Strongly Disagree / Disagree / Neutral / Agree / Strongly Agree

(j) I am comfortable with wearing the Twin Exoskeleton in the future.

- Strongly Disagree / Disagree / Neutral / Agree / Strongly Agree

3. Please rank the following tasks that were performed *with* the Twin Exoskeleton from 1 to 5. 1 means the easiest, 5 means the most difficult.

Sit-to-stand

Stand-to-sit

Turning

Manual Walk Mode (each step triggered manually)

Automatic Walk Mode (each step triggered by incline)

4. Additional Comments (feel free to add as many details as you like!): E.g. What other exercises do you think would be helpful for the preparation?

Appendix B

Human and Exoskeleton Marker Layout

The marker layout used for the STS biomechanics experiment is adapted from Qualisys PAF (qfl.qualisys.com/#!/project/qcs) and the KIT MMM (mmm.humanoids.kit.edu/markerset.html). Asymmetry and further details are modified by Jonathan Lin from CERC HCRMI Lab at the University of Waterloo. TWIN and crutches marker labelling are created by Giorgos Marinou from ORB Lab of Heidelberg University. Further modifications are made by Jan Lau from CERC HCRMI Lab at the University of Waterloo.

TWIN MARKERING PROTOCOL: 62 MARKERS IN TOTAL

Name	Segment	Location	Location (bone, landmark)
MODIFIED MARKER SET ON HUMAN UPPER BODY (25 markers)			
L_HEAD	Head	Left temple	Between os frontale and os parietale
R_HEAD	Head	Right temple	Between os frontal and os parietale
SGL	Head	Forehead, between eyebrows (glabella)	Glabella
SJN	Upper torso	Between collarbone, just above the keyhole divot	Sternum, jugular notch
SXS	Upper torso	Bottom of sternum	Sternum, xiphisterna joint
CV7	Upper torso	Largest vertebra in the neck	Cervical vertebra 7
TV2	Upper torso	Aligned with shoulder markers SAE	Thoracic vertebra 2
L_SAE	L upper arm	Top of shoulder	Scapula, acromial edge
L_HUM	L upper arm	Roughly 1/3 up from elbow, outside edge of arm (lateral), In line with L_SAE and L_HLE	(Not on bony landmark)
L_HLE	L upper arm	Elbow outside side (lateral). Elbow landmarks on upper arm. May be easier to find if the subject bends their arm, the bony landmark will become more obvious	Humerus, lateral epicondyle
L_HME	L upper arm	Elbow inside side (medial)	Humerus, medial epicondyle
L_OLE	L lower arm	Roughly 1/3 down from elbow, outside edge of arm, in line with L_HLE and L_RSP	(Not on bony landmark)
L_RSP	L lower arm	Wrist thumb side (lateral)	Radius, styloid process
L_USP	L lower arm	Wrist pinky side (medial)	Ulna, styloid process
L_HM2	L hand	Second knuckle	Forefinger basis
L_HM5	L hand	Fifth knuckle	Small finger basis
R_SAE	R upper arm	Top of shoulder	Scapula, acromial edge
R_HUM	R upper arm	Roughly 1/3 down from shoulder. outside edge of arm (lateral), In line with R_SAE and R_HLE	(Not on bony landmark)
R_HLE	R upper arm	Elbow outside side (lateral)	Humerus, lateral epicondyle
R_HME	R upper arm	Elbow inside side (medial)	Humerus, medial epicondyle
R_OLE	R lower arm	Roughly 1/3 up from wrist, outside edge of arm (lateral), in line with L_HLE and L_RSP	(Not on bony landmark)
R_RSP	R lower arm	Wrist thumb side (lateral)	Radius, styloid process
R_USP	R lower arm	Wrist pinky side (medial)	Ulna, styloid process
R_HM2	R lower arm	Second knuckle	Forefinger basis
R_HM5	R lower arm	Fifth knuckle	Small finger basis

Figure B.1: Marker layout on human upper body.
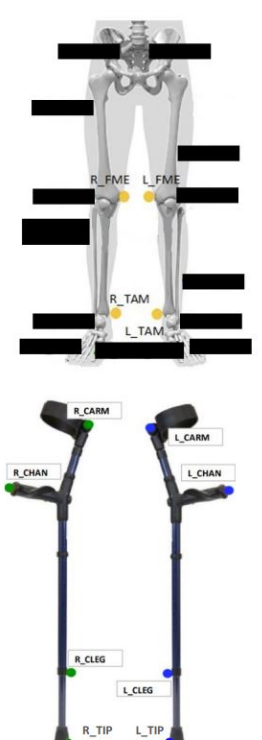
		TWIN MARKERING PROTOCOL	
Name	**Segment**	**Location**	**Location (bone, landmark)**
		MODIFIED MARKER SET ON HUMAN LOWER BODY (4 markers)	
L_FME	L thigh	Knee inside (medial)	Femur, medial epicondyle
R_FME	R thigh	Knee inside (medial)	Femur medial epicondyle
L_TAM	L shank	Ankle inside (medial)	Medial malleolus, medial prominence
R_TAM	R shank	Ankle inside (medial)	Medial malleolus, medial prominence
		NEW MARKERS ON CRUTCHES (8 markers)	
L_CARM	L crutch	Posterior middle side of arm brace	-
L_CHAN	L crutch	Tip of the handle	-
L_LEG	L crutch	Posterior side at distal end of upper tube	-
L_TIP	L crutch	Tip of the crutch	-
R_ARM	R crutch	Posterior middle side at distal end of upper tube	-
R_CHAN	R crutch	Tip of the handle	-
R_LEG	R crutch	Posterior middle side of arm brace	-
R_TIP	R crutch	Tip of the crutch	-

Figure B.2: Marker layout on human lower body and crutches.

TWIN MARKERING PROTOCOL

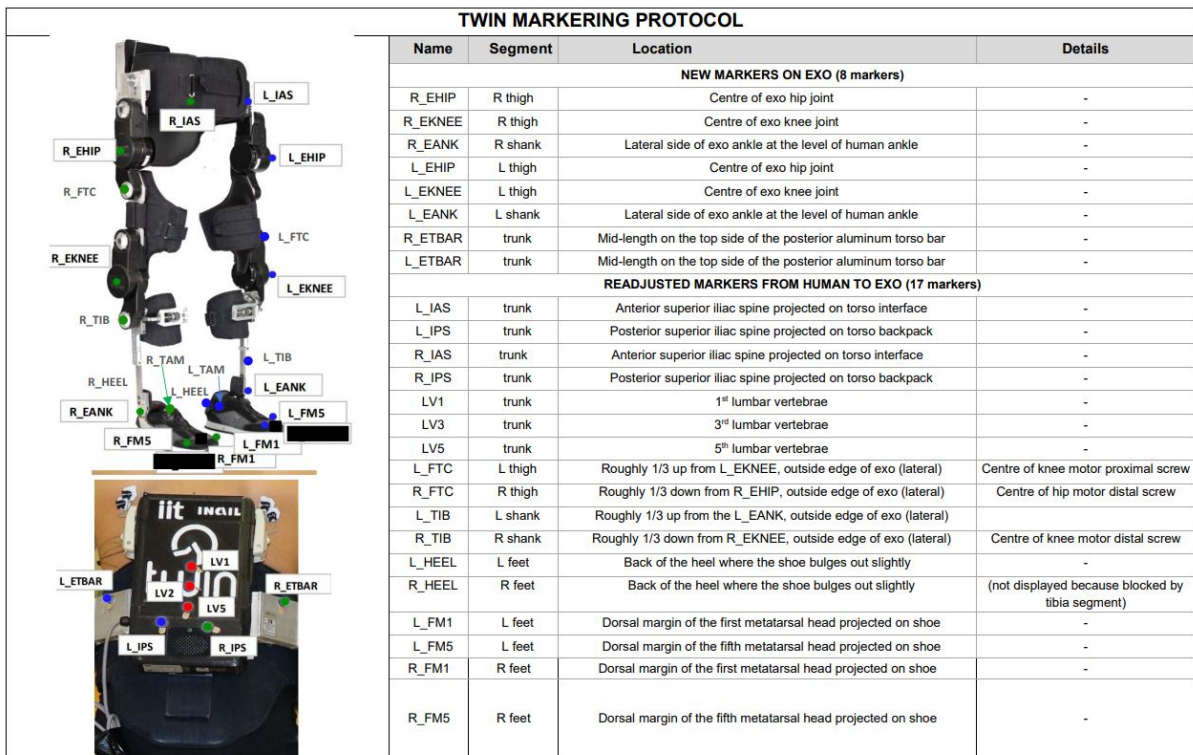| Name	Segment	Location	Details
NEW MARKERS ON EXO (8 markers)			
R_EHIP	R thigh	Centre of exo hip joint	-
R_EKNEE	R thigh	Centre of exo knee joint	-
R_EANK	R shank	Lateral side of exo ankle at the level of human ankle	-
L_EHIP	L thigh	Centre of exo hip joint	-
L_EKNEE	L thigh	Centre of exo knee joint	-
L_EANK	L shank	Lateral side of exo ankle at the level of human ankle	-
R_ETBAR	trunk	Mid-length on the top side of the posterior aluminum torso bar	-
L_ETBAR	trunk	Mid-length on the top side of the posterior aluminum torso bar	-
READJUSTED MARKERS FROM HUMAN TO EXO (17 markers)			
L_IAS	trunk	Anterior superior iliac spine projected on torso interface	-
L_IPS	trunk	Posterior superior iliac spine projected on torso backpack	-
R_IAS	trunk	Anterior superior iliac spine projected on torso interface	-
R_IPS	trunk	Posterior superior iliac spine projected on torso backpack	-
LV1	trunk	1st lumbar vertebrae	-
LV3	trunk	3rd lumbar vertebrae	-
LV5	trunk	5th lumbar vertebrae	-
L_FTC	L thigh	Roughly 1/3 up from L_EKNEE, outside edge of exo (lateral)	Centre of knee motor proximal screw
R_FTC	R thigh	Roughly 1/3 down from R_EHIP, outside edge of exo (lateral)	Centre of hip motor distal screw
L_TIB	L shank	Roughly 1/3 up from the L_EANK, outside edge of exo (lateral)	
R_TIB	R shank	Roughly 1/3 down from R_EKNEE, outside edge of exo (lateral)	Centre of knee motor distal screw
L_HEEL	L feet	Back of the heel where the shoe bulges out slightly	-
R_HEEL	R feet	Back of the heel where the shoe bulges out slightly	(not displayed because blocked by tibia segment)
L_FM1	L feet	Dorsal margin of the first metatarsal head projected on shoe	-
L_FM5	L feet	Dorsal margin of the fifth metatarsal head projected on shoe	-
R_FM1	R feet	Dorsal margin of the first metatarsal head projected on shoe	-
R_FM5	R feet	Dorsal margin of the fifth metatarsal head projected on shoe	-

Figure B.3: Marker layout on TWIN exoskeleton.

138